THE ADDITION AND HYDROGEN ABSTRACTION REACTIONS OF A FLUORINATED RADICAL IN AQUEOUS SOLUTION

By

LI ZHANG

A DISSERTATION PRESENTED TO THE GRADUATE SCHOOL
OF THE UNIVERSITY OF FLORIDA IN PARTIAL FULFILLMENT
OF THE REQUIREMENTS FOR THE DEGREE OF
DOCTOR OF PHILOSOPHY

UNIVERSITY OF FLORIDA

2001

To my Heavenly Father

To my Mom, Dad, Jing, and my church family

ACKNOWLEDGMENTS

Among many people with whom I have interacted throughout the course of my graduate study at the University of Florida, I would like to extend my sincere appreciation to the special few that have supported, motivated, and inspired me.

I would like to express my gratitude to my research advisor, Dr. William R. Dolbier, Jr., for helping me to become a researcher and for his continuous guidance during my time in the Ph.D. program. I would especially like to thank him for his motivation and for challenging me to pursue excellence.

For the supervision during my time as a graduate student, I would like to thank the members of my supervisory committee for their advice and encouragement. These include Dr. Merle Battiste, Dr. Kirk Schanze, Dr. Robert Kennedy, and Dr. Wolfgang Sigmund.

I would like to thank Dr. Keith U. Ingold for his collaboration on this project, for his help and support, and for allowing me work in his lab to conduct the LFP experiments.

Special thanks go to the staff of the Spectroscopic Services Laboratories in the Department of Chemistry. Dr. Ion Ghiviriga, Mr. Robert Harker, Dr. David Powell, and Dr. Lidia Matveeva have been very helpful for getting spectra with special requirements, for interpretating of spectra, and for solving instrumental problems. I truly appreciate their skill, kindness, and patience.

It is always a pleasure for me to be in the Dolbier group. I would like to say special thanks to Dr. Conrad Burkholder, Dr. Jian-Xin Duan, Dr. An-Rong Li, Dr. Alexander B. Shtarev, Dr. Samia Ait-Mohand and Dr. Yue-Lian Xu for their helpful discussion and friendship; Dr. Feng Tian for his friendship and encouragement; Dr. Michelle Fletcher for her help during the early stage of my graduate study in the United States; Mr. Marshall Baker and Mr. Bob Shelton for their help and patience to check the English of my dissertation and reports; Mr. Joe Cradlebaugh for his contributions to the projects; and the Dolbier group members, both past and present, for their helpful discussion and friendship.

The Gainesville Chinese Christian Church has been a constant source of support and encouragement for me and my academic endeavors. It is impossible to name all the people who have helped me. I would like to acknowledge all of the friends for their love and prayers.

Last and definitely not least, I thank my family for the endless love and support that makes my dream become true. I thank my mother and father for their belief in me, especially during some difficult times. I would also thank my sister Jing for her encouragement.

TABLE OF CONTENTS

ACKNOWLEDGMENTS iii

KEY TO SYMBOLS OR ABBREVIATIONS vii

ABSTRACT viii

CHAPTERS

1 AN OVERVIEW OF RADICAL REACTIONS AND THE REACTIVITIES OF FLUORINATED RADICALS IN ORGANIC SOLVENTS 1

- General Overview of Addition and H-Abstraction Reactions of Free Radicals 2
- Reactivities of Fluorinated Radicals in Organic Solvents 15
- Solvent Effects on Free Radical Reactions 28
- Conclusion 33

2 ADDITION REACTIONS OF PERFLUORO-N-ALKYL RADICAL IN AQUEOUS SOLUTION 35

- Synthesis of Water-Soluble Substrates 36
- Laser Flash Photolysis Experiments 40
- Results and Discussion 46
- Conclusion 52

3 HYDROGEN ATOM ABSTRACTION REACTIONS OF PERFLUORO-N-ALKYL RADICAL IN AQUEOUS SOLUTION 53

- Absolute Rate Determination - Competition between Addition and H-Abstraction Reactions 54
- Absolute Rate Constants of Hydrogen Abstraction Reactions by Perfluoro-n-alkyl Radical in Aqueous Solution 64
- Solvent Effect of the H-abstraction Reactions by $\cdot R_fSO_3Na$ Radical 80
- Kinetic Isotope Effects of H-abstraction Reactions by $\cdot R_fSO_3Na$ Radical in Aqueous Solution 81
- Conclusion 84

4 SUMMARY 86

Addition Reactions of Perfluoro-n-alkyl Radical in Aqueous Solution 86
Hydrogen Atom Abstraction Reactions of Perfluoro-n-alkyl Radical in Aqueous Solution 87

5 EXPERIMENTAL 90

General Procedures 90
Experiments for Chapter 2 91
Experiments for Chapter 3 104

APPENDIX SELECTED ^{19}F NMR SPECTRA 140

REFERENCES 145

BIOGRAPHICAL SKETCH 152

KEY TO SYMBOLS AND ABBREVIATIONS

Acronym Names and IUPAC Names

Acronyms Name	IUPAC Name
1,3-BTB	1,3-Bis(trifluoromethyl)benzene
F113	1,1,2-Trichloro-trifluoroethane
THF	Tetrahydrofuran

Abbreviations and Explanations

Abbreviation	Explanation
$R\cdot$ radical	Hydrocarbon alkyl radical
$R_f\cdot$ radical	Perfluoro-n-alkyl radical
$\cdot R_fSO_3Na$ radical	$\cdot\ CF_2CF_2OCF_2CF_2SO_3Na$ Radical
k_{add}	Addition reaction rate constant of a radical to an alkene
k_H	H-Abstraction reaction rate constant of a radical
k_{exptl}	Pseudo 1st order rate constant of addition reaction measured by LFP technique
k_{gl}	Global rate constant of a radical and alkene reaction
$k_{D,\ THF\text{-}d8}$	Absolute D-abstraction rate constant from THF-d_8 by a radical
$k_{H\ overall}$	Overall H-abstraction rate constant from substrates by a radical
$k_{H\ per\ H}$	H-Abstraction rate constant by a radical from each active H-transfer site in the substrate molecule
LFP	Laser Flash Photolysis

Abstract of Dissertation Presented to the Graduate School
of the University of Florida in Partial Fulfillment of the
Requirements for the Degree of Doctor of Philosophy

THE ADDITION AND HYDROGEN ABSTRACTION REACTIONS OF A FLUORINATED RADICAL IN AQUEOUS SOLUTION

By

Li Zhang

December 2001

Chairman: William R. Dolbier, Jr.
Major Department: Chemistry

The kinetics of addition and hydrogen abstraction reactions of a fluorinated radical are investigated by a combination of laser flash photolysis (LFP) experiments, competition kinetic methodology, and product analysis in aqueous solution.

Absolute rate constants of addition reactions of $\cdot CF_2CF_2OCF_2CF_2SO_3Na$ radical to water-soluble alkenes are measured by the LFP technique in water at room temperature. The results imply that thermodynamic effects, polar effects, and steric effects all play roles in such addition reactions. The rate constants obtained in aqueous solution are compared with those of the analogous reactions obtained in the nonpolar organic solvent 1,1,2-trichloro-1,2,2-trifluoroethane (F113). It is found that the addition reactions of perfluoro-n-alkyl radicals to alkenes are somewhat faster in water than in F113. These rate enhancements are sufficient to demonstrate the importance of solvent polar effects in the addition of electrophilic perfluoro-n-alkyl radicals to alkenes.

By using competition kinetic methodology, absolute rate constants of hydrogen abstraction reactions by $\cdot CF_2CF_2OCF_2CF_2SO_3Na$ radical from a variety of hydrogen donors are determined in water. The substrates are alcohols, alkoxides, ethers, acetone, carboxylic acids and salts, thiol, silanes, and phosphorous acid. A wide range of substrate reactivity (63,400 fold) is observed, acetic acid being the slowest one, and $HSCH_2CH_2SO_3Na$ being the most reactive one.

The results indicate that the aqueous hydrogen abstraction reactions of perfluoro-n-alkyl radical are controlled by a combination of thermodynamic, transition state polar, and field effects. When the rate constants are compared with those obtained in the nonpolar organic solvent 1,3-bis(trifluoromethyl)benzene (1,3-BTB), a significant solvent polar effect is revealed. The perfluoro-n-alkyl radical is observed to react with hydrogen donors faster in water than in 1,3-BTB.

Kinetic isotope effects are investigated for the H-abstraction reaction by the $\cdot CF_2CF_2OCF_2CF_2SO_3Na$ radical in aqueous solution. A relationship between the substrate reactivity and KIE is noticed: the more reactive the substrate, the smaller the KIE value. Large KIE's (11~22) are obtained for some unreactive compounds, with tunneling effect thought to be involved.

CHAPTER 1
AN OVERVIEW OF RADICAL REACTIONS AND THE REACTIVITIES OF FLUORINATED RADICALS IN ORGANIC SOLVENTS

As one of the reactive intermediates in organic reactions, free radicals have been extensively used in organic synthesis.[1-7] At the same time, radical polymerization has been widely adopted for both industrial and laboratory scale polymer syntheses.[8-10] Free radical reactions often are tolerant of functional groups, highly selective, and proceed under mild conditions.[11] They can also give products that are not accessible by means of the more conventional polar routes.

There are several elementary reactions of free radicals (Scheme 1-1):[12]

1. Atom abstraction: $R\cdot + X\text{-}Y \longrightarrow R\text{-}X + Y\cdot$
2. Recombination: $R\cdot + R'\cdot \longrightarrow R\text{-}R'$
3. Disproportionation: $R\text{-}CH_2\text{-}CH_2\cdot \longrightarrow RCH_2CH_3 + R\text{-}CH{=}CH_2$
4. Addition: $R\cdot +$ 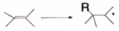
5. Electron Transfer: $R\cdot + M^{n+} \longrightarrow R^+ + M^{(n-1)+}$

Scheme 1-1 Elementary Reactions of Free Radicals

Most free radical reactions proceed through chain processes, where different elementary reactions can occur in each step, and free radical processes often have several competing pathways. It is important to be able to quantify the reactivities of radicals toward different reagents under various reaction conditions, so that one can predict expected outcomes by carefully designing the reaction. Indeed, the kinetics of alkyl radicals in addition reactions, cyclization reactions, and H-abstraction reactions have been extensively studied and reviewed.[13-18]

General Overview of Addition and H-Abstraction Reactions of Free Radicals

This chapter will focus on radical addition reactions and H-abstraction reactions.

Philicity of Radicals

According to the variable electronic demand in a particular reaction, free radicals can be categorized as being either nucleophilic or electrophilic. The nucleophilicity or electrophilicity of radicals has been established by means of Hammett studies. As shown in Table 1-1, the addition reactions of radicals with substituted styrenes and the H-abstraction reactions of radicals from substituted toluenes were used to evaluate the philicities of different radicals. It was demonstrated that simple alkyl radicals have nucleophilic character,[19, 20] whereas haloalkyl radicals[21] and oxygen-centered radicals[22] have electrophilic character.

Addition Reactions to Carbon-Carbon Double Bonds

Additions of carbon-centered radicals to alkenes are generally strongly exothermic, since a σ-bond is formed at the expense of a π-bond. For example, the addition of methyl radical to ethylene has a $\Delta H° =$ ca. -22.6 kcal/mol.[23, 24] According to the Hammond postulate,[25] such reactions should have early transition states with little bond-making and bond-breaking. This is supported by both experimental[26] and theoretical data.[23, 27-30]

Therefore, the stabilization of the incipient radical is not the major factor that determines the rate and regiochemistry of the addition reactions, unless the substituents on the double bond have π-orbitals (e.g., $-CH=CH_2$, -Ph) that can overlap with the half-filled atomic orbital of the generated radical center.[16, 39-42] Rather, the outcomes of free radical addition to alkenes depend on "a complex interplay of polar, steric, and bond strength terms."[13: P.191, 16: P.701]

Table 1-1 Hammett ρ and ρ^+ Parameters for Reactions of radicals

Radical	Addition to Styrene		H-Abstraction from Toluene	
	ρ^+	ρ	ρ^+	ρ
$(CH_3)_3C\cdot$	1.1 [a]	-	-	0.49 [b]
$c\text{-}C_6H_{11}\cdot$	0.68 [a]	-	-	-
$n\text{-}C_6H_{13}\cdot$	0.45 [a]	-	-	-
$n\text{-}C_{11}H_{23}\cdot$	-	-	-	0.45 [c]
$CH_3\cdot$	-	-	-0.1 [d]	-0.12 [d]
$(CH_3)_3CO\cdot$	-0.27 [e]	-0.31 [e]	-0.32 [f]	-0.36 [f]
$(CH_3)_3COO\cdot$	-	-	-0.56 [g]	-0.78 [g]
$(CH_3)_2N\cdot$	-	-	-1.08 [h]	-1.66 [h]
$CCl_3\cdot$	-0.42 [i]	-0.43 [i]	-1.46 [j]	-1.46 [j]
$n\text{-}C_8F_{17}\cdot$		-0.53 [k]		

a. 42°C, ref 19; b. 80°C, ref 31; c. 42°C, ref 32; d. 100°C, ref 33; e. 60°C, benzene, ref 22; f. 45°C, chlorobenzene, ref 34; g. 40°C, ref 35; h. 136°C, ref 36; i. 70°C, ref 21; j. 50°C, ref 37; k. 25°C, ref 38.

The importance of polarity in determining the overall rate of addition of radicals to symmetrical alkenes is well illustrated by the relative rates of addition of the radicals $CH_3\cdot$, $CH_2F\cdot$, $CHF_2\cdot$, $CF_3\cdot$ to ethylene and tetrafluoroethylene, as listed in Table 1-2.

Table 1-2 Relative Rates of Radicals Addition to $CF_2=CF_2/CH_2=CH_2$

Radical	$k_{CF2=CF2} / k_{CH2=CH2}$ (164°C)
$CH_3\cdot$ [a]	9.5
$CH_2F\cdot$ [b]	3.4
$CHF_2\cdot$ [b]	1.1
$CF_3\cdot$ [c]	0.1

a. ref 43; b. ref 44; c. ref 45.

In general, polarity is a major factor in controlling the overall rate of addition. With the fluorine-substituents increasing on a methyl radical, the radical becomes more electrophilic and the addition to electron-deficient alkenes becomes slower. The electrophilicity of the $CF_3\cdot$ radical and its polar effect on overall addition rates were also demonstrated in a study of the relative rates of its addition to various olefins.[46] As illustrated in Table 1-3, the more electron rich the olefin, the faster the addition reaction goes.

Table 1-3 Relative Addition Rate of $CF_3\cdot$ to Olefins

Olefin	k_{rel}
Isobutene	3.7
Propylene	1.4
Ethylene	1
Tetrafluoroethylene	0.15

With few exceptions, radicals are observed to add preferentially to the less substituted end (α-position) of unsymmetrically substituted alkenes. Tedder and Walton summarized a lot of addition reactions and pointed out "the attack occurs at the α-position in most cases not because this position is activated but because the β- or substituted site is very deactivated."[16: P.701] Some examples were given in Table 1-4, and the β-position is seen to be strongly deactivated because of steric hindrance.

Table 1-4 Relative Rates ($2k_\alpha/k_e$) and Orientation Ratios (α: β) for the Addition of $CH_3\cdot$, $CF_3\cdot$, and $CCl_3\cdot$ Radical to Mono-Substituted Ethenes ($\overset{\alpha}{CH_2}=\overset{\beta}{CH}\text{-}X$)

X	$CH_3\cdot$		$CF_3\cdot$		$CCl_3\cdot$	
	$2k_\alpha/k_e^*$	α: β	$2k_\alpha/k_e^*$	α: β	$2k_\alpha/k_e^*$	α: β
H	1	1:1	1	1:1	1	1:1
CH_3	0.7	1:0.15	2.3	1:0.1	4	1:0.07
F	0.9	1:0.20	0.48	1:0.09	0.7	1:0.08
CF_3	0.9	1:0.33	0.40	1:>0.02	0.9	1:>0.01

* k_e is the addition rate to ethylene.

The size of the attacking radical can also affect the addition reaction, with the bulkier the radical, the slower the reaction.

There is not a single factor that determines the outcome of radical addition reactions. Instead it is the combination of polar, steric, bond strength, and stereoelectronic factors.[47] Polarity can have a major effect on the overall rate of addition. It also influences the magnitude of the regioselectivity, making it larger or smaller depending on the relative electronegativity of the radical and the substituents on the alkene. The regioselectivity of addition to polysubstituted alkenes is primarily controlled by the degree of steric compression associated with forming the new bond, and factors which favor bond formation facilitate addition reaction.

Radical addition reactions can be described in terms of frontier molecular orbital theory (FMO)[48] because they have early transition states and the activation energies are dominated by polar effects.[49-51] The interaction of the highest occupied molecular orbital (HOMO) of one reactant and the lowest unoccupied molecular orbital (LUMO) of the other determines the reaction rate. The smaller the energy difference between them, the faster the reaction goes.[52, 53] The frontier orbital of a radical is that bearing the free spin, the singly occupied molecular orbital (SOMO). During the addition reaction, The SOMO of a radical will interact with both the π^* antibonding orbital (the LUMO) and the π-orbital (the HOMO) of the alkene. Both the SOMO-HOMO and the SOMO-LUMO interactions lead to energy drop (Scheme 1-2).

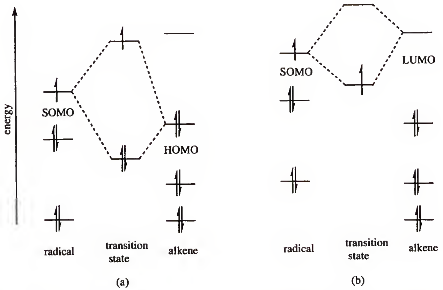

Scheme 1-2 FMO diagram of radical addition to a double bond. (a) SOMO-HOMO interaction; (b) SOMO-LUMO interaction

The dominant interaction and the reaction rates depend on the relative energies of these orbitals. Nucleophilic radicals have high energy SOMO, and the SOMO-LUMO interaction is the most important interaction. With electrophilic radicals, the SOMO energy may be low enough for the SOMO-HOMO interaction to be dominant.

Hydrogen Atom Abstraction Reactions

Atom or radical transfer reactions generally proceed via a S_H2 mechanism. Usually the atom that is transferred is a hydrogen atom or a halogen atom. When it is a hydrogen atom, the reaction is also known as hydrogen atom abstraction. Atom transfer reactions have been the subject of a number of significant reviews. [54, 39, 17, 55] This chapter will be limited to hydrogen atom abstraction from aliphatic substrates and the factors influencing the rate.

The activation parameters and bond dissociation energies (BDE) of the products of hydrogen abstraction from methane by radicals are provided in Table 1-5.[17] The pre-exponential term (A-factor) varies very little for different radicals abstracting hydrogen atom from methane.

Table 1-5 The Activation Parameters for Hydrogen Abstraction from Methane

Radical	logA	Ea / kcal mol^{-1}	BDE / kcal mol^{-1}
$CH_3\cdot$	8.8	14.3	104
$CF_3\cdot$	9.2	11.5	106
$CH_3O\cdot$	8.8	11.0	104
$C_2H_5\cdot$	8.7	17.7	98
$(CH_3)_2CH\cdot$	8.7	19.6	94.5
$(CH_3)_3C\cdot$	8.9	21.0	92

Table 1-6 gives the logA, activation energies, and the rate constants for hydrogen abstraction by methyl radical from different sites in branched chain alkanes. The A factor also varies very slightly. The change in rate by a factor of 500 is entirely attributable to the decrease in activation energy. The factors that control the activation energy of hydrogen abstraction reactions will determine the reaction rates and these will be discussed in the following context.

Table 1-6 The Activation Parameters for Hydrogen Abstraction from Branched Alkanes by Methyl Radical

Alkane	logA	Ea / kcal mol^{-1}	k_H / M^{-1}s^{-1}
$C\underline{H}_4$	8.76	14.23	44.7
$CH_3C\underline{H}_3$	8.83	11.83	912
$CH_3C\underline{H}_2CH_3$	8.82	10.13	5623
$(CH_3)_3C\underline{H}$	8.38	8.03	22909

The first factor that affects the hydrogen abstraction reaction is the strength of bonds being broken and formed. Evans and Polanyi[56] recognized this and suggested the following relationship (the Evans-Polanyi equation, eq. 1-1) between the activation energy for the hydrogen atom abstraction (Ea) and the difference between BDE for the bonds being formed and broken (ΔH°).

$$Ea = \alpha\, \Delta H° + \beta \qquad \text{(eq.1-1)}$$

If it is the abstraction by a given radical, the strength of the bond being formed is a constant, and there should be a straight line relationship between the activation energy and the strength of the bond being broken [D(R-H)] (eq. 1-2).

$$Ea = \alpha' \, [D(R\text{-}H)] + \beta' \qquad \text{(eq. 1-2)}$$

In the absence of severe steric constraints, straight line correlations between the relative reactivity of substrates towards a given radical can be found for systems (a) where there is little polarity in the transition state, or (b) when the transition states are of like polarity.[47]

A good correlation between the activation energy (Ea) of hydrogen abstraction by methyl radical from hydrocarbon C-H bonds and the bond dissociation energies (BDE) was summarized by Trotman-Dickenson (Table 1-7 and Figure 1-1).[57]

Table 1-7 Activation Energy of H-Abstraction from C-H bonds by Methyl Radical and BDE of C-H Bonds

Substrate	Ea / kcal mol^{-1}	BDE / kcal mol^{-1}
CH_3-H	14.5	103.8
CH_3CH_2-H	11.9	98.0
$(CH_3)_2C$-H	10.3	94.5
$CH_3CH_2(CH_3)C$-H	9.7	94.6
$(CH_3)_3C$-H	8.2	91.0

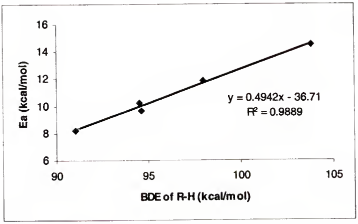

Figure 1-1 Evans-Polanyi Relationship of H-abstraction by $\cdot CH_3$ radical from Hydrocarbon C-H bonds: Plot of Activation Energy (Ea) vs. BDE of C-H Bonds

The second factor is the polar effect. Polar effects can play an extremely important role in determining the overall reactivity and specificity of hydrogen abstraction reactions. Theoretical studies on atom abstraction reactions support this view by showing that the transition state has a degree of charge separation.[58, 59]

The traditional way to determine to what extent polarity has an effect on the reaction is a linear free energy study. As shown in Table 1-1, good correlation was established for hydrogen abstraction reactions of different radicals from various substituted toluenes. Methyl radical was usually considered to be a nucleophilic radical, but it has a slightly negative ρ value. Other alkyl radicals have positive ρ values, and they are all nucleophilic radicals. The haloalkyl radicals, oxygen-centered radicals, and nitrogen-centered radicals all have negative ρ values, and they are electrophilic radicals.

There is a very good example to demonstrate the polar effect in hydrogen abstraction reaction from C-H bonds. Table 1-8 provides the relative hydrogen abstraction rates from ethane and acetone by $CH_3\cdot$ and $CF_3\cdot$ radicals in gas phase.[60] The rates of ethane were used as standard for each radical.

Table 1-8 Relative Hydrogen abstraction Rates from C-H bonds in Gas Phase

Substrate	BDE / kcal mol^{-1}	k_{real} at 164°C	
		$CH_3\cdot$	$CF_3\cdot$
CH_3CH_2-H	98	1	1
CH_3COCH_2-H	92	2.1	0.5

Ethane and acetone have opposite reactivity orders towards hydrogen abstraction by methyl and trifluoromethyl radicals. Acetone provides hydrogen to methyl radical 2 times faster than ethane does, while hydrogen abstraction by trifluoromethyl radical from acetone is 2 times slower than from ethane.

The electrophilic $CF_3\cdot$ radical prefers to form a polar transition state with electron-rich ethane (Figure 1-2 a), but the C=O in acetone opposes the polarity of trifluoromethyl group (Figure 1-2 b). In contrast, the polarity of $CH_3\cdot$ radical matches with the C=O of acetone, which makes the acetone 2 times more reactive than ethane towards $CH_3\cdot$ radical (Figure 1-2 c).

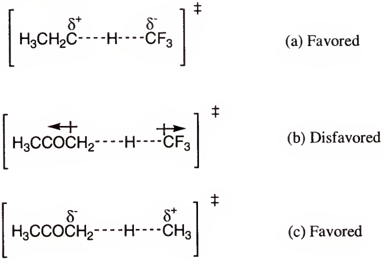

$$\left[\mathrm{H_3CH_2\overset{\delta^+}{C}\text{----}H\text{----}\overset{\delta^-}{C}F_3}\right]^{\ddagger}$$

(a) Favored

$$\left[\mathrm{H_3CC\overset{\leftarrow\!+}{O}CH_2\text{----}H\text{----}\overset{+\!\rightarrow}{C}F_3}\right]^{\ddagger}$$

(b) Disfavored

$$\left[\mathrm{H_3CC\overset{\delta^-}{O}CH_2\text{----}H\text{----}\overset{\delta^+}{C}H_3}\right]^{\ddagger}$$

(c) Favored

Figure 1-2 The Polar Transition States of H-abstraction by $CF_3\cdot$ and $CH_3\cdot$ radicals from Ethane and Acetone

Hydrogen abstraction reactions are also affected by steric factors.[17, 47, 54] Steric factors include changing steric compression due to rehybridization in the transition state, steric hindrance of the approach of the attacking radical to the hydrogen in the substrate, and steric inhibition of resonance which prevents the incipient radical from being stabilized by electron delocalization. Generally the steric compression change during the reaction is very important. The attacking radical turns to sp^3 from sp^2 hybridization as the substituents are brought closer. Steric compression is released on the site where hydrogen is abstracted. Rüchardt even attributed the decreasing order of C-H BDE in primary, secondary, and tertiary alkanes to increasing release of steric strain.[61]

Stereoelectronic effect has also been noticed to play a role in hydrogen abstraction reactions, especially in intramolecular processes.[47]

Kinetic Methods to Determine the Rate of Radical Reactions

The rate constants of radical reactions can be obtained by direct measurement to give absolute numbers, or indirect competition methods to provide relative ratios of rates.

Direct kinetic methods-time-resolved techniques. The rate of a reaction is the rate of reactant consumption and the product formation, and it is expressed as change of reactant and product concentrations versus time. In the discussion of the radical reaction rates, one's goal is to measure the rate of radical concentration decrease or of the product concentration increase. Although it is impossible to analyze the real concentration of most radicals because of their high reactivities and instabilities, spectroscopic methods can be used to monitor radicals and can provide information of the radical concentration.

There are many different time-resolved techniques available now to measure absolute rate constants of elementary radical reactions.[18] Three of them have been widely used:

1. Rotating sector method: [62, 63] The reaction is followed by measuring the heat evolved in the exothermic chain process.

2. Kinetic electron paramagnetic resonance (EPR) and electron spin resonance (ESR) spectroscopy:[64, 65, 14] The decay of the radical is monitored by its EPR or ESR spectroscopy in a period of time after the radical is generated.

3. Kinetic absorption spectroscopy:[66] the rate of the radical reaction is obtained by monitoring the growth rate of product concentration via its absorption spectroscopy, e.g., time-resolved (TRIR) infrared, time-resolved unltraviolet (TRUV), and time-resolved visible (TRVis) spectroscopies.[67]

As stated by Ingold,[18] these three techniques are complementary, not competitive. It is the reaction type, condition, and time scale that decide which method to use. The last one was employed to conduct the study in this report, and it will be discussed in more detail.

Kinetic absorption spectroscopy is also known as time-resolved laser flash photolysis method (LFP). With the rapid development of the instruments, nanosecond and picosecond LFP experiments are used extensively on the absolute rate measurements for many reactions.[38, 66, 68-70]

The apparatus and experimental process have been well demonstrated by Kazanis et al.[71] Radicals are generated from suitable precursors by laser pulse with appropriate wavelength. The radical precursors could be alkyl iodide, alkyl peroxide, diacyl peroxide, Barton esters, etc.

The radicals generated then undergo further transformations, commonly bimolecular reactions or unimolecular cyclizations, to provide new species that have distinguishable absorption spectroscopy. Bimolecular addition to a styrene type compound[70] or intramolecular cyclization[72] with aryl group at the end of double bond has been generally utilized because of the characteristic UV-Vis. spectroscopy of the so generated benzylic radicals (shown in Scheme 1-3). The growth rate of the benzylic radical could be scrutinized within an appropriate period of time. The absolute rate constants of the radical reactions could be obtained from that.

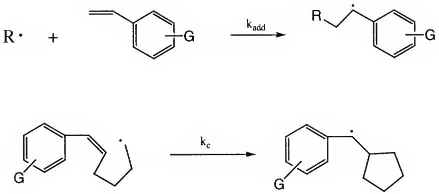

Scheme 1-3 LFP Study to Determine the Absolute Radical Addition and Cyclization Rate Constants

Indirect method-competition kinetic technique. The competition kinetic method has been used for a long time; and it remains a very useful method [15] because a lot of reaction rate constants can not be obtained by those direct measuring methods due to the unsuitable reaction conditions, spectropically undetectable radical species, or lack of instruments.

Once the radicals are generated, there are two competing pathways for them to follow, one with a known rate constant and the other whose rate constant is to be determined. After the reaction, product analysis by chromatography or a spectroscopic technique can provide the ratio of the two rate constants. In principle, any competing reactions can be employed, but practically one prefers a situation where a bimolecular reaction competes with a unimolecular reaction or another bimolecular reaction.

The radical hydrogen abstraction reaction rate constants can therefore be determined by competition with addition reactions, whose rates can be obtained by LFP. Scheme 1-4 illustrates the competition between radical hydrogen abstraction and addition reactions. The radical is generated in the presence of a styrene and a H-donor. It adds to the styrene to form a benzylic radical, which abstracts hydrogen from the hydrogen donor to give the final addition product. In the same reaction mixture, the radical abstracts hydrogen from H-donor and forms the reduced product. Both reactions are second order, but the amounts of styrene and H-donor are in much excess (at least ten times than the amount of R-I) and they become pseudo-first order reactions. Equation 1-3 applies to give the ratio of the two rate constants, which is the slope of the plot of two product ratios versus various ratios of the two reagents, provided that the addition reaction is not reversible.

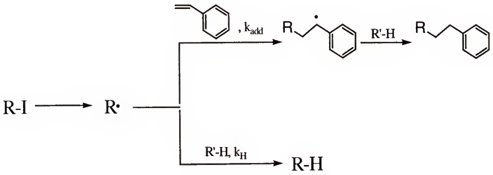

Scheme 1-4 Competition Between H-Abstraction and Addition Reactions

$$\frac{[\text{Addition Product}]}{[\text{Reduced Product}]} = \frac{k_{add}\,[\text{Styrene}]}{k_H\,[\text{R-H}]} \qquad \text{(eq. 1-3)}$$

Reactivities of Fluorinated Radicals in Organic Solvents

The commercial interest in compounds containing carbon-fluorine bonds has increased dramatically, mainly owing to work on biologically active fluororganics-particularly agrochemicals, the relentless search for the new markets for fluoropolymers and fluorocarbon fluids, developments in the fields of medical diagnostics, and the drive to find replacements for ozone-depleting CFCs and halon fire-extinguishing agents.[73] Among all the methods to prepare fluorinated compounds, the addition of fluorinated radicals onto double or triple bonds has been studied extensively.[74-79] The fluoroalkyl radicals can be generated thermally, photochemically, by radical initiation, and electron transfer processes. Fluorinated radicals are also the key intermediates in free radical chain polymerization of fluoroolefins, which comprised perhaps the most effective pathway for the preparation of this diverse and commercially very important class of polymers.[80-82]

It is theoretically and practically necessary to study the structure, reactivity, and chemistry of fluoroalkyl radicals. The kinetics of small fluorinated and hydrocarbon radicals in gas phase were investigated thoroughly in the 60s and 70s. Some reaction rates were provided in Table 1-2, 1-3, and 1-8, and from these data it can be concluded that the more fluorine substitution on the methyl radical, the more electrophilic the radical is, such radical thus reacting faster with electron rich substrates.

In the early 90's Dolbier and Ingold group began a program to measure the absolute kinetics of prototypical fluoroalkyl radical reactions in solution by a combination of laser flash photolysis (LFP), product analyses, and conventional competitive kinetics.[70] Kinetic studies of fluorinated radicals have been conducted with three types of reactions with fundamental importance to free radical chemistry: the addition reactions to π-bond,[38, 83] intramolecular cyclization reactions,[84, 85] and H-abstraction reactions from stannane, silanes, thiols, and C-H bonds in various functionalized organic compounds.[86-88]

Structure of Fluorinated Radicals

Fluorine substituents have dramatic impact upon the structure of alkyl radicals.[89] The methyl radical itself is planar. Fluoromethyl radicals, on the other hand, are increasingly pyramidal, with the trifluoromethyl radical being essentially tetrahedral with a significant barrier to inversion.

Such a strong influence of fluorine substituents on the geometry of a radical can be understood largely in terms of the effect of the σ inductive influence of the fluorine substituent on the thermodynamics of bonding. There is a thermodynamic advantage for the carbon orbitals used in bonding to fluorine to be relatively high in p character, as they would be in an increasingly bent radical. In such a case, the orbital containing the unpaired electron in a fluoromethyl radical would have increasing s character as the number of fluorines is increased.

Nonconjugated carbon radicals bearing at least two fluorine substituents are strongly pyramidal, σ-radicals, while β-fluorine substituents appear to have little influence on the geometry of a radical. The strong σ character of CF_3, CHF_2, and perfluoro-n-alkyl radicals has a considerable influence on their reactivity.

Addition Reactions

The absolute rate constants of alkene addition reactions of $C_2F_5\cdot$, n-$C_3F_7\cdot$, and n-$C_7F_{15}\cdot$ radicals in $CFCl_2CF_2Cl$ (F113) were obtained by laser flash photolysis and competition experiments.[70, 38] As shown in Table 1-9 (entry 1-4), these perfluoroalkyl radicals are much more reactive than their hydrocarbon counterparts toward electron rich alkenes.

The pyramidal geometry of the perfluoroalkyl radicals and the stronger (ca. 11kcal/mol) C-C bond formed when $R_f\cdot$ vs $R\cdot$ adds to an alkene are all relevant to their high reactivity. But radical additions to double bonds involve early transition states, and therefore the overall enthalpies of reaction should be relatively unimportant.[90] This must be true because when reacting with electron deficient alkene (entry 5 in Table 1-9) fluorinated alkyl radicals have almost the same rate as alkyl radicals.

Table 1-9 Absolute Rate Constants for the Reactions of Perfluoro-n-alkyl Radicals with Various Unsaturated Substrates at 298 ± 2 K, as Measured by FLP in F113.[38]

Entry	Substrate	k_{add} / 10^6 $M^{-1}s^{-1}$			k_{add} / 10^6 $M^{-1}s^{-1}$	
		$n\text{-}C_3F_7\cdot$	$n\text{-}C_7F_{15}\cdot$	$C_2F_5\cdot$	$RCH_2CH_2\cdot$	$(CH_3)_3C\cdot$
1	β-methylstyrene	3.8 ± 0.2	3.7 ± 0.2	7.0 ± 0.8		
2	α-methylstyrene	78 ± 8	89 ± 1	94 ± 16	0.059	
3	styrene	43 ± 1	46 ± 6		0.12	0.132
4	1-hexene	6.2 ± 0.2	7.9 ± 0.7	16 ± 1	2.0×10^{-4}	
5	CH_2=CHCN	2.2 ± 0.1	1.6 ± 0.3	3.2 ± 0.3		2.4

The electrophilicities of perfluoroalkyl radicals are probably the dominant factors for their high reactivities towards electron-rich alkenes. As stated earlier in this chapter, FMO theory is very useful to describe radical reactions. In the reaction of electrophilic perfluoroalkyl radicals with alkenes, the main interaction should be the SOMO-HOMO interaction. The higher the HOMO energy of the alkene, the smaller the energy difference between the two orbitals, the easier the reaction takes place. The energy of HOMO orbital of alkenes could be reflected by their ionization potentials (IP). A good correlation of log k_{add} for these three perfluoroalkyl radicals with terminal alkene IPs was obtained (<r> = 0.97).[38] This does indicate the interaction of the SOMO of electrophilic perfluoro-n-alkyl radicals with the HOMO of the alkenes, and that polar effects are therefore important in determining the rates of the addition reactions.

Linear free energy relationships are traditionally used to investigate how sensitive a reaction is to polar effects. A Hammett study of addition reactions to a series of para-substituted styrenes by n-$C_8F_{17}\cdot$ was carried out in C_6D_6.[38] The rate constants were summarized in Table 1-10. The log of the rate constants correlated extremely well with Hammett σ value, with <r> = 0.99. The ρ value is negative (–0.53), as would be expected for an electrophilic reactant.

Table 1-10 Absolute Rate Constants for the Reactions of n-$C_8F_{17}\cdot$ Radical with Para-Substituted Styrenes at 298 ± 2 K, as Measured by Competition Kinetic Method with nBu_3SnH in C_6D_6.

Substrate	$k_{add}/\ 10^7\ M^{-1}s^{-1}$	σ
4-methoxystyrene	6.5	-0.28
4-methylstyrene	6.1	-0.14
Styrene	4.6	0
4-chlorostyrene	3.6	0.24
4-(trifluoromethyl)styrene	2.5	0.54

These results imply that the dominant factor giving rise to the high reactivities of perfluoro-n-alkyl radicals in their additions to alkenes, particularly to electron-rich alkenes, is the high electrophilicities of these very electron-deficient radicals. That is, charge transfer interactions (Figure 1-3) stabilize an early transition state and lower both the enthalpic and entropic barriers to reaction, and, consequently, the reaction rate is increased.[90]

$$\left[\overset{\delta^-}{\text{n-R}_f\cdot}\ \text{----------}\ \overset{\delta^+}{\text{Alkene}}\right]^{\ddagger}$$

Figure 1-3 Polar Transition State of $R_f\cdot$ Radical Addition to Alkene

It was also noticed that $C_2F_5\cdot$ was a little bit more reactive than n-$C_3F_7\cdot$ (shown in Table 1-8), while there is little or no difference in the rates of addition of n-$C_3F_7\cdot$, n-$C_7F_{15}\cdot$, and n-$C_8F_{17}\cdot$ to alkenes. Thus it seems likely that the reactivities of all homologous perfluoro-n-alkyl radicals can be defined by the reactivities of the n-$C_3F_7\cdot$, n-$C_7F_{15}\cdot$, and n-$C_8F_{17}\cdot$ radicals.[38]

The reactivity of perfluoro-n-alkyl radicals with fluorinated alkenes, $R_fCH_2CH=CH_2$ and $R_fCH=CH_2$, provides more evidence of the importance of polar effect in the addition reactions.[83] By using the competition kinetic methodology, the addition rate constants of $C_4F_9\cdot$ radical to $C_4F_9CH_2CH=CH_2$ and $C_4F_9CH=CH_2$ were determined in trifluoromethylbenzene and 1,3-bis-(trifluoromethyl)benzene, respectively. As shown in Table 1-11, direct attachment of perfluoroalkyl group to a π-bond significantly decreases its reactivity towards addition by a perfluoro-n-alkyl radical. The large inductive electron-withdrawing effect of the perfluoroalkyl group lowers the nucleophilicity of the hydrocarbon alkene; therefore the electrophilic perfluoro-n-alkyl radical adds much slower to this alkene. When the C_4F_9 group is placed at the allylic position of the alkene, the addition rate is ~7 times smaller than that for 1-hexene by $C_4F_9\cdot$ radical.

Table 1-11 Absolute Rate Constants for the Reactions of n-$C_4F_9\cdot$ Radical with Fluorinated and Unfluorinated 1-Alkene, Measured by Competition Kinetic Method with Et_3SiH

Substrate	$k_{add}/\ 10^6\ M^{-1}s^{-1}$	k_{rel}
1-hexene	7.9 (± 0.7)	30
$C_4F_9CH_2CH=CH_2$	1.15 (±0.11)	4.4
$C_4F_9CH=CH_2$	0.26 (±0.02)	1

Hydrogen Atom Abstraction Reactions from Sn-H, Si-H, and S-H bonds

LFP data of the addition reactions was used in conjunction with a series of bimolecular competition experiments in C_6D_6 to determine absolute rate constants for some hydrogen atom transfer reactions of the n-$C_7F_{15}\cdot$ radical with nBu_3SnH, substituted silanes and thiophenol.[38, 83, 86] The absolute rate constants were summarized in Table 1-12 and compared with those of n-alkyl radicals.

Table 1-12 Rate Constants for Hydrogen Atom Abstraction at 303K

Radical	$k_H/ 10^6 M^{-1}s^{-1}$				
	nBu_3SnH	$(TMS)_3SiH$	$(TMS)_2SiMeH$	Et_3SiH	PhSH
n-$C_7F_{15}\cdot$	203 (±14)	51 (±5)	16.3 (±1.5)	0.50 (±0.04)	0.28 (±0.03)
R-$CH_2\cdot$	2.7	0.46	0.037	0.00085	150

The rate of hydrogen atom transfer to n-$C_7F_{15}\cdot$ from nBu_3SnH was ~75 times faster than that to n-alkyl radicals at 30°C in C_6D_6. $(TMS)_3SiH$ was ~110 times more reactive with n-$C_7F_{15}\cdot$ than with n-alkyl radical, and $(TMS)_2SiMeH$ was ~440 times more reactive with n-$C_7F_{15}\cdot$ than with n-alkyl radical at 30°C in C_6D_6. The least reactive reducing agent Et_3SiH showed the largest difference in reactivity for $R_f\cdot$ and R·. It transfers hydrogen atom 588 times more rapidly, respectively, to perfluoro-n-alkyl radicals than to the analogous hydrocarbon radicals!

The BDE of R_f-H is ca. 9 kcal/mol more than that of the R-H,[91] so the greater exothermicity of the hydrogen atom transfer to $R_f\cdot$ is one of the factors counting for their high reactivity. At this point, special attention has to be paid to the reducing ability of PhS-H towards R_fI. Benzenethiol is a very efficient hydrogen atom donor to hydrocarbon radicals, but it transfers hydrogen to $R_f\cdot$ radicals 536 times slower than to hydrocarbon radicals. This indicates that there must be other factors besides exothermicity controlling the hydrogen abstraction reactions of fluorinated and hydrocarbon radicals. The stannane and silanes are all electropositive hydrogen donors; the polarity of transition state is favored when they react with electrophilic $R_f\cdot$ radicals (Figure 1-4). While the PhS-H is electronegative hydrogen donor, its reaction with nucleophilic alkyl radicals is faster than with electrophilic $R_f\cdot$ radicals. This result shows that transition state polar effects must also play a significant role in such hydrogen atom transfer reactions.

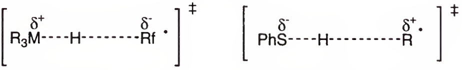

$$\left[\overset{\delta^+}{R_3M}\text{----}H\text{--------}\overset{\delta^-}{Rf}\ \cdot\right]^{\ddagger} \qquad \left[\overset{\delta^-}{PhS}\text{----}H\text{----------}\overset{\delta^+\cdot}{R}\right]^{\ddagger}$$

(a) Fluorinated radical favored (c) Alkyl radical favored

Figure 1-4 Polar Transition State of Hydrogen Abstraction Reactions

The abstraction of hydrogen from arene thiols by perfluoro-n-alkyl radicals is a very exothermic process [for: $R_f\cdot + PhSH \rightarrow Rf\text{-}H + PhS\cdot$, $\Delta H = -24$ kcal/mol],[92] and the activation energy for this reaction must be very low (i.e., ≤ 3 kcal/mol).[15] With such an energy profile, the reaction should have a reactant-like transition state, with little bond-breaking and little transfer of radical character to the thiyl site. It is for such transition states that FMO interactions and polarization effects would be expected to play their most important role. In order to provide corroboration for the role of polar effects in such reactions, a Hammett study was carried out for the reduction of $n\text{-}C_7F_{15}I$ by a series of arene thiols.[93] As shown in Table1-13, there's a definite relationship between the rates of hydrogen transfer and the "electron-richness" or "-poorness" of the arene thiol.

Table1-13 Absolute Rate Constants for Hydrogen Atom Abstraction from Arene thiols at 303K in C_6D_6, Measured by Competition kinetic Method with 1-Hexene

Aryl Substituent	k_H / 10^5 $M^{-1}s^{-1}$	σ^+
p-OCH_3	9.9 (±0.9)	-0.78
p-CH_3	6.6 (±0.6)	-0.31
H	3.3 (±0.3)	0
m-OCH_3	3.0 (±0.3)	+0.12
p-CF_3	1.8 (±0.2)	+0.61

The best correlation was obtained when $\log k_H$ was plotted versus σ^+, and a negative ρ^+ value of –0.56 (<r> = 0.986) was consistent with the electrophilic character of the $R_f\cdot$ radical.

Hydrogen Atom Abstraction Reactions from C-H Bonds

Not only the hydrogen atom abstraction reactions were accelerated for the reaction between perfluoro-n-alkyl radicals and electropositive reducing reagents, e.g. stannanes and silanes; but also $R_f\cdot$ radicals abstract hydrogens more rapidly than their hydrocarbon counterparts from C-H bonds of some organic compounds. While C-H bonds are commonly considered inert to alkyl radicals, in fact, fluorinated radicals can abstract hydrogen from active C-H bonds fast enough that it can be used as a key propagation step in the chain reactions of fluoroolefins with alcohols, diols, and oxolanes, equation 1-4 giving an example.[94, 95]

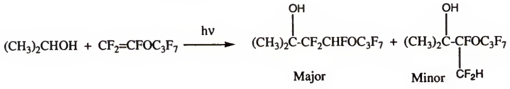

$$(CH_3)_2CHOH + CF_2{=}CFOC_3F_7 \xrightarrow{h\nu} \underset{\text{Major}}{(CH_3)_2\overset{OH}{C}\text{-}CF_2CHFOC_3F_7} + \underset{\text{Minor}}{(CH_3)_2\overset{OH}{C}\text{-}\underset{CF_2H}{C}FOC_3F_7}$$

(eq. 1-4)

Although fluorinated radicals abstract hydrogen from active C-H bonds fairly rapidly, these reactions are still slower than the reactions of fluorinated radicals with nBu_3SnH and silanes. Rate constants of H-abstraction reactions by $R_f\cdot$ radicals from nBu_3SnH and silanes are in the range of $5 \times 10^5 \sim 2 \times 10^8$ $M^{-1}s^{-1}$ in non-polar organic solvents.

To obtain the rate constants of these relatively slow reactions, $t\text{-}BuSiMe_2D$ was used as the deuterium donor in a bimolecular competition with C-H transfer from the substrates.[87] $t\text{-}BuSiMe_2D$ reduces $R_f\cdot$ radicals at a relatively slow rate ($k_D = 1.49 \times 10^5$ $M^{-1}s^{-1}$) in 1,3-bistrifluoromethyl benzene (1,3-BTB),[96] and the hydrogens on the side chains are unreactive towards $R_f\cdot$ radicals.

The absolute rate constants for bimolecular hydrogen abstraction from a variety of organic substrates in solution have been obtained for the $n\text{-}C_4H_9CF_2CF_2\cdot$, $n\text{-}C_4F_9\cdot$, and $i\text{-}C_3F_7\cdot$ radicals. The molecules chosen for study were alkanes, aromatic hydrocarbons, haloalkanes, ethers, thioether, alcohols, and esters. A wide range of substrate reactivities was observed (5200-fold), with 1,2-dichloroethane being the slowest, and tetrahydrothiophene being the fastest one measured. Some examples of the hydrogen abstraction rate constants from different types of organic substrates by $n\text{-}C_4F_9\cdot$ are given in Table 1-14.

The rate constants for hydrogen abstraction from each position of n-heptane and 1-chlorohexane (as shown in Tables 1-15 and 1-16) were derived from their overall rate constants and the known regiochemistry of free radical iodination.[97]

Table 1-14 Absolute Rate Constants for Hydrogen Atom Abstraction from Organic Substrates at 298±2 K in 1,3-BTB, Measured by Competition Kinetic Method with t-$BuSiMe_2D$

Substrate	k_H overall / 10^2 $M^{-1}s^{-1}$	Substrate	k_H overall / 10^2 $M^{-1}s^{-1}$
$ClCH_2CH_2Cl$	0.6 (±0.25)	THP	70 (±15)
$C_6H_{13}Cl$	21 (±6)	$CH_3OCH_2OCH_3$	19 (±5)
n-heptane	76 (±16)	$(CH_3OCH_2)_2$	67 (±14)
CH_3OH	9.2 (±1.9)	$CH_3CH_2OCH_2CH_3$	220 (±50)
$(CH_3)_2CHOH$	163 (±33)	1,3-dioxolane	140 (±29)
$(CH_3CHOH)_2$	50 (±11)	THF	310 (±61)
CH_3OCH_3	28 (±7)	Tetrahydothiophene	355 (±73)
1,3,5-trioxane	9.7 (±2.3)	Cyclohexane	93 (±20)
1,4-dioxane	31 (±7)	Cyclopentane	104 (±22)

Table 1-15 Rate Constants for Hydrogen Abstraction from Each Position of n-Heptane by n-$C_4F_9\cdot$, Derived from Overall Rate Constants and Regiochemistry of Iodination of n-Heptane

Position	1-CH_3	2-CH_2	3-CH_2	4-CH_2
k_H per H / 10^2 $M^{-1}s^{-1}$	0.52	9.7	5.8	5.6

Table 1-16 Rate Constants for Hydrogen Abstraction from Each Position of 1-Chlorohexane by n-$C_4F_9\cdot$, Derived from Overall Rate Constants and Regiochemistry of Iodination of 1-Chlorohexane

Position	1-CH_2Cl	2-CH_2	3-CH_2	4-CH_2	5-CH_2	6-CH_3
k_H per H / 10^2 $M^{-1}s^{-1}$	0.22	0.37	1.3	2.8	5.3	0.4

The C_2 hydrogens of n-heptane are seen to be ~19 times more reactive than its methyl hydrogen, a result quite consistent with the ~3 kcal/mol greater stabilization of a secondary versus a primary alkyl radical. Thermodynamic effect also counts for the 54 times greater reactivity of $(CH_3)_2CHOH$ than CH_3OH.

Transition state polar effects are still very important in this reaction. Although an α-chloro substituent is thermodynamically radical-stabilizing, the overall per hydrogen reactivity of 1-chlorohexane is 3 times less than that of n-heptane. And the rate constant for C-H abstraction from a methyl group of n-heptane is 2.4 times larger than that for the CH_2Cl carbon of 1-chlorohexane.

Moreover, none of the CH_2 or CH_3 groups of 1-chlorohexane is as reactive as the analogous site in n-heptane. Because the transition state polar effect of the chlorine substituent should not be expected to extend more than two or three C-C bonds from C-1, this result indicated that field effects were intervening in these reactions. The hydrogens of 1,2-dichloroethane are even less reactive ($k_{rel} = 0.67$) than those of the chloromethyl group of 1-chlorohexane. The chlorine substituents in 1,2-dichloroethane and 1-chlorohexane not only inductively destabilize their hydrogen abstraction transition states, but they also give rise to the destabilizing electrostatic field interactions with the fluorine substituents of the perfluoroalkyl radicals within their abstraction transition states.

A study of regiochemistry study showed that the α-CH_2 hydrogens of ether and THF have reactivities (per H) of 7 and 9, relative to those of cyclohexane. Likewise, the C-H bonds of methanol and dimethyl ether are 6 and 9 times more reactive, respectively, than those of n-heptane's methyl groups. Such rate factors are generally consistent with the smaller bond dissociation energy (BDE) of such bonds.

Although a single ether function clearly activates its α-hydrogens with respect to abstraction, two or more ether functions in the same molecule give rise to a decrease in reactivity, for example, the reactivity decreases from THP to 1,4-dioxane to 1,3,5-trioxane. Similarly, the C-2 hydrogens of THF are 1.7 times more reactive (per H) than those of 1,3-dioxolane. Not only the BDE differences make the reactivities different, but polar, and especially field effects, also play an important role.

The study of the hydrogen atom abstraction reactions from different functionalized C-H bonds by fluoro-alkyl radicals in 1,3-BTB implies that this reaction is affected by a combination of thermodynamic, polar, steric, stereoelectronic, and field effects.

Reactivities of Perfluoro-n-alkyl radicals

The great electrophilicity of perfluoro-n-alkyl radicals has been demonstrated in its addition reactions to alkenes and hydrogen atom transfer from stannane, silanes, arene thiols, and C-H bonds of organic compounds. The reactivities of $R_f\cdot$ radicals were much greater than these of their hydrocarbon counterparts when they reacted with electron-rich substrates. But the reactions were rather slow if the electronic matchup was not good.

The same factors, which influence the reactivities of other carbon-centered radicals, also affect the reaction of perfluoro-n-alkyl radicals. The pyramidal geometry of the σ- $R_f\cdot$ radicals makes them more reactive than the planar π-alkyl radicals. Because of the stronger R_f-C and R_f-H bonds formed in the addition reactions and hydrogen abstraction reactions, the exothermicity of the $R_f\cdot$ reaction also has an advantage over the hydrocarbon radical reactions.

But the enthalpic factor couldn't be very important for these reactions since they all have early transition states. Therefore the transition state polar effect plays an extremely important role for the reactions of perfluoro-n-alkyl radicals.

Solvent Effects on Free Radical Reactions

It is a commonly held misconception that the reactions of neutral free radicals are insensitive to the effect of solvent.[98] Although it is true that in general the rate and selectivity of radical reactions are only nominally influenced by solvent in comparison to reactions of polar species (i.e., nucleophilic and electrophilic), there are several examples in the free radical literature where solvent profoundly affects the outcome of a process. There are several possible ways solvent can affect the reactions of free radicals: solvent polarity, internal pressure, solvent viscosity, and the formation of a new complex through the interaction of the radical and the solvent.

Solvent Polar Effects on Free Radical Reactions

Solvent polarity will influence the rate of a chemical reaction if the dipole moment of the reactants and transition state are different. Although solvent polarity effects have been studied more thoroughly for polar processes, they have also been observed in some free radical reactions.

In the reaction of free radical chlorination of alkanes with t-butyl hypochlorite (t-BuOCl), the propagating t-butoxyl radical has two pathways: hydrogen atom abstraction from the alkane to continue the chain process, and/or β-scission to yield acetone and a methyl radical (as shown in Scheme 1-5).

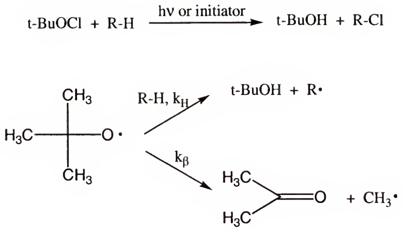

Scheme 1-5 Reaction of t-BuOCl with Alkane

Walling and Wagner studied the effect of solvent on the partitioning of t-BuO· radical between hydrogen abstraction and β-scission. By GC analysis of the product mixture, the relative rate constants of two pathways could be obtained. The ratio of k_H versus k_β (k_H/ k_β) varied as a function of solvent, changed from 5.5 in F113 to 1.78 in CH_3CN to 0.7 in CH_3CO_2H (with cyclohexane as the hydrogen atom source).[99]

The authors thought that the hydrogen abstraction reaction was relatively insensitive to solvent effects, and the observed trend as ascribed to an increase in k_β. This conclusion was based on the premise that the C=O bond of the product is highly polar and much of this polarity is expected to be present in the transition state of the β-scission process. Thus, an increase in solvent polarity would cause an increase in solvent stabilization of the developing carbonyl in the transition state, resulting in an enhancement of k_β in polar solvents.

This hypothesis was verified later on by Lusztyk and his coworkers.[67] They studied the solvent effects on the β-scission and hydrogen atom abstraction reactions of cumyloxyl radical via LFP and product analysis in six solvents. As shown in Table 1-17, the absolute rate constant for hydrogen abstraction from cyclohexane by cumyloxyl radical is essentially independent of the solvent. In contrast, the absolute rate constant for β-scission of this radical varied considerably as a function of solvent polarity. The increase in k_β with the increase in solvent polarity is attributable to the increase in stabilization of the transition state for β-scission via increased solvation of the incipient acetophenone product.

The log k_β correlated with Dimroth-Reichardt $E_T(30)$ values reasonably well (<r> = 0.965). An even better correlation was obtained between log k_β and the nitrogen hyperfine splitting, α^N, for the 4-amino-2,2,6,6,-tetramethylpiperdinyl-N-oxyl radical.

Table 1-17 Absolute Rate Constants for Cumyloxyl Radical Reactions in Six Solvents at 303K, Measured by LFP

Solvent	k_H (cyclohexane as H source)/ 10^6 $M^{-1}s^{-1}$	k_β / 10^5 $M^{-1}s^{-1}$
CCl_4	1.1	2.6
C_6H_6	1.2	3.7
C_6H_5Cl	1.1	5.5
$(CH_3)_3COH$	1.3	5.8
CH_3CN	1.2	6.3
CH_3COOH	1.3	19

Because of the high electrophilicities of perfluoro-n-alkyl radicals and the importance of the transition state polar effect on their reactivities, one assumes that the reactions of n-$R_f\cdot$ could be affected by the polarities of different solvent media. Surprisingly, solvent polar effects on the reactivities of these strongly electrophilic perfluoro-alkyl radicals have received scarce attention.

Dolbier and his coworkers did notice the solvent effect for the addition reactions of $CF_3\cdot$ and n-$C_3F_7\cdot$ radicals and the results were mentioned as a footnote in one of their papers.[90] They found that the addition of perfluoro-n-alkyl radicals to alkenes was faster in CH_3CN than in F113, with this solvent effect being greater for the more electron-rich alkenes. For example, the rate acceleration in CH_3CN relative to the F113 solvent for addition to styrene by $CF_3\cdot$ and n-$C_3F_7\cdot$ is about a factor of 3, but for the addition of these two radicals to pentafluorostyrene the rate acceleration is only ca. 50%.

Until now there have been no systematic studies on the influence of solvents on the reactions of fluorinated radicals, so that a more complete profile of their reactivities could be available. The reaction rate constants of $R_f\cdot$ radicals should be obtained unambiguously in different solvents. We have initiated a program to investigate the kinetics of the addition and hydrogen atom abstraction reactions of $R_f\cdot$ radicals in water, which is, of course, a very polar solvent. With the rate constants of these reactions in non-polar organic solvents (F113, C_6D_6, and 1,3-BTB) available, it will then be possible to compare the reactivities of perfluoro-alkyl radicals in solvents with greatly different polarities.

Free Radical Reactions in Aqueous Solutions

Organic reactions in aqueous media have attracted a lot of attention since the eighties because there are specific effects produced in water.[100-102] Water can stabilize a polar transition state because of its high dielectric constant ($\varepsilon = 78$). Thus the well-known S_N1 solvolysis reactions are accelerated in water by strong interactions between the carbenium ions and the solvent in the transition state. The hydrophobic effect of water due to its high cohesive energy density (c.e.d.) also facilitates some non-polar reactions, for instance the Diels-Alder reaction. Furthermore, reactions in water media are considered much better than those in general organic media from an environmental point of view.

Studies on radical reactions in an aqueous solution have so far been limited. In the early nineties, Breslow[103] and Collum[104] made water-soluble tin reagents and utilized them in aqueous radical reactions. Later on, several other papers about tin-free radical reactions in water were presented,[105-107] but they only focused on the environmental advantages offered by using water as the solvent. The "powerful solvent effect of water in radical reaction", as the title of the paper suggests, was not disclosed until last year,[108] when the triethylborane-induced atom-transfer radical cyclization was found to occur in water much better than in traditional organic solvents.

Polymer chemistry is quite different from organic chemistry on this issue. Radical polymerization in aqueous solution has been extensively used in industry.[109, 110] Radical polymerization in aqueous solution allows the synthesis of high molecular weight polymers at high polymerization rates. Heat can be excellently transferred as a result of the relatively low viscosity of the continuous aqueous phase, thus giving good temperature control. Toxic and flammable organic solvents do not have to be used and the reaction can proceed to high conversion. The molecular weight can easily be controlled by the use of chain-transfer agents.

Because of the unique properties of fluorine-containing polymers, the fluoro polymer industry developed very rapidly. Radical polymerization in aqueous media is an extremely important method in this field. As a matter of fact, perfluoroalkenes can be converted to high molecular weight polymeric products only under free radical conditions.[111] For example, the homopolymerization of TFE (tetrafluoroethylene) to make PTFE can be accomplished in aqueous media by two different free radical processes. Solution polymerization is of no practical value since the physical form of the precipitated polymer makes it useless in subsequent processing operations.

Although most commercial fluoropolymers are now made by dispersion, emulsion, or suspension polymerization in aqueous media, there are still problems in this field. One of the difficulties is the chain transfer or termination reaction in the presence of many organic compounds (surfactants and initiators) that contain C-H bonds because polymerization in aqueous media normally requires dispersing or emulsifying agents. The presence of such compounds results in polymers with lower molecular weights than desired and /or a lowered yield of polymer.[112]

In order for companies to develop new, superior initiators and surfactants for polymerizations of fluoroolefins, it is necessary to have knowledge of structure-reactivity relationship with respect to C-H abstraction by fluorinated radicals in water. Until this study, there has been no thorough kinetic data on this subject.

Conclusion

This chapter discusses the addition and H-abstraction reactions of perfluoro-n-alkyl radicals in non-polar organic solvents.

The addition reactions and H-abstraction reactions from aliphatic substrates of carbon-centered alkyl radicals are reviewed first. The radical addition reactions are controlled by a combination of polar, steric, bond strength, and stereoelectronic factors. Polarity can have a major effect on the overall rate of addition.

The radical H-abstraction reactions are affected by the strength of bonds being formed and broken, polar effects, steric effects, and stereoelectronic effects. Hammett studies showed that simple alkyl radicals have nucleophilic character, while haloalkyl radicals and oxy-centered radicals have electrophilic character.

The kinetics of addition reactions of perfluoro-n-alkyl radicals to alkenes in F113 were studied by a combination of LFP experiments and competition methods. It was demonstrated that $R_f\cdot$ radicals reacted more rapidly with electron-rich alkenes than did the corresponding hydrocarbon radicals. Transition polar effects were shown to be the main reason for such rate acceleration. Other factors, such as the pyramidal geometry of the $R_f\cdot$ radicals and stronger C-C bonds formed by $R_f\cdot$ radical addition than $R\cdot$ radical addition, also help account for the higher reactivities of $R_f\cdot$ radicals.

Transition state polar effects are also the main factor controlling the H-abstraction reactions by perfluoro-n-alkyl radicals from stannane, silanes and thiols in non-polar organic solvent. The kinetic study of H-abstraction reaction by $R_f\cdot$ radicals from C-H bonds in 1,3-BTB revealed that polar effects, and field effects are all very important in such processes. Other factors such as thermodynamic, steric, and stereoelectronic effects also play a role in this reaction.

Making fluorinated polymers by radical polymerization from fluoro monomers in aqueous media is widely used in polymer industry. But the chain transfer or termination reactions by H-abstraction of the propagating fluorinated radicals from C-H bonds often give trouble to the polymerization. In the current study, the kinetics of the H-abstraction reactions by perfluoro-n-alkyl radicals are scrutinized in aqueous solution.

Solvent polar effects can affect a radical reaction that goes through a polar transition state. Since the polar effect is the dominant factor controlling the addition reactions and H-abstraction reactions of $R_f\cdot$ radicals, we are also interested in the kinetics of the perfluoro-n-alkyl radicals' addition and H-abstraction reactions in the polar aqueous media.

CHAPTER 2

ADDITION REACTIONS OF PERFLUORO-N-ALKYL RADICAL IN AQUEOUS SOLUTION

The addition reactions of perfluoro-n-alkyl radicals ($C_2F_5\cdot$, n-$C_3F_7\cdot$, n-$C_7F_{15}\cdot$, and n-$C_8F_{17}\cdot$) to alkenes in nonpolar organic solvents (F113 and C_6D_6) were studied previously. The absolute rate constants of these reactions were determined by a combination of product analyses, LFP technique, and competition kinetic methods.[70, 38] It was demonstrated that the dominant factor in the addition reactions of the $R_f\cdot$ radicals is the transition state polar effect, which controls the overall rate. The results also showed that n-$C_3F_7\cdot$, n-$C_7F_{15}\cdot$, and n-$C_8F_{17}\cdot$ radicals had essentially the same reactivity; thus their reactivities can represent the reactivities of all homologous perfluoro-n-alkyl radicals.

With the increasing interest in radical reactions in aqueous solutions and the practical advantages that one can gain when water is used as solvent, kinetic data for reactions in aqueous solution are in strong demand. We started this program to investigate the reactivities of fluorinated radicals in water.

In the current study, water-soluble substrates with appropriate structures were first synthesized. Then the absolute rate constants of addition reactions of a water-soluble perfluoro-n-alkyl radical to these substrate alkenes were measured by LFP experiments, and were compared with those obtained in organic solvents.

Synthesis of Water-Soluble Substrates

To study the reactions of perfluoro-n-alkyl radicals with alkenes in aqueous solution, one has to use substrates that have reasonable solubilities in water. Both the perfluoroalkyl-diacyl peroxides and perfluoroalkyl iodides, as well as all the styrenes and alkenes used in previous studies, are not soluble in water. Therefore new compounds were chosen for use in this study, whose structures are similar to the compounds used in the organic solvent studies, so that the results could be compared.

There are several ways to make compounds water-soluble. For instance, one can append an unreactive ionic site or polyether chains to the substrates. In this chapter, we simply affixed an ionic moiety to the compounds, because polyether chains might donate hydrogens to fluorinated radicals.

Water-Soluble Radical Precursor

Sodium 5-Iodo-3-oxaoctafluoropentanesulfonate **1** ($ICF_2CF_2OCF_2CF_2SO_3Na$) was made by hydrolysis of $ICF_2CF_2OCF_2CF_2SO_2F$ (eq. 2-1) in H_2O. Water was removed by vacuum, leaving a white solid residue as a mixture of compound **1** and NaF. Because their solubility in ethanol is so different (compound **1** is very soluble in ethanol, while NaF does not dissolve in it), they could be easily separated. Compound **1** was obtained as a white solid with a very clean ^{19}F NMR spectrum. Nevertheless, for our kinetic studies, the solid was purified further by recrystallization from water. Elemental analysis demonstrated that the obtained compound was $ICF_2CF_2OCF_2CF_2SO_3Na{\cdot}H_2O$. Compound **1** will be abbreviated as **IR$_f$SO$_3$Na** in this report. It has the UV/vis. spectrum shown in Figure 2-1.

$$ICF_2CF_2OCF_2CF_2SO_2F + 2NaOH \xrightarrow[\text{overnight, 87\%}]{H_2O,\ 90\ ^{\circ}C} \underset{\mathbf{1}}{ICF_2CF_2OCF_2CF_2SO_3Na} \quad \text{(eq. 2-1)}$$

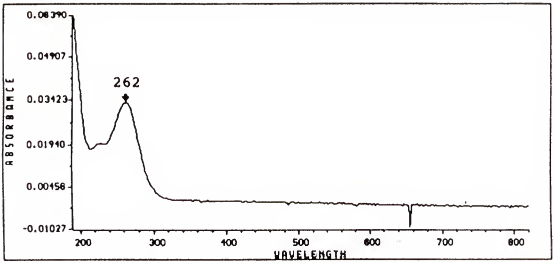

Figure 2-1 UV/Vis Spectrum of Compound IR_fSO_3Na

Synthesis of Water-Soluble Alkenes

Five water-soluble styrene type compounds and one terminal alkene (as listed in Scheme 2-1) were synthesized. The sodium carboxylate group was used to make each substrate soluble in water. The –COONa group was connected to the phenyl ring directly for compounds **2a, 2b**, and **2c**. To check if the conjugation between them has any influence on the addition reactions, we also studied the addition reaction of **2d**, in which the –COONa is separated from the phenyl ring by a methylene group.

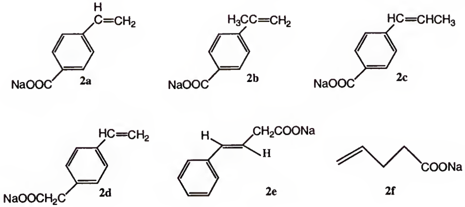

Scheme 2-1 Water-Soluble Alkenes

The p-vinylbenzoic acid is a commercially available compound, it was expected that it would be very easy to get its sodium salt. First the acid was treated with NaOH in water, but only polymer was obtained when vacuum was applied to remove water. Finally this conversion was carried out in MeOH (eq. 2-2), with phenolphthalein as the indicator.[113] MeOH could be easily removed with rotary evaporator, and any organic impurity was washed off with ether.

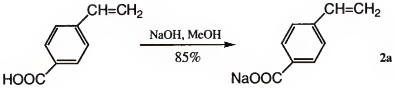

(eq. 2-2)

The 4-(α-methyl)vinylbenzoic acid was prepared from 4'-bromo-acetophenone in two steps[114] (eq. 2-3): a Wittig reaction to get 4-bromo-α-methylstyrene, and lithium-halogen exchange with n-BuLi in ether followed by carbonation with CO_2(gas). Finally the salt **2b** was made in EtOH from the acid and NaOH.

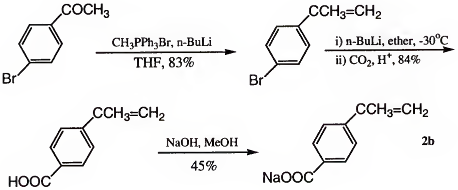

(eq. 2-3)

The β-methyl compound **2c** was prepared using almost the same method (eq. 2-4) as for **2b**, except t-BuLi was used in the second step for the lithium-halogen exchange at a lower temperature.

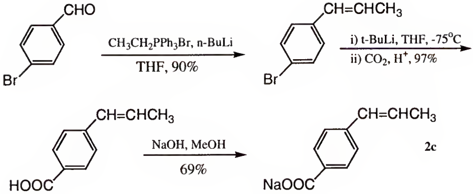

2c

(eq. 2-4)

Starting from 4-vinylbenzyl chloride, the chloride was converted to nitrile by reaction with dry potassium cyanide and dicyclohexyl-18-crown-6 in acetonitrile, and then hydrolyzed to the acid (eq. 2-5).[115] Finally it was treated with NaOH in MeOH to get **2d**.

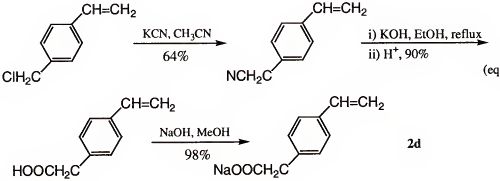

2d

(eq. 2-5)

Compound **2e** was made from the commercially available trans-styrylacetic acid (eq. 2-6) in MeOH. And 4-pentenoic acid reacted with NaOH in water to give sodium 4-pentenate (**2f**) (eq. 2-7).

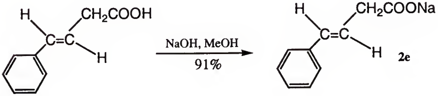

2e

(eq. 2-6)

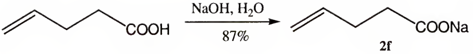

(eq. 2-7)

Laser Flash Photolysis Experiments

The absolute rate constants of $\cdot R_fSO_3Na$ addition to water soluble alkenes were measured by LFP experiments. A schematic diagram of the LFP apparatus used in this study is shown in Figure 2-2. An aqueous solution of IR_fSO_3Na and styrenes (**2a**-**2e**) was placed in a quartz cuvette (sample cell). The pulse of laser beam passed through the cuvette and irradiated IR_fSO_3Na to generate the $\cdot R_fSO_3Na$ radical. Then the UV/Vis. light, as the monitoring beam, was used to detect growth of the benzylic radicals formed by addition of $\cdot R_fSO_3Na$ to the styrene within the limited time frame.

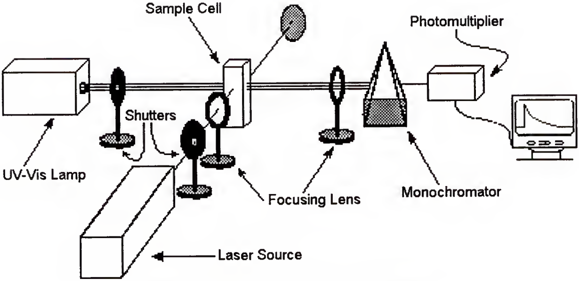

Figure 2-2 Laser Flash Photolysis Apparatus

Although IR_fSO_3Na has good UV/Vis. absorption in the range of 240nm to 300 nm wavelengths, the styrenes have very similar UV/Vis spectra in this range with stronger absorption. An example is provided in Figure 2-3, the absorption coefficient of styrene **2b** is 476 $M^{-1}cm^{-1}$ at 298nm, which is about 17 times more than that of IR_fSO_3Na.

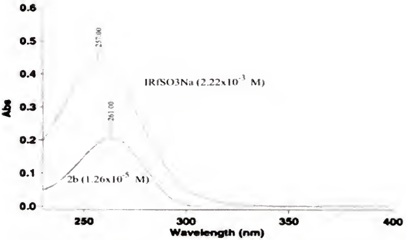

Figure 2-3 UV/Vis. Spectra of IR_fSO_3Na and Styrene **2b**

Fortunately the absorption of IR_fSO_3Na becomes comparable to that of styrene at wavelengths longer than 300nm, and the 308nm excimer laser was therefore a good candidate for photochemical generation of the desired radical. A reasonable concentration IR_fSO_3Na solution (C = 0.027M) has sufficient absorption (A = 0.36) at 308 nm to generate detectable $\cdot R_fSO_3Na$ radicals. When an appropriate amount of water-soluble styrene solution was added to the IR_fSO_3Na solution, the additional absorption derived from the added styrene was fortunately less than 0.1 at 308 nm.

Therefore the 308nm light pulses from an excimer laser could be used to generate the $\cdot R_fSO_3Na$ radical by 308nm irradiation of a solution containing IR_fSO_3Na and the water-soluble styrenes (eq. 2-8).

$$\mathbf{IR_fSO_3Na} \xrightarrow{h\nu,\ 308\ \text{nm}} \cdot\,\mathbf{R_fSO_3Na} \qquad \text{(eq. 2-8)}$$

Results from $\cdot R_fSO_3Na$ Radical Addition to Styrenes

The addition reactions of the $\cdot R_fSO_3Na$ radical to the water-soluble styrenes were monitored directly *via* observation of the pseudo-first-order growth of the absorption at 320 nm, which resulted from the formation of the benzylic radicals (eq. 2-9), as shown in

Figure 2-4. The rate constants for the global reactions of $\cdot R_fSO_3Na$ radical with the styrenes, k_{gl}, were calculated from the experimental growth curves measured over a range of substrate concentrations (eq. 2-10).

$$\bullet \mathbf{R_fSO_3Na + p\text{-}R_3C_6H_4CR_2{=}CHR_1} \underset{\mathbf{2a\text{-}e}}{\xrightarrow{\hspace{3em}}} \mathbf{p\text{-}\ R_3C_6H_4\dot{C}R_2\text{-}CHR_1R_f} \qquad \text{(eq. 2-9)}$$

2a: $R_1 = R_2 = H$, $R_3 = COONa$; **2b**: $R_1 = H$, $R_2 = CH_3$, $R_3 = COONa$; **2c**: $R_1 = CH_3$, $R_2 = H$, $R_3 = COONa$; **2d**: $R_1 = R_2 = H$, $R_3 = CH_2COONa$; **2e**: $R_1 = CH_2COONa$, $R_2 = R_3 = H$

$$\mathbf{k_{exptl} = k_0 + k_{gl}\,[Styrene]} \qquad \text{(eq. 2-10)}$$

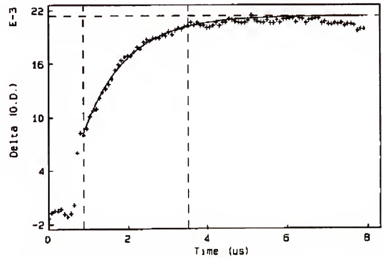

Figure 2-4 1st Order Growth of the Benzylic Radical Absorption

IR_fSO_3Na is very stable in water. A stock solution of IR_fSO_3Na (0.027M) was used in this study. The study was initiated by measuring the pseudo-first order rate constants for addition of $\cdot R_fSO_3Na$ to styrene **2a** at various concentrations of **2a**. A nice growth curve corresponding to the generated benzylic radical could be seen if freshly made styrene solutions were used. However, if a solution of the styrene that had been dissolved in water for about three hours was used, the addition reaction could not be observed. It seems that styrene compound **2a** is not very stable in water.

The sample preparation procedure was therefore modified so that all measurements could be completed within one and a half hour from when the styrene solution was made. Into a series of cuvettes (6 to 8), 1.5ml IR_fSO_3Na solution was charged with a pipette. All of the cuvettes were sealed with rubber septa and degassed by bubbling N_2 through the solutions for ~15 minutes. The styrene solution was prepared during this time and degassed immediately. Different portions of styrene solutions were added to the cuvettes via micro-syringe and the sample was immediately irradiated to obtain the pseudo-first order rate constants. In this manner, one series of samples could be measured within one and a half hours from the time when the styrene solution had been made. Excellent kinetic behavior was observed for the reaction of IR_fSO_3Na and p-$NaOOCC_6H_4CH{=}CH_2$ (**2a**). The amounts of the IR_fSO_3Na and **2a** used are listed in Table 2-1, and the plot giving the second order rate constant is shown in Figure 2-5.

Table 2-1 Pseudo 1st Order Rate Constants of $\cdot R_fSO_3Na$ Addition to **2a**

Entry	V_{2a} (μl)	C_{2a} (x 10^{-3} mol/l)	1st Order Rate (x 10^5 s^{-1})	R
1	25	0.520	1.82	0.981
2	45	0.923	2.78	0.990
3	70	1.41	4.02	0.986
4	100	1.98	4.89	0.996
5	130	2.53	5.38	0.992
6	160	3.06	6.84	0.993
7	200	3.73	9.10	0.995
8	250	4.53	11.6	0.983

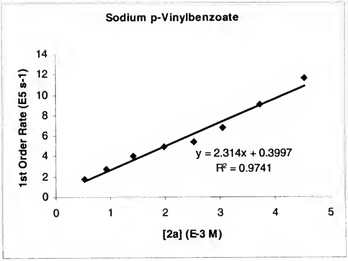

Figure 2-5 Plot of the Pseudo 1st Order Rates vs. Concentration of **2a**

The rate constants of IR_fSO_3Na with all of other styrenes (**2b-2e**) were measured in the same way: freshly made styrene solutions were used and the 2nd order rate constants were obtained by plotting pseudo1st order rates versus various concentration of the styrenes.

Addition of $\cdot R_fSO_3Na$ Radical to Aliphatic Alkene – Use of Probe Techniques

Rate constants for the global reactions of $\cdot$ R_fSO_3Na with an aliphatic alkene (CH_2=$CHCH_2CH_2COONa$) that does not form readily observed radical products, was measured by using a probe technique. A substrate that will form an easily observed product was added to the samples as a spectroscopic probe.[38] In this study, the addition rate constant of IR_fSO_3Na with CH_2=$CHCH_2CH_2COONa$ was obtained by LFP at room temperature using ca. 0.0019 M sodium 4-(βmethyl)vinylbenzoate (**2c**) as the spectroscopic probe (eq. 2-11)

$$k_{exptl} = k_O + k_\beta[2c] + k_{gl}[alkene] \qquad \text{(eq. 2-11)}$$

In each of the six samples, 1.5ml IR_fSO_3Na solution, 100μl β-methylstyrene (**2c**) solution, and various amount of sodium pentenate (**2f**) solution were mixed. Because the total volume of the mixture increased along the series, the concentration of the styrene **2c** is not constant (instead, it decreased slightly along the series). The values of $\{k_{exptl} - k_{\beta}[2c]\}$, all of the pseudo1st order rates, and alkene concentrations are listed in Table 2-2. The plotting of $\{k_{exptl} - k_{\beta}[2c]\}$ versus C_{2f} provides the 2nd order rate constant for $\cdot R_fSO_3Na$ radical addition to alkene **2f** (Figure 2-6).

Table 2-2 Pseudo 1st Order Rate Constants of $\cdot$ R_fSO_3Na Addition to Alkene

Entry	C_{2f}/ 10^{-3} mol/l	k_{exptl} / 10^5 s^{-1}	C_{2c} /10^{-3} mol/l	$k_{exptl} - k_{2c}$[**2c**] / 10^4 s^{-1}
1	1.09	1.25	1.98	5.97
2	1.61	1.38	1.95	7.36
3	2.12	1.64	1.92	10.1
4	3.08	1.75	1.86	11.4
5	4.00	1.80	1.81	12.0
6	4.86	2.03	1.76	14.5

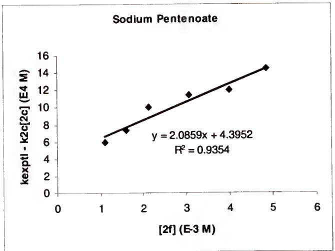

Figure 2-6 Plot of $\{k_{exptl} - k_{\beta}C_{Styrene}\}$ vs. concentration of **2f**

Results and Discussion

Absolute Rate Constants for Addition of ·R_fSO_3Na Radical to Alkenes

The rate constants, k_{add}, obtained from LFP experiments, for addition of the ·R_fSO_3Na radical to various water-soluble alkenes are given in Table 2-3.

Table 2-3 Absolute Rate Constants for the Reactions of · R_fSO_3Na with Various Unsaturated Substrates at 295K in H_2O, Measured by LFP

Entry	Substrate	$k_{add}/10^7\ M^{-1}s^{-1}$	Relative k_{add}
1	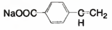 (2a)	23.2 ± 0.16	1
2	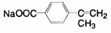 (2b)	55.3 ± 0.25	2.38
3	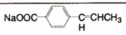 (2c)	3.31 ± 0.28	0.143
4	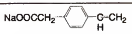 (2d)	20.2 ± 0.13	0.871
5	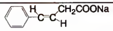 (2e)	1.88 ± 0.11	0.081
6	CH_2=$CHCH_2CH_2COONa$ (2f)	2.08 ± 0.26	0.090

The reactivity of alkenes towards ·R_fSO_3Na radical decreases in the order of: **2b** > **2a** ~ **2d** > **2c** > **2f** ~ **2e,** with the α-methyl substituted styrene the most reactive. Comparing styrenes **2a** and **2b**, the α-methyl substituent enhances the reactivity of the alkene by more than a factor of two. This is consistent with a more electron-rich alkene being more reactive with the electrophilic fluorinated radical.

However, when the methyl group is at β-position, the addition reaction is inhibited, with **2c** reacting seven times slower than **2a**! This indicates that the addition reaction of the ·R_fSO_3Na radical is sensitive to steric effects.

The same effect of α- and β-methyl substitution on the reactivity of alkenes towards perfluoro-n-alkyl radicals has been observed in F113.[38] Some related absolute addition rate constants of $C_3F_7\cdot$ and $C_8F_{17}\cdot$ to alkenes in nonpolar organic solvent (F113) are provided in Table 2-4. α-Methyl styrene is 1.81 and 1.93 times more reactive than styrene, respectively, towards n-$C_3F_7\cdot$ and n-$C_8F_{17}\cdot$ radicals in F113. Therefore the reactivity enhancement caused by the α-methyl group is almost the same for addition of perfluoro-n-alkyl radicals, whether the reaction is carried out in nonpolar F113 or in water.

Table 2-4 Absolute Rate Constants for the Reactions of Perfluoro-n-alkyl Radicals with Unsaturated Substrates at 298 ± 2 K, as Measured by LFP[38]

Entry	Substrate	$k_{add}/10^6$ M^{-1} s^{-1}			
		n-$C_3F_7\cdot$	Relative k	n-$C_8F_{17}\cdot$	Relative k
1	styrene	43 ± 1	1	46 ± 6	1
2	4-methylstyrene	/	/	61	1.33
3	α-methylstyrene	78 ± 8	1.81	89 ± 1	1.93
4	β-methylstyrene	3.8 ± 0.2	0.088	3.7 ± 0.2	0.080
5	1-hexene	6.2 ± 0.2	0.144	7.9 ± 0.7	0.172

β-Methyl styrene is 11 times less reactive than styrene towards n-$C_3F_7\cdot$ radical addition in F113, a somewhat larger factor than the seven fold decrease observed in H_2O.

The rate constants for **2a** and **2d** are very similar, **2a** reacting a bit more rapidly than **2d**. This is consistent with their Hammett inductive/field substituent constants. The F values for $-COO^-$ and $-CH_2COO^-$ are –0.10 and 0.19, respectively.[116] This indicates that inductively -COO$^-$ is a weak electron-donating group, while –CH_2COO^- is a weak electron-withdrawing group.

The respective σ_p values for –COO$^-$ and –CH_2COO^- are 0.00 and –0.16, respectively[116] which are not consistent with the observed trend in rate constants. Thus it appears that the para-substituents mainly influence the observed addition reactions by inductive/field effects.

Comparison of Perfluoro-n-alkyl Radical Addition Reactions in Nonpolar Organic Solvent and Aqueous Solution

By necessity, different fluorinated radicals were used for the respective studies in nonpolar organic solvents and aqueous solutions. It is necessary to consider the similarities and differences on the two radical types before we can reach conclusions about the observed rate differences in the two solvents. As discussed in chapter one, n-$C_3F_7\cdot$, n-$C_7F_{15}\cdot$, and n-$C_8F_{17}\cdot$ radicals have virtually the same reactivities with respect to alkene addition reactions, and thus the reactivities of all homologous perfluoro-n-alkyl radicals can be defined by the reactivities of these radicals.[38] The water-soluble fluorinated radical $\cdot CF_2CF_2OCF_2CF_2SO_3Na$, which was used in this project, differs structurally from a prototypical perfluoro-n-alkyl radical ($\cdot CF_2CF_2CF_2CF_2CF_3$) in two ways, as shown in Figure 2-7.

$$\cdot CF_2CF_2\ \underline{O}\ CF_2\underline{CF_2SO_3Na}$$

$$\cdot CF_2CF_2\underline{CF_2}CF_2\underline{CF_3}$$

Figure 2-7 Comparison of the Structures of $\cdot CF_2CF_2OCF_2CF_2SO_3Na$ and $\cdot CF_2CF_2CF_2CF_2CF_3$ Radicals

The ionic substituent of the $\cdot CF_2CF_2OCF_2CF_2SO_3Na$ radical is located far from the radical site. Therefore we don't believe that this should give rise to significant reactivity differences between the two types radicals. However, the replacement of a $-CF_2-$ moiety with an oxygen atom at the 3-position could potentially alter the electrophilicity of the radical. Because this can only have an effect on the radical reactivity through inductive/field factors, the F values are considered. $-OCF_2CF_3$ group is reported to have an F value of 0.55, which is greater than that of $-CF_2CF_2CF_3$ (F value of 0.44).[116] This indicates that $-OCF_2CF_3$ is a somewhat stronger electron-withdrawing group than $-CF_2CF_2CF_3$. Because of this reason, the radical used in the aqueous study ($\cdot CF_2CF_2OCF_2CF_2SO_3Na$) might be somewhat more electrophilic than the perfluoro-n-alkyl radicals studied earlier in the nonpolar organic solvents.

To compare the rate constants obtained in water and F113, the relative rate constants for the substrates with similar structures are summarized in Table 2-5. It is noticed that the addition rate constants in aqueous solution are generally larger than the analogous reactions in F113. The addition reactions of the $\cdot R_fSO_3Na$ radical to alkenes in water are between 3~9 times faster than those of $\cdot R_f$ radicals to alkenes in F113! However, all of the water-soluble alkenes have an ionic substituent not present in organic solvent experiments. The effect of the carboxylate substituent on substrate reactivities needs to be considered before any conclusions can be drawn.

In the Hammett study carried out in C_6D_6 of the reaction between $\cdot R_f$ and para-substituted styrenes (given in Table 1-10), the best correlation was obtained with Hammett σ value to give a ρ value as -0.53.[38] The relatively small ρ value indicates that the addition reactions of perfluoro-n-alkyl radicals to styrene are not very sensitive to the nature of para-substituents. For instance, 4-methylstyrene has a σ value of -0.14, and it reacts only 1.3 times faster than styrene. As mentioned earlier in this chapter, inductively $-CO_2^-$ is a weak electron-donating group. Therefore, although the presence of a $-CO_2^-$ group at the para-position of the styrenes might slightly facilitate the addition reactions of the electrophilic $\cdot R_fSO_3Na$ radical, such enhancement should not be very large.

Table 2-5 Comparisons of Addition Reactions of Perfluoro-n-alkyl Radicals in H_2O and Freon 113

Entry	Substrate	k_{add} in H_2O / k_{add} in Freon 113	
		$\cdot R_fSO_3Na$ vs $C_3F_7\cdot$	$\cdot R_fSO_3Na$ vs $C_8F_{17}\cdot$
1	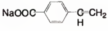 **(2a)**, styrene	5.40	5.04
2	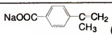 **(2b)**, α-methylstyrene	7.09	6.21
3	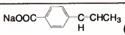 **(2c)**, β-methylstyrene	8.71	8.94
4	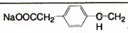 **(2d)**, styrene	4.70	4.39
5	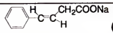 (2e), β-methylstyrene	4.95	5.08
6	$CH_2=CHCH_2CH_2COONa$ **(2f)**, 1-hexene	3.35	2.63

The rate constants of $\cdot R_fSO_3Na$ addition to compounds **2a**, **2b**, and **2c** are about 5, 7, and 9 times larger, respectively, than those for addition of $\cdot R_f$ to styrene, α-methyl styrene, and β-methyl styrene (entries 1-3 in Table 2-5). Such rate increases in aqueous solution compared with organic solution (F113 or C_6D_6 as solvents) must derive from (a) the above mentioned beneficial $-COO^-$ substitution on the styrenes used in water, (b) the beneficial 3-oxygen atom in the $\cdot R_fSO_3Na$ radical, and lastly (c) a positive influence of the polar solvent water.

The addition reaction of $\cdot R_fSO_3Na$ radical to compound **2d** in water is more than four times faster than that of $\cdot R_f$ radical to styrene in F113. And compound **2e** reacts with $\cdot R_fSO_3Na$ radical in aqueous solution five times faster than does β-methyl styrene with $\cdot R_f$ radical in F113. The rate difference must also be caused by the $-CH_2COO^-$ substitution on the styrene, the presence of 3-oxygen in $\cdot R_fSO_3Na$ radical, and polar solvent effect. However, in these two cases (entries 4 and 5 in Table 2-5), the $-CH_2COO^-$ substituent is considered as a weak electron-withdrawing group. Thus the rate enhancement is not as much as that for entries 1, 2 and 3.

Although electrostatic inhibition originated from the carboxylate group might be present, the aliphatic alkene $CH_2{=}CHCH_2CH_2COONa$ (**2f**) and 1-hexene are perhaps the most comparable pair of substrates because they have the most similar structures among those pairs of compounds being compared in these two solvents. Contrasted with the addition of $\cdot R_f$ radical to 1-hexene in F113, a ca. three times rate enhancement was observed for the addition of $\cdot R_fSO_3Na$ radical to **2f** in water. Those three factors mentioned earlier must also count for the different reactivies observed for compound **2f** and 1-hexene in different solvents.

Compared with the rate constants obtained in F113 and C_6D_6 for addition reactions of $\cdot R_f$ with alkenes, the rates in aqueous solution are observed to increase. Besides the influences derived from different compounds used in aqueous solution and organic solvents, a polar solvent effect in the transition state is definitely implied by the rate enhancement in aqueous solution than in F113. The solvent effect is not very large because of (a) general radical reaction characteristics, and (b) the very fast rates (low activation barriers) for these addition reactions (i.e. leveling effect).

Conclusion

In the current study, absolute rate constants of $\cdot R_fSO_3Na$ addition to water-soluble alkenes containing ionic substituents in aqueous solution are measured by LFP experiments. Thermodynamic, polar, and steric effects all play roles in such a reaction.

The rate constants are compared with those of some analogous reactions, which have been determined in a non-polar organic solvent, F113. Aqueous reactions are all faster than the analogous reactions carried out in F113, and 3~9 folds rate increase are observed. Although the solvent effect is not large, it is unambiguous that the addition reactions of electrophilic perfluoro-n-alkyl radicals are faster in polar solvent water than in a non-polar organic solvent.

CHAPTER 3
HYDROGEN ATOM ABSTRACTION REACTIONS OF PERFLUORO-N-ALKYL RADICAL IN AQUEOUS SOLUTION

A preliminary investigation of the C-H abstraction by fluorinated radicals from several typically functionalized organic substrates was carried out in 1,3-BTB (1,3-bistrifluoromethyl benzene).[87] The absolute rate constants for bimolecular hydrogen abstraction from a variety of organic substrates in solution have been obtained for the n-$C_4H_9CF_2CF_2\cdot$, *n*-$C_4F_9\cdot$, and *i*-$C_3F_7\cdot$ radicals by competition kinetic methods. The molecules chosen for study were alkanes, aromatic hydrocarbons, haloalkanes, ethers, thioethers, alcohols, and esters. A wide range of substrate reactivities (5200-fold) was observed. The results indicate that the thermochemical, polar, steric, stereoelectronic, and field effects all play a role in the H-abstraction process of fluorinated radicals.

In the present study, with the addition reaction rates of $\cdot R_fSO_3Na$ radical to alkenes available, absolute rate constant of hydrogen abstraction from $HSCH_2CH_2SO_3Na$ by $\cdot R_fSO_3Na$ in aqueous solution was determined with competitive technique. Another competition of H-transfer from $HSCH_2CH_2SO_3Na$ with D-transfer from THF-d8 gives the absolute D-transfer rate to $\cdot R_fSO_3Na$ in water.

The kinetics of hydrogen abstraction by $\cdot R_fSO_3Na$ from several types of functionalized organic compounds were studied, with the competition between C-H compounds and THF-d8. The absolute rate constants obtained in water were used to study the solvent effect of this reaction. Kinetic isotope effects were measured for several substrates and fairly large k_H/k_D was observed for those unreactive substrates.

Absolute Rate Determination – Competition Between Addition and H-Abstraction Reactions

With the absolute rate constants of $\cdot R_fSO_3Na$ addition to alkenes in water available, several competition experiments were tested to obtain absolute rates of hydrogen abstraction (Scheme 3-1). The relative amount of the two products could be determined with ^{19}F NMR. To get accurate results, the two pathways ought to be comparable so that both products could be detected in NMR and their amounts do not differ very much. This requires that the value of k_H[H-Donor] is comparable to that of k_a[alkene], and the radical formed from the addition reaction could be reduced by the H-donor at a reasonable rate. At the same time, there should not be other competing pathways for the radical.

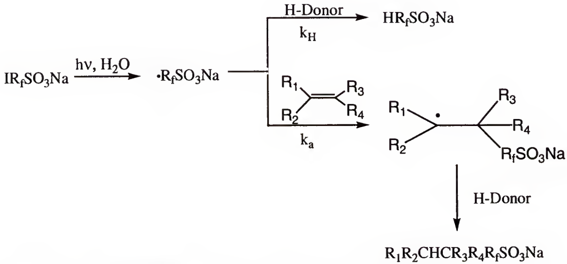

Scheme 3-1 Competing Reactions of Addition and H-Abstraction by $\cdot R_fSO_3Na$ Radical

The absolute addition rates are in the range of 10^7 to 10^8 $M^{-1}s^{-1}$, so a comparable hydrogen transfer reaction is required to compete with the addition reaction.

The Preparation of Authentic Samples

Photochemically reducing IR_fSO_3Na with THF gives the reduced product **3a** (Eq. 3-1). THF is the reducing agent and solvent, ^{19}F NMR showed complete consumption of starting material after 24 hours. Then solvent was removed, and the solid residue was washed with diethyl ether to give white crystals in 88% yield.

$$\underset{\mathbf{1}}{IR_fSO_3Na} + THF \xrightarrow{h\nu,\ 24hrs} \underset{\mathbf{3a}}{HR_fSO_3Na} \qquad \text{(eq. 3-1)}$$

Radical addition of compound **5** to pentenoic acid was initiated with AIBN,[117] and the reaction mixture was used for the zinc reduction without purification. Then compound **6** was hydrolyzed with NaOH in EtOH /H_2O. ^{19}F NMR showed that there was some impurity in the mixture. Conc. HCl was used to precipitate the acid, which gave a white solid identified as the monoacid **7** in 26% overall yield. **7** was treated with NaOH to give the final addition-reduction product **4**.

$$\underset{\mathbf{5}}{ICF_2CF_2OCF_2CF_2SO_2F} + CH_2{=}CHCH_2CH_2COOH \xrightarrow{AIBN,\ 80^{o}C} \xrightarrow[Reflux]{Zn,\ EtOH}$$

$$\underset{\mathbf{6}}{FSO_2(CF_2)_2O(CF_2)_2(CH_2)_4COOH} \xrightarrow[2)\ HCl]{1)\ NaOH,\ EtOH/H_2O}$$

$$\underset{\mathbf{7}}{NaSO_3(CF_2)_2O(CF_2)_2(CH_2)_4COOH} \xrightarrow{NaOH} \underset{\mathbf{4}}{NaSO_3(CF_2)_2O(CF_2)_2(CH_2)_4COONa}$$

Scheme 3-2 Preparation of Addition Product **4**

The Competition between THF and Alkenes in Water

Among all the compounds studied previously for the hydrogen abstraction reaction in 1,3-BTB, THF has the second highest overall reactivity towards $C_4F_9\cdot$ radical. The most reactive compound is tetrahydrothiophene, which is insoluble in water. In organic solvents, the overall hydrogen-donating rate from THF to $C_4F_9\cdot$ radical is 3.1x

10^4 $M^{-1}s^{-1}$, which is about 1400 times slower than $C_3F_7\cdot$ radical addition to styrene and 200 times slower than the addition to 1-hexene. Therefore the rate difference between H-abstraction from THF and addition to alkenes by perfluoro-n-alkyl radicals might also be very large in the aqueous solution. Regardless, the competition reactions of THF and water-soluble alkenes towards $\cdot R_fSO_3Na$ radical were carried out. At least the results could tell us whether the aqueous H-transfer from THF to $\cdot R_fSO_3Na$ radical is fast enough to compete with the addition reaction or not.

A competition reaction (Eq. 3-2) was conducted. THF was used in ten times excess of the amount of styrene **2a**. However, only addition products could be detected by ^{19}F NMR, and no reduced product HR_fSO_3Na could be detected. With 98% conversion of the IR_fSO_3Na shown in ^{19}F NMR, the product mixture gave messy peaks in the range of –114ppm to –118ppm on ^{19}F NMR spectrum; this range is commonly corresponding to $-CF_2CH_2-$ structure. Thus the products are very likely to be oligomers or polymers formed by addition reactions (Eq. 3-2).

$$\underset{\mathbf{1}}{IR_fSO_3Na} + \underset{\mathbf{2a}}{p\text{-}NaOOCC_6H_4CH{=}CH_2} + THF \xrightarrow{hv,\ H_2O} \underset{\text{Oligomers or polymers}}{H(ArCHCH_2)_nR_fSO_3Na} \qquad \text{(eq. 3-2)}$$

As shown on the previous page, when compound IR_fSO_3Na is irradiated with UV light in the presence of THF in water, IR_fSO_3Na is reduced to HR_fSO_3Na in quantitative yield. However, the presence of alkene **2a** in the reaction mixture totally blocks the reduction reaction. This indicates that the hydrogen abstraction reaction is much slower than the addition reaction to alkene **2a** so that H-abstraction could not compete with the addition reaction.

The alkene $CH_2{=}CHCH_2CH_2COONa$, with a rate ten times less than that of **2a**, was used in the competition experiment (eq. 3-3). The reaction was initiated photochemically (UV reactor) or thermally with ACVA [4,4'-Azobis (4-cyanovaleric acid)] as the initiator. The reactions were carried out at different conditions, and the results are summarized in Table 3-1. The results in Table 3-1 show that none of the competition experiments were clean and gave compounds **3a** and **4** as major products.

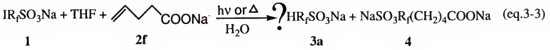

Table 3-1 The Competition Experiments of THF and **2f** towards ·R$_f$SO$_3$Na Radical

Entry	I/THF/2f	Condition	Conversion (%)	Yields*
1	1:250:17	hν, 24hrs	100	~2% **3a**, ~32% **4**, and unknown**
2	1:765:17	hν, 24hrs	100	~10% **3a**, ~30% **4**, and unknown**
3	1:241:10	ACVA, 75°C	100	~10% **3a**, and unknown, no **4****
4	1:141:2	ACVA, 75°C	100	~25% **3**, and unknown, no **4****
5	1:241:11	ACVA, 65°C	100	~8% **3a**, and unknown, no **4****
6	1:245:11	ACVA, 96°C	100	~10% **3a**, and unknown, no **4****

* ^{19}F NMR yields.

** The major product for these reactions is an unknown compound. ^{19}F NMR shows that this product has several peaks in the range of -114ppm to –118ppm. It looks like the 1,1-addition product, but we did not separate and identify it.

Although excess amount of THF was used, especially for entries 2 and 4, the addition-reduction reactions forming product **4** still could not be accomplished. The yield of the reduced product was always low. The maximum yield of **3a** was 25%, when the amount of THF was 70 times as that of alkene **2f**. The results may be caused by two reasons: low reactivity of THF compared with the alkene so the addition reaction dominated in all cases. Secondly, THF could not transfer hydrogen efficiently to $\cdot CH(CH_2R_fSO_3Na)CH_2CH_2COONa$, which is the radical formed by $\cdot R_fSO_3Na$ addition.

The competition experiments imply that hydrogen abstraction from THF by $\cdot R_fSO_3Na$ radical is much slower than the radical addition to $CH_2{=}CHCH_2CH_2COONa$ in aqueous solution. A better H-donor is needed to compete with the addition reaction. Since compound $CH_2{=}CHCH_2CH_2COONa$ has almost the lowest reactivity among all of the alkenes and the radical addition to terminal alkene has very good regioselectivity, we used this compound to try competition experiments with other H-donors.

The Competition between Silanes and Alkene 2f in Water

In the organic solvents, silanes donate hydrogen to perfluoro-n-alkyl radicals at a reasonably fast rate. For instance, the hydrogen transfer reaction has a rate constant of $5 \times 10^5 M^{-1}s^{-1}$ between $n\text{-}C_7F_{15}\cdot$ radical and Et_3SiH.[83] We attempted to make water-soluble silanes as H-donor for this study.

The reactions shown in Scheme 3-3 were used to make ionic silanes.

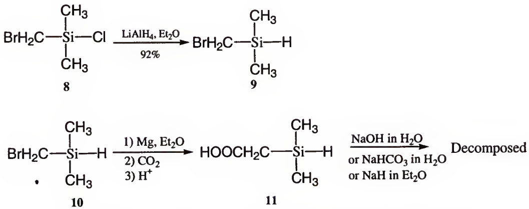

Scheme 3-3 Attempts for Preparation of $NaOOCCH_2Si(CH_3)_2H$

The first two reaction worked out well, and the acid **11** was obtained in 68% overall yield. While this compound decomposed when treated with NaOH in water, none of the expected salt was formed even when a weaker base ($NaHCO_3$) was used. NaH in ether could not give the desired compound $NaOOCCH_2Si(CH_3)_2H$, either.

Then we tried to prepare an ammonium salt from compound **10** (Scheme3-4), the salt was obtained as a white solid. ^1H NMR showed the proton signal of Si-H, but there were some impurities at high field, the ionic characteristic of compound **12** makes the purification difficult. Thus it is not very useful in a kinetic study.

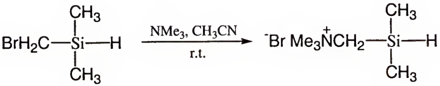

$$BrH_2C{-}\overset{CH_3}{\underset{CH_3}{Si}}{-}H \xrightarrow[\text{r.t.}]{NMe_3,\ CH_3CN} {}^{-}Br\ Me_3\overset{+}{N}CH_2{-}\overset{CH_3}{\underset{CH_3}{Si}}{-}H$$

10 **12**

Scheme 3-4 Attempts for the Preparation of $Br^-Me_3N^+CH_2SiMe_2H$

At this point, we would like to make a silane compound containing hydroxyl groups so that it could dissolve in water. Scheme 3-5 provides the synthesis strategy to get this water-soluble silane.

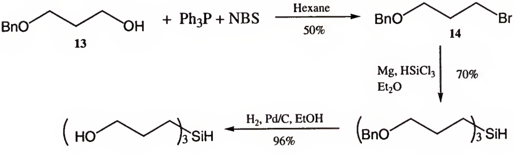

Scheme 3-5 Synthesis of Water-Soluble Silane **16**

In the second step, the Grignard reaction goes smoothly with 4 equivalent of the bromide and magnesium, and compound **15** was obtained in 70% yield after column chromatography (Scheme 3-4). The benzyl group can be deprotected easily by H_2 with

Pd/C as catalyst to give the final product **16** as an oil, which solidifies with diethyl ether to give a white solid. Compound **16** is able to dissolve in water; at room temperature the maximum concentration could reach ca. 0.15M.

The competition of silane **16** and alkene **2f** was carried out (eq. 3-4), photochemically and thermally. Reaction conditions and results are given in Table 3-2. The photoreaction didn't give the addition-reduction product as expected (entry 1), instead the major product has an AB pattern in the range of –114 to –118 ppm, and there are some impurities as well. The thermal reactions are cleaner, but the major product is still the same one obtained in the photoreaction. Increasing the amount of silane used does not help to give product **4** (entry5).

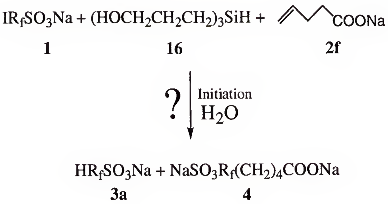
IR_fSO_3Na + $(HOCH_2CH_2CH_2)_3SiH$ +
COONa
1
16
2f
?
Initiation
H_2O
HR_fSO_3Na + $NaSO_3R_f(CH_2)_4COONa$
3a
4

(eq.3-4)

Because of the solubility limitation of the silane, it is hard to use much excess amount of it. We lowered the concentration of IR_fSO_3Na, at the same time the relative amounts of **3a** and **16** were increased to make the reaction pseudo-first order (entry 2). Photoreaction did give product **4**, but the yield was not satisfying. Acetic acid was then used as a co-solvent to increase the solubility of silane. We noticed that the addition of acetic acid helped silane **16** to dissolve, but the yield of addition product was still poor.

Table 3-2 The Competition Experiments of **16** and **2f** towards $\cdot R_fSO_3Na$ Radical

Entry	I/16/2f	Condition	Conversion (%)	Yields*
1	1:5:2	hν	100	~2.5% **3a**, no **4**
2	1:44:6	hν	100	~24.7% **3a**, 31% **4**
3	1:135:6	hν**	100	~5.5% **3a**, 39% **4**
4	1:6:2	ACVA, 75°C***	100	~3% **3a**, no **4**
5	1:16:2	ACVA, 75°C	100	~8% **3a**, no **4**

* ^{19}F NMR Yields.
** 27% (by volume) CH_3COOH in H_2O as solvent.
*** This reaction was carried out in H_2O, and 0.01M PBS buffer (pH = 7.0) solution. Same results were obtained in both reactions.

As mentioned before, silanes are not good reducing agents for hydrocarbon radicals because the hydrogen transfer reaction is slow (primary alkyl radicals abstract hydrogen atom from Et_3SiH at a rate of 850 $M^{-1}s^{-1}$).[15] We believe this is the reason that the addition-reduced product could not be obtained in good yield.

The Competition between Thiol and Alkene 2f in Water

Thiol is also widely used as a reducing reagent; it donates hydrogen to hydrocarbon radicals very fast. For example, PhSH has a rate ca. 1.5×10^8 $M^{-1}s^{-1}$ to transfer hydrogen to primary alkyl radicals.[15] In C_6D_6, the absolute rate constant of hydrogen abstraction reaction from PhSH by perfluoro-n-alkyl radical is 2.8×10^5 $M^{-1}s^{-1}$. The hydrogen abstraction from a S-H bond might be able to compete with addition reaction to alkene $CH_2=CHCH_2CH_2COONa$ of $\cdot R_fSO_3Na$ radical.

We used the commercially available compound 2-mercaptoethanesulfonic acid, sodium salt (MESAS) $HSCH_2CH_2SO_3Na$ (**17**) in the competition experiments. Two reactions were conducted with various amounts of $HSCH_2CH_2SO_3Na$ (eq. 3-5). As shown in Table 3-3, both reactions gave the two desired products with almost quantitative overall yields, and the amount of reduced product increased when more thiol was used.

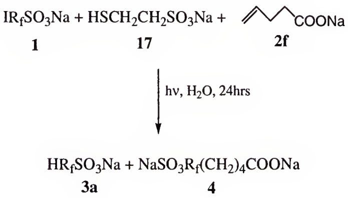

IR_fSO_3Na + $HSCH_2CH_2SO_3Na$ +
COONa
1
17
2f
hv, H_2O, 24hrs
HR_fSO_3Na + $NaSO_3R_f(CH_2)_4COONa$
3a
4

(eq. 3-5)

Table 3-3 The Competition Experiments of **17** and **2f** towards $\cdot R_fSO_3Na$ Radical

Entry	**1/17/2f**	Conversion (%)	Overall Yield * (%)	**3a/4**
1	1:10:10	100	99	0.0137
2	1:20:10	100	99	0.0876

* Based on ^{19}F NMR, and it is the total yield of products **3a** and **4.**

A kinetic competition was carried out with the concentration of $HSCH_2CH_2SO_3Na$ varying in a series of six samples, while the concentrations of IR_fSO_3Na and alkene $CH_2{=}CHCH_2CH_2COONa$ were kept constant. Reaction results are listed in Table 3-4, with all of the overall yields more than 90%, there is a good correlation between the products ratio **(3a/4)** and the substrate ratio **(17/2f).**

Table **3-4** The Competition Kinetic of **17** with **2f** towards $\cdot R_fSO_3Na$ Radical in H_2O at Room Temperature*

Entry	[17] / mol·l^{-1}	[17] / [2f]	[3a] / [4]	Yield (%)
1	0.106	0.993	0.0190	98
2	0.142	1.325	0.0493	93
3	0.178	1.657	0.112	98
4	0.213	1.987	0.153	98
5	0.249	2.316	0.190_5	99
6	0.320	2.980	0.260_5	99

* All of the reactions were initiated photochemically, with [IR_fSO_3Na] = 0.011 M, and [2f] = 0.107 M.

According to equation 1-3, a plot of the product ratios (**3a/4**) versus substrate ratios (**17/2f**) gives a straight line, the slope of the line is the ratio of the rate constants (k_H/k_a) as illustrated in Figure 3-1.

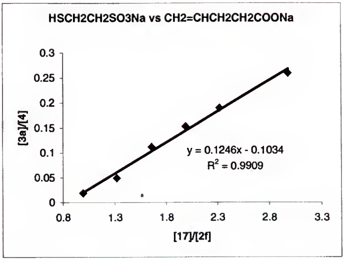

Figure 3-1 Plot of Products Ratio (**3a/4**) versus Substrates Ratio (**17/2f**)
k_H/k_a = Slope = 0.125 ± 0.006

With the addition rate constant k_a known, which is 2.08 (±0.26) x 10^7 $M^{-1}s^{-1}$, the absolute rate constant of hydrogen abstraction from $HSCH_2CH_2SO_3Na$ by $\cdot R_fSO_3Na$ radical could be calculated as $k_H = k_a$ x slope.

The addition rate constant and the rate constant ratio k_H/k_a have errors, therefore the errors accumulate for the rate constant of hydrogen abstraction reaction k_H. Statistical theory demonstrates the way to combine the relative standard deviations for multiplication and division. For the relationship y = ab/c, the absolute standard deviation is given in equation 3-6.

$$(s_y/y)^2 = (s_a/a)^2 + (s_b/b)^2 + (s_c/c)^2 \qquad \text{(eq. 3-6)}$$

So the H-abstraction rate constant from $HSCH_2CH_2SO_3Na$ by $\cdot R_fSO_3Na$ radical is 2.60 (± 0.35) x 10^6 $M^{-1}s^{-1}$ in aqueous solution.

Absolute Rate Constants of Hydrogen Abstraction Reactions by Perfluoro-n-alkyl Radical in Aqueous Solution

We want to use a deuterium abstraction reaction as the standard reaction to study kinetics of hydrogen abstraction reactions by perfluoro-n-alkyl radical in water, as shown in equation 3-7. The two reduced products can get baseline separation on ^{19}F NMR for the signals of $-\underline{CF_2}H$ and $-\underline{CF_2}D$. NMR integration gives the ratio of the two products.

$$\underset{\mathbf{1}}{IR_fSO_3Na} + \text{H-Donor} + \text{D-Donor} \xrightarrow{H_2O} \underset{\mathbf{3a}}{HR_fSO_3Na} + \underset{\mathbf{3b}}{DR_fSO_3Na} \qquad \text{(eq. 3-7)}$$

By varying the amount of H-donor and D-donor, a series of relative concentrations of the two products can be obtained. A plot made of the product ratios versus donor ratios gives the relative rate constant k_H/k_D (Scheme 3-6).

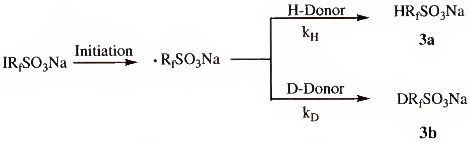
IR_fSO₃Na
Initiation
• R_fSO₃Na
H-Donor
k_H
HR_fSO₃Na
3a
D-Donor
k_D
DR_fSO₃Na
3b

$$\frac{[HR_fSO_3Na]}{[DR_fSO_3Na]} = \frac{k_H[\text{H-Donor}]}{k_D[\text{D-Donor}]}$$

Scheme 3-6 Competition Kinetic between H-, and D-abstraction

Selection of the Standard Deuterium Donor

To apply the competition method, we studied the deuterium donating ability of three deuterated compounds: CD_3OD, $(CD_3)_2CO$, and THF-d8 (eq. 3-8). THF-d8 gave the best results among these three substrates. It reduces the IR_fSO_3Na very rapidly with quantitative yield (Table 3-5).

$$IR_fSO_3Na + \text{D-Donor} \xrightarrow{h\nu,\ H_2O} DR_fSO_3Na \qquad \text{(eq. 3-8)}$$

Table 3-5 Reactions of IR_fSO_3Na with D-Compounds in H_2O^*

D-Donor	[D-Donor]/[IR_fSO_3Na]	Time (hour)	Conversion (%)	Yield (%) **
CD_3OD	192.6	47	28.4	12.6
$(CD_3)_2CO$	115.8	47	55.4	22
THF-d8	96.2	19	100	100

* [IR_fSO_3Na] = 0.011M, reaction in pyrex NMR tubes, UV irradiation.
** Based on ^{19}F NMR.

Competition experiments between $HSCH_2CH_2SO_3Na$ and THF-d8 give D-abstraction rate from THF-d8 by $\cdot R_fSO_3Na$ radical (eq. 3-9). Table 3-6 provides the results of the kinetic study with all of the yields higher than 95%. The plot of **3a/3b** versus [**17**]/[THF-d8] gives the $k_H/k_{D\ THF\text{-}d8}$ ratio in Figure 3-2.

$$\underset{\mathbf{1}}{IR_fSO_3Na} + HSCH_2CH_2SO_3Na + THF\text{-}d_8 \xrightarrow{h\nu,\ H_2O} \underset{\mathbf{3a}}{HR_fSO_3Na} + \underset{\mathbf{3b}}{DR_fSO_3Na} \qquad \text{(eq. 3-9)}$$

Table 3-6 The Competition Kinetic of **$HSCH_2CH_2SO_3Na$ (17)** with **THF-d8** towards $\cdot R_fSO_3Na$ Radical in H_2O at Room Temperature*

Entry	[17] / $mol \cdot l^{-1}$	[17] / [THF-d8]	**3a / 3b**	Yield (%)**
1	0.118	0.174	20.1	97
2	0.157	0.232	27.3	97
3	0.196	0.291	29.1	97
4	0.235	0.349	38.9	96
5	0.275	0.408	41.0	96
6	0.314	0.460	48.7	97

* [IR_fSO_3Na] = 0.011M, [THF-d8] = 0.677M, reaction in pyrex NMR tubes, UV irradiation.

** Based on ^{19}F NMR.

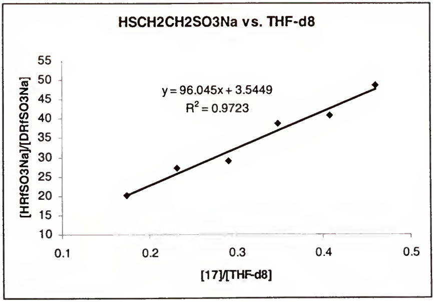

$k_H / k_{D\ THF\text{-}d8}$ = Slope = 96.0 (±8.1)

Figure 3-2 Plot of Products Ratio (**3a/3b**) versus Substrates ratio (**17/THF-d8**)

The absolute rate constant of overall deuterium abstraction reaction from THF-d8 by $\cdot R_fSO_3Na$ radical is calculated to be 2.71 (±0.43) x 10^4 $M^{-1}s^{-1}$.

Determination of Absolute Rate Constants of Hydrogen Abstraction Reactions by $\cdot R_fSO_3Na$ Radical in Aqueous Solution

The competition kinetic method is shown in equation 3-7 and Scheme 3-6. THF-d8 was used as the standard D-donor.

The organic substrates used in this study were chosen on the basis of two main criteria: (a) structural simplicity, the molecules having a minimum of different C-H bonds, and (b) to provide a reasonable variety of structural (functional group) types. The molecules we studied were:

Alcohols: **CH_3OH, CH_3CH_2OH, $(CH_3)_2CHOH$, $HOCH_2CH_2OH$, $(CH_3CHOH)_2$, $HOCH_2COOCH_3$, CF_3CH_2OH, $(CF_3)_2CHOH$**

Alkoxides: **CF_3CH_2ONa, $(CF_3)_2CHONa$**

Ether: **THF, $CH_3OCH_2CH_2OCH_3$**

Carbonyl compounds: **CH_3COCH_3, CH_3COOH, CH_3COONa, CH_3CH_2COOH,**

CH_3CH_2COONa

Thiol: **$HSCH_2CH_2SO_3Na$**

Silanes: **$(HOCH_2CH_2CH_2)_3SiH$, $Br^-Me_3N^+CH_2SiMe_2H$**

Phosphorous acid: **H_3PO_3**

In a typical kinetic study, a stock solution of IR_fSO_3Na in H_2O (17.8% by wt%), H-Donor, THF-d8, and H_2O were mixed in a series of NMR tubes. The amount of H-donor varies and the amount of all the other compounds was kept constant. A sealed capillary tube containing $CFCl_3/C_6D_6$ was also placed in the NMR tube as internal standard. The tubes were degassed by three cycles of freeze-pump-thaw and irradiated in a Rayonet UV reactor equipped with 254 nm wavelength light bulbs. The yields of the reactions and product ratios were obtained from the integrals of ^{19}F NMR. The results will be presented according to the substrates type.

Alcohols. The absolute rate constants for hydrogen abstraction reactions from the compounds with –OH group by $\cdot R_fSO_3Na$ radical in water are provided in Table 3-7.

1,1,1,3,3,3-Hexafluoroisopropanol is only slightly soluble in water, and the small amount dissolved in water was not enough for the kinetic studies even in the presence of THF-d8. Thus a direct competition of $(CF_3)_2CHOH$ with THF-d8 does not work.

Fortunately it was noticed that addition of methanol to water can increase the solubility of $(CF_3)_2CHOH$. Therefore a competition of $(CF_3)_2CHOH$ with CD_3OD is possible, and the rate constant of hydrogen abstraction from $(CF_3)_2CHOH$ by $\cdot R_fSO_3Na$ radical was achieved by a series of competitions: $(CF_3)_2CHOH$ versus CD_3OD, CD_3OD versus CH_3OH, and CH_3OH versus THF-d8.

Table 3-7 Absolute Rates of H-abstraction from Alcohols by $\cdot R_fSO_3Na$ radical, Measured by Competition with THF-d8 in Aqueous Solution at 298K

Substrate	$k_{H\ overall}/k_{D\ THF\text{-}d8}$	$k_{H\ Overall}$ / $10^4\ M^{-1}s^{-1}$	$k_{H\ per\ H}$/ $10^4\ M^{-1}s^{-1}$
CH_3OH	0.434 (±0.010)	1.18 (±0.19)	0.393 (±0.063)
CH_3CH_2OH	2.48 (±0.15)	6.72 (±1.14)	3.36 (±0.57)
$(CH_3)_2CHOH$	13.0 (±0.8)	35.2 (±6.0)	35.2 (±6.0)
$HOCH_2CH_2OH$	1.28 (±0.03)	3.47 (±0.56)	0.868 (±0.140)
$(CH_3CHOH)_2$	5.55 (±0.23)	15.0 (±2.4)	7.50 (±1.20)
$HOCH_2COOCH_3$	0.593 (±0.028)	1.61 (±0.27)	0.805 (±0.135)
CF_3CH_2OH	0.0188 (±0.0007)	0.0509 (±0.0083)	0.0254 (±0.0041)
$(CF_3)_2CHOH$*	0.0942 (±0.0061)	0.255 (±0.043)	0.255 (±0.043)

* Indirect measurement, please read the following text.

The competition between $(CF_3)_2CHOH$ and CD_3OD gives:

$$k_{H\ (CF3)2CHOH} / k_{D\ Methanol\text{-}d4} = 2.47\ (\pm\ 0.12)$$

The competition between CD_3OD and CH_3OH gives:

$$k_{H\ Methanol} / k_{D\ Methanol\text{-}d4} = 11.4\ (\pm\ 0.4)$$

And the competition between CH_3OH and THF-d8 gives:

$$k_{H\ Methanol} / k_{D\ THF\text{-}d8} = 0.434\ (\pm 0.011)$$

A simple calculation could convert these relative rate constants to the one between $(CF_3)_2CHOH$ and THF-d8: $k_{H\ (CF3)2CHOH} / k_{D\ THF\text{-}d8} = 0.0942\ (\pm 0.0061)$. The standard deviations of them were propagated using equation 3-6 to give the error of the final number, the value shown in Table 3-7.

The reactivity increases along the series of CH_3OH, CH_3CH_2OH, and $(CH_3)_2OH$. With the secondary alcohol reacts 8.5 times (per H) more rapidly than the primary one, and the tertiary alcohol is 10.5 times more reactive (per H) than the secondary one. This is consistent with the thermodynamic expectation, with the decrease of BDE in the same order (Table 3-8). Isopropanol transfers hydrogen to perfluoro-n-alkyl radical at a rate of $3.52 \times 10^5\ M^{-1}s^{-1}$ in water. It is a fairly fast reaction.

It is also because of thermodynamic reason that 2,3-butanediol is 8.6 times more reactive (per H) than ethylene glycol towards $\cdot R_fSO_3Na$ radical.

Table 3-8 C-H Bond Dissociation Energies

C-H Bond	$\underline{CH_3}OH$	$CH_3\underline{CH_2}OH$	$(CH_3)_2\underline{CH}OH$
BDE (kcal.mol)	94 (±2)	93 (±1)	90.7

Compared with ethanol and isopropanol, trifluoroethanol and hexafluoroisopropanol have very low reactivities towards H-abstraction by $\cdot R_fSO_3Na$ radical. The strong electron-withdrawing CF_3- group lowers their reactivity to the electrophilic radical. Therefore the transition state polar effect must have significant influence on the H-abstraction reaction of $\cdot R_fSO_3Na$ radical in the aqueous media. The rate decrease might also come from the field effect: the repulsion between the lone pairs of electrons on the fluorine atoms when the radical is approaching the C-H bond in the fluorinated alcohols.

Field effects are clearly illustrated in the comparison of the mono alcohols with diols. With one more –OH group, ethylene glycol is about 4 times less reactive (per H) than ethanol, and 2,3-butanediol is 4.7 times less reactive (per H) than isopropanol.

The reactions of aqueous trifluoromethyl radicals were studied by Bullock and Cooper in 1970.[118] The reaction between the solvated electron and trifluoromethyl halides was used as a source of trifluoromethyl radicals in aqueous solution. Combination of pulse radiolysis studies and competition kinetic methods enabled the rate constants for the hydrogen abstraction reactions by $CF_3\cdot$ radical from methanol, ethanol, and iso-propanol in water (summarized in Table 3-9).

Table 3-9 Rate Constants for Hydrogen Abstraction Reactions in Water

Substrate	$K_{H\ overall}$ / $10^4\ M^{-1}s^{-1}$ in water	
	$\cdot CF_2CF_2OCF_2CF_2SO_3Na$ *	$CF_3\cdot$ **
Methanol	1.18 (±0.19)	0.8 (±0.12)
Ethanol	6.72 (±1.14)	4.6 (± 0.5)
Iso-propanol	35.2 (±6.0)	9.2 (±0.9)

* This work; ** ref 118

It is noticed that the aqueous H-abstraction rate constants measured by us for the $\cdot R_fSO_3Na$ radical are in good consistent with those measured by Bullock for $CF_3\cdot$ radical. All of the numbers are in the same order of magnitude.

Alkoxides. We are very interested in the H-donating ability of alkoxides towards fluorinated radicals. The oxygen bearing negative charge might affect the reaction in two opposite manners: thermodynamic stabilization of the radical next to the oxygen could facilitate the reaction, meanwhile the electrostatic repulsion between O^- and the fluorine atoms could retard the reaction.

We used the alkoxides whose corresponding alcohols are more acidic than water so that they could survive in water. The pKa values of CF_3CH_2OH and $(CF_3)_2CHOH$ are

11.4 and 9.3, respectively.[119] In the 0.1M aqueous solutions of CF_3CH_2ONa and $(CF_3)_2CHONa$, more than 90% of the compounds are the ionic species.

CF_3CH_2ONa and $(CF_3)_2CHONa$ were easily made from the corresponding alcohols. Treating CF_3CH_2OH and $(CF_3)_2CHOH$ with NaH in diethyl ether (eq. 3-10, 3-11) gave the two salts as white solids.

$$CF_3CH_2OH + NaH \xrightarrow[\text{Quant. yield}]{\text{Diethyl ether}} CF_3CH_2ONa \qquad \text{(eq. 3-10)}$$

$$(CF_3)_2CHOH + NaH \xrightarrow[\text{Quant. yield}]{\text{Diethyl ether}} (CF_3)_2CHONa \qquad \text{(eq. 3-11)}$$

The results in Table 3-10 show that the alkoxides are unexpectedly reactive towards H-abstraction by $\cdot R_fSO_3Na$ radical. Their global H-donating rates are all more than $7 \times 10^5\ M^{-1}s^{-1}$!

Both of CF_3CH_2ONa and $(CF_3)_2CHONa$ are bases. A control reaction was run to check whether the product HR_fSO_3Na was from radical process or from ionic process. IR_fSO_3Na reacted with 15 equivalents of CF_3CH_2ONa in D_2O under the same reaction conditions of the kinetic studies (degassed, and irradiated with UV light) for 14.5 hours. ^{19}F NMR showed complete consumption of the iodide compound, and HR_fSO_3Na was formed as a single product. This confirms that the reactions of IR_fSO_3Na and alkoxides go through a radical process.

Table 3-11 shows the reactivity difference between alcohols and the corresponding alkoxides. CF_3CH_2ONa is 1400 times more reactive than CF_3CH_2OH, and $(CF_3)_2CHONa$ is 300 times more reactive than $(CF_3)_2CHOH$!

Table 3-10 Absolute Rates of H-abstraction from Alkoxides by $\cdot R_fSO_3Na$ Radical, Measured by Competition in Aqueous Solution at 298K

Substrate	$k_{H\ overall}/k_{D\ THF\text{-}d8}$	$k_{H\ Overall}$ / 10^4 $M^{-1}s^{-1}$	$k_{H\ per\ H}$/ 10^4 $M^{-1}s^{-1}$
CF_3CH_2ONa	26.5 (±1.3)	71.8 (±11.9)	35.9 (±6.0)
$(CF_3)_2CHONa$	28.2 (±1.1)	76.4 (±12.5)	76.4 (±12.5)

Table 3-11 Comparison of the Rate Constants of Alcohols and Alkoxides towards H-Abstraction by $\cdot R_fSO_3Na$ Radical

Substrate	$k_{H\ per\ H}$/ 10^4 $M^{-1}s^{-1}$	Relative $k_{H\ per\ H}$
CF_3CH_2ONa	35.9 (±6.0)	1410 (±86)
CF_3CH_2OH	0.0254 (±0.0041)	1
$(CF_3)_2CHONa$	76.4 (±12.5)	299 (±23)
$(CF_3)_2CHOH$*	0.255 (±0.043)	1

* Indirect measurement by $(CF_3)_2CHOH$–CD_3OD–CH_3OH–THF-d8

The rate constant of H-abstraction from $(CF_3)_2CHOH$ by $\cdot R_fSO_3Na$ radical was obtained by an indirect competition with THF-d8 through three conversions. The error must been accumulated thus the reliability of the data is lower than that of other data. Because the direct competition was between $(CF_3)_2CHOH$ and CD_3OD, the competition experiment of $(CF_3)_2CHONa$ and CD_3OD was carried out (shown in Table 3-12). Compared with the same D-donor: CD_3OD, the relative rates also show that $(CF_3)_2CHONa$ is 280 times more reactive than $(CF_3)_2CHOH$. The rate enhancement is the same as measured by the indirect way when errors are considered.

Table 3-12 Comparison of the Relative Rate Constants of Alcohols and Alkoxides towards H-Abstraction by $\cdot R_fSO_3Na$ Radical, Relative to D-Abstraction Rate from CD_3OD

Substrates	$k_{H\ overall}/k_{D\ Methanol\text{-}d4}$	Relative $k_{H\ overall}$
$(CF_3)_2CHONa$	693 (±35)	280 (±20)
$(CF_3)_2CHOH$	2.47 (±0.12)	1

The C-H bond dissociation energies of these compounds in gas phase were calculated and summarized in Table 3-13.[120] The BDE of CF_3CH_2OH and $CF_3CH_2O^-$ could be calculated with CBS4 and B3LYP methods. Though the absolute numbers of the BDE calculated using the two methods exhibit large differences (ca. 5 kcal/mol), the ΔBDE's are very similar. Compared with –OH group, the oxygen anion weakens its α-CH bond by about 23 kcal/mol in gas phase!

The BDE's of $(CF_3)_2CHOH$ and $(CF_3)_2CHO^-$ were not able to be obtained using CBS4 method, and they were calculated only by the B3LYP method. We believe B3LYP is a fairly reliable method for the calculation of ΔBDE, because by using either method the calculated values of ΔBDE for CF_3CH_2OH and $CF_3CH_2O^-$ are very similar. The C-H bond ΔBDE for $(CF_3)_2CHOH$ and $(CF_3)_2CHO^-$ is calculated to be 23.7kcal/mol!

The calculated gas phase α-C-H bond BDE differences for alkoxides and their corresponding alcohols are very large (ca. 23 kcal/mol). The number will differ for aqueous reactions because of the solvation by water molecules, but the gas phase ΔBDE's nevertheless give one an idea as why the alkoxides are much more reactive than their corresponding alcohols. The O^- weakens it's α-C-H bond much more effectively than an –OH group. In other words, the radicals are stabilized more by an adjacent O^- than by an –OH group.

Table 3-13 Calculated C-H BDE Using CBS4 and B3LYP Methods

Substrate	CBS4 Calculation		B3LYP Calculation	
	BDE (kcal/mol)	ΔBDE (kcal/mol)	BDE (kcal/mol)	ΔBDE (kcal/mol)
CF_3CH_2OH	97.5	22.6	92.6	23.5
$CF_3CH_2O^-$	74.9	/	69.1	/
$(CF_3)_2CHOH$	/	/	90.7	23.7
$(CF_3)_2CHO^-$	/	/	67.0	/

The huge activation effect of anionic oxygen towards α-bond cleavage has been observed before. For example, oxy-Cope reactions are markedly catalyzed by base, [121, 122] such base-catalyzed reactions being called anionic oxy-Cope rearrangement. When the C-3 hydroxyl group is converted to its alkoxide, the reaction is accelerated by factors of 10^{10}-10^{17}.[123]

Ethers. The absolute rate constants of $CH_3OCH_2CH_2OCH_3$ and THF are provided in Table 3-14.

Table 3-14 Absolute Rates of H-abstraction from Ethers by $\cdot R_fSO_3Na$ Radical, Measured by Competition in Aqueous Solution at 298K

Substrate	$k_{H\ overall}/k_{D\ THF\text{-}d8}$	$k_{H\ Overall}$ / 10^4 $M^{-1}s^{-1}$	$k_{H\ per\ H}$/ 10^4 $M^{-1}s^{-1}$
$CH_3OCH_2CH_2OCH_3$	1.31(±0.02)	3.55 (±0.56)	0.888 (±0.140)
THF	7.87 (±0.38)	21.3 (±3.5)	5.32 (±0.88)

Carbonyl compounds. The absolute rate constants of carbonyl compounds are provided in Table 3-15. Acetone and acetic acid both have very low reactivity towards H-abstraction by $\cdot R_fSO_3Na$ radical in aqueous solution. The rate constants of CH_3COCH_3 and CH_3COOH are 60 and 96 times (per H), respectively, less than that of CH_3OH! The electron-withdrawing groups (-CO- and –COOH) slow down the H-abstraction reaction by the electrophilic $\cdot R_fSO_3Na$ radical. This indicates that transition state polar effects are very important for this reaction.

Propionic acid is 40 times more reactive than acetic acid ($k_{H\ overall}$). This rate enhancement is much more than that from methanol to ethanol (ethanol is only 5.7 times more reactive than methanol for the overall rate constant). We think it is necessary to consider the regiochemistry of hydrogen transfer reaction from CH_3CH_2COOH. Chlorine atom, a strong electrophilic radical, prefers to abstract hydrogens from the β position of CH_3CH_2COOH because of polar effect. At 80°C, the relative H-abstraction rate of α-H is only 0.03 times as that of the β-H (per H) towards Cl· radical.[124] In this study, the CH_3- group of CH_3CH_2COOH should also make large contribution for the hydrogen transfer by the electrophilic $\cdot R_fSO_3Na$ radicals.

It is interesting to notice that the salts of the carboxylic acids are more reactive than their corresponding acids. CH_3COONa reacts 6 times faster than CH_3COOH, and CH_3CH_2COONa reacts 2 times faster than CH_3CH_2COOH. The F value of $-COO^-$ is –0.10, and that of –COOH is 0.34.[116] Inductively $-COO^-$ is an electron-donating group, while –COOH is an electron-withdrawing group. This must cause the carboxylate compounds to be more reactive than their corresponding carboxylic acids towards the $\cdot R_fSO_3Na$ radical.

Table 3-15 Absolute Rates of H-abstraction from Carbonyl Compounds by $\cdot R_fSO_3Na$ Radical, Measured by Competition in Aqueous Solution at 298K

Substrate	$k_{H\ overall}/k_{D\ THF\text{-}d8}$	$k_{H\ Overall}$ / $10^4\ M^{-1}s^{-1}$	$k_{H\ per\ H}$/ $10^4\ M^{-1}s^{-1}$
CH_3COCH_3	0.0146 (±0.0010)	0.0396 (±0.0068)	0.00660 (±0.00113)
CH_3COOH	0.00455 (±0.00053)	0.0123 (±0.0024)	0.00410 (±0.00080)
CH_3COONa	0.0284 (±0.0020)	0.0770 (±0.0134)	0.0257 (±0.0045)
CH_3CH_2COOH	0.180 (±0.006)	0.488 (±0.079)	0.163 (±0.026)*
CH_3CH_2COONa	0.362 (±0.021)	0.981 (±0.166)	0.327 (±0.055)*

* Only hydrogens from CH_3- are counted.

Other hydrogen sources – thiol, silanes, and phosphorus acid. The absolute rate constants of water-soluble thiol ($HSCH_2CH_2SO_3Na$), two silanes, and phosphorus acid are provided in Table 3-16.

Table 3-16 Absolute Rates of H-abstraction from Thiol, Silanes, and Phosphorus Acid by $\cdot R_fSO_3Na$ Radical, Measured by Competition in Aqueous Solution at 298K

Substrate	$k_{H\ overall}/k_{D\ THF\text{-}d8}$	$k_{H\ Overall}$ / $10^4\ M^{-1}s^{-1}$	$k_{H\ per\ H}$/ $10^4\ M^{-1}s^{-1}$
$HSCH_2CH_2SO_3Na$	96.0 (±8.1)	260 (±35)[b]	260 (±35)[b]
$(HOCH_2CH_2CH_2)_3SiH$	28.1 (±1.6)	76.2 (±12.8)	76.2 (±12.8)
$Me_3N^+CH_2SiMe_2H\ Br^-$*	20.5 (±0.8)	55.6 (±9.1)	55.6 (±9.1)
H_3PO_3	3.48 (±0.10)	9.43 (±1.52)	9.43 (±1.52)

* Used without purification.

Thiol is the most reactive compound among all the substrates studied. This has been recognized by mechanistic and synthetic chemists. Actually benzene thiol and tert-butyl thiol are widely used reducing reagents.[125-127]

The two water-soluble silanes are all pretty reactive compounds. The reduction reactions are very efficient because the reactions of IR_fSO_3Na and the silanes could be complete in 2~3 hours, which is much less than the 24 hours reaction time needed for other substrates. They all give quantitative yield of the reduced product. The radical chain must proceed better with the silanes as H-Donors than the C-H compounds.

The H_3PO_3 is also a pretty good H-Donor. Actually several recent publications have described the use of phosphorus-centered radicals as chain carrier in reactions such as de-oxygenations and de-halogenations.[105, 128]

Summary of the Absolute Rate Constants of H-abstraction by $\cdot R_fSO_3Na$ Radical in Aqueous Solution

Table 3-17 Absolute Rates of H-abstraction from Organic Substrates by $\cdot R_fSO_3Na$ Radical, Measured by Competition in Aqueous Solution at 298K

Substrate	$k_{H\ Overall}$ / 10^4 $M^{-1}s^{-1}$	$k_{H\ per\ H}$/ 10^4 $M^{-1}s^{-1}$	$k_{H\ rel}$
CH_3OH	1.18 (±0.19)	0.393 (±0.063)	1
CH_3CH_2OH	6.72 (±1.14)	3.36 (±0.57)	8.55
$(CH_3)_2CHOH$	35.2 (±6.0)	35.2 (±6.0)	89.6
$HOCH_2CH_2OH$	3.47 (±0.56)	0.868 (±0.140)	2.21
$(CH_3CHOH)_2$	15.0 (±2.4)	7.50 (±1.20)	19.1
$HOCH_2COOCH_3$	1.61 (±0.27)	0.805 (±0.135)	2.05
CF_3CH_2OH	0.0509 (±0.0083)	0.0254 (±0.0041)	0.0646
$(CF_3)_2CHOH^*$	0.255 (±0.043)	0.255 (±0.043)	0.649
CF_3CH_2ONa	71.8 (±11.9)	35.9 (±6.0)	91.3

Table 3-17 –continued

Substrate	$k_{H\ Overall}$ / $10^4\ M^{-1}s^{-1}$	$k_{H\ per\ H}$/ $10^4\ M^{-1}s^{-1}$	$k_{H\ rel}$
$(CF_3)_2CHONa$	76.4 (±12.5)	76.4 (±12.5)	194
$CH_3OCH_2CH_2OCH_3$	3.55 (±0.56)	0.888 (±0.140)	2.26
THF	21.3 (±3.5)	5.32 (±0.88)	13.5
CH_3COCH_3	0.0396 (±0.0068)	0.00660 (±0.00113)	0.0168
CH_3COOH	0.0123 (±0.0024)	0.00410 (±0.00080)	0.0104
CH_3COONa	0.0770 (±0.0134)	0.0257 (±0.0045)	0.0654
CH_3CH_2COOH	0.488 (±0.079)	0.163 (±0.026)**	0.415
CH_3CH_2COONa	0.981 (±0.166)	0.327 (±0.055)**	0.832
$HSCH_2CH_2SO_3Na$***	260 (±35)	260 (±35)	662
$(HOCH_2CH_2CH_2)_3SiH$	76.2 (±12.8)	76.2 (±12.8)	194
$Me_3N^+CH_2SiMe_2H\ Br^-$	55.6 (±9.1)	55.6 (±9.1)	141
H_3PO_3	9.43 (±1.52)	9.43 (±1.52)	24.0

* Indirect measurement by $(CF_3)_2CHOH$ ----- CH_3OH -d4 ----- CH_3OH ----- THF-d8
** Only hydrogens of CH_3- are counted
*** Rate and standard deviation is from the competition between $HSCH_2CH_2SO_3Na$ and $CH_2{=}CHCH_2CH_2COONa$

This study covers substrates with a wide range of reactivities (63,400 fold per H). The huge reactivity differences of these compounds derive from a combination of thermodynamic, transition polar, and field effect.

It is obvious that the polarity of the transition state plays a significant role in the H-abstraction reaction by $\cdot R_fSO_3Na$ radical in aqueous solution. All of the unreactive substrates are electron-deficient compounds: CF_3CH_2OH, $(CF_3)_2CHOH$, CH_3COCH_3, CH_3COOH, CH_3COONa, and CH_3CH_2COOH.

The anionic moiety of the molecule could increase reactivity towards H-abstraction by $\cdot R_fSO_3Na$ radical. Alkoxides have much higher reactivities than their corresponding alcohols. And carboxylates also react faster than the carboxylic acids.

Solvent Effect of the H-abstraction Reactions by $\cdot R_fSO_3Na$ Radical

The rate constants of hydrogen abstraction reactions by perfluoro-n-alkyl radical from some of the compounds in nonpolar solvents were determined in previous study.[87] The results were compared in Table 3-18.

Table 3-18 Absolute Rate Constants of H-Abstraction Reactions by Fluorinated Radicals in Solution, Measured by Competition Method

Substrate	k_H overall in $H_2O/10^4M^{-1}s^{-1}$ (by $\cdot R_fSO_3Na$)	k_H overall in 1,3-BTB/$10^4M^{-1}s^{-1}$ (by $\cdot C_4F_9$)	k_H overall in H_2O/ k_H overall in 1,3-BTB
CH_3OH	1.18 (±0.19)	0.092 (±0.019)*	13
CH_3CH_2OH	6.72 (±1.14)	0.301 (±0.065)	22
$(CH_3)_2CHOH$	35.2 (±6.0)	1.63 (±0.33)*	22
$(CH_3CHOH)_2$	15.0 (±2.4)	0.50 (±0.11)*	30
$CH_3OCH_2CH_2OCH_3$	3.55 (±0.56)	0.67 (±0.14)*	5.3
THF	21.3 (±3.5)	3.10 (±0.61)*	6.9

*Ref 87

All of the H-abstraction reactions by the $\cdot R_fSO_3Na$ radical in water are faster than those by $\cdot C_4F_9$ radical in the non-polar organic solvent, 1,3-BTB. Because of the importance of transition state polar effects, the H-abstraction reaction by the electrophilic fluorinated radicals is accelerated in the polar solvent, water.

The rate enhancement is more for the compounds with –OH groups than the ethers. This might be because of the H-bonding formed between the –OH group and H_2O molecules. As discussed earlier in this chapter, the anionic oxygen of alkoxides weakens its α-CH bond, thus the hydrogen transfer process is facilitated greatly. The H-bonding of ROH in aqueous solutions can make the oxygen bearing partially negative charge, as shown in Figure 3-3. This can activate the α-CH bond of the hydroxyl group, make the alcohols better hydrogen donors in water than in 1,3-BTB.

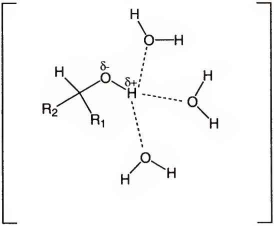

Figure 3-3 Activation of α-CH Bond by H-Bonding in H_2O

Kinetic Isotope Effects of H-abstraction Reactions by $\cdot R_fSO_3Na$ Radical in Aqueous Solution

The competition between CH_3OH and CD_3OD towards H-abstraction by $\cdot R_fSO_3Na$ radical shows a fairly large isotope effect:

$$k_{H\ Methanol} / k_{Methanol\text{-}d4} = 11.4\ (\pm\ 0.4)$$

This value differs a lot from the isotope effect of THF:

$$k_{H\ THF}/k_{D\ THF\text{-}d8} = 7.87\ (\pm 0.38)$$

We noticed that methanol has a larger kinetic isotope effect (KIE) than THF, while methanol is less reactive than THF towards H-abstraction by $\cdot R_fSO_3Na$ radicals. The kinetic isotope effects of several substrates with different reactivities were measured, to determine whether there is a general relationship between the KIE and the H-transfer reactivity towards $\cdot R_fSO_3Na$ radicals. We chose compounds with a broad range of C-H transfer reactivities.

As expected, among the six compounds studied the faster the compound donates hydrogen to $\cdot R_fSO_3Na$ radical, the smaller is its KIE value. The most reactive, $(CH_3)_2CHOH$, has a KIE of 5.84, whereas the KIE for CH_3COOH is 22.2. All of the KIE values are given in Table 3-19.

Table 3-19 Kinetic Isotope Effect of H-abstraction Reactions by $\cdot R_fSO_3Na$ Radical in Water, Photochemical Reaction at 298K

Entry	Substrates	k_H/k_D	$k_{H\ overall}$ / 10^4 $M^{-1}s^{-1}$
1	Iso-propanol	5.84 (±0.10)	35.2 (±6.0)
2	THF	7.87 (±0.38)	21.3 (±3.5)
3	Ethanol	8.78 (±0.18)	6.72 (±1.14)
4	Methanol	11.4 (±0.4)	1.18 (±0.19)
5	Acetone	17.0 (±0.4)	0.0396 (±0.0068)
6	Acetic Acid	22.2 (±0.7)	0.0123 (±0.0024)

It is noticed that the KIE values are fairly large, especially for methanol, acetone, and acetic acid. The values for these three compounds are much larger than the normal primary kinetic isotope effect. Is this possibly caused by tunneling?

To obtain evidence for tunneling effect of this reaction, a temperature dependence of the KIE of acetone was studied by Dolbier and his coworkers.[129] As shown in Table 3-20, the KIE value decreases at higher temperature. There is a linear relationship between $\ln(k_H/k_D)$ and 1/T (Figure 3-4).

Table 3-20 Temperature Dependence of KIE of Acetone, towards the H-abstraction Reactions of $\cdot R_fSO_3Na$ Radicals in Water

Entry	T(°K)	1/T	k_H/k_D	$\ln(k_H/k_D)$
1	24	0.00337	16.6 (± 0.7)	2.81
2	56	0.00304	12.6 (±0.1)	2.53
3	80	0.00283	10.2 (±0.5)	2.32

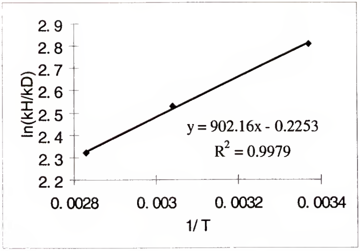

$$Ea^D - Ea^H = 1.79 \text{ kcal/mol}$$

$$A^D/A^H = 1.25$$

Figure 3-4 Plot of $\ln(k_H/k_D)$ of Acetone vs. 1/T

There are three criteria for establishing the occurrence of tunneling: (a) ($Ea^D - Ea^H$) is more than 1.2kcal/mol, (b) A^D/A^H is greater than unity, and (c) an observed k_H/k_D

is greater than that calculated for the system.[130] The first two criteria are met for such a reaction.

A model calculation is carried out by Dolbier and his coworker.[131] DFT calculation gives the KIE value for hydrogen abstraction reaction by $CF_3\cdot$ radical from acetone at room temperature to be 6.79. This value is much lower than the experimental result. This indicates that tunneling effect involves in the hydrogen abstraction reactions by perfluoro-n-alkyl radicals from acetone.

Conclusion

The kinetics of H-abstraction reaction in aqueous solution by $\cdot R_fSO_3Na$ radical from a variety of organic compounds are studied. The absolute H-abstraction reaction rate constants are measured with competition kinetic methodology, by competing with D-abstraction from THF-d8.

The substrates are alcohols, diols, alkoxides, ethers, ketone, carboxylic acids and salts, thiol, silanes, and phosphorous acid. A wide range of substrate reactivities (63,400-fold) was observed. The results imply that thermodynamic effects, transition state polar effects, and field effects all play a role in such H-abstraction reactions. Among the neutral hydrocarbon compounds, alcohols are more reactive than ketone and carboxylic acids. It is noticed that the α-CH bonds of alkoxides are so activated that the alkoxides are much more reactive than their corresponding alcohols towards the $\cdot R_fSO_3Na$ radical. The gas phase BDE's of the alcohols and alkoxides are calculated by Dolbier and his coworker. The α-CH bond is weakened greatly by the anionic oxygen.

Significant solvent effects are observed for the H-abstraction reactions by fluorinated radicals. It is found that H-abstraction reactions are faster in water than in the non-polar organic solvent, 1,3-BTB.

Kinetic isotope effects for H-abstraction reactions by $\cdot R_fSO_3Na$ radical in aqueous solution are also studied. Larger KIE's are observed for compounds having less reactive C-H bonds. A temperature dependence study of the KIE and DFT calculation indicate that there is tunneling effect involved in such a reaction.

CHAPTER 4
SUMMARY

The absolute kinetics of prototypical fluoroalkyl radical reactions in solution have been measured previously by a combination of laser flash photolysis (LFP), product analyses, and conventional competitive kinetics. Kinetic studies of perfluoro-n-alkyl radical addition reactions and hydrogen abstraction reactions have been conducted in non-polar organic solvents, such as F113, benzene, and 1,3-BTB. The great electrophilicity of perfluoro-n-alkyl radicals has been demonstrated in those reactions. The transition state polar effect plays an extremely important role for the reactions of $R_f\cdot$ radicals.

Solvent polar effects can affect a radical reaction that goes through a polar transition state. In the current study, the kinetics of addition reactions and hydrogen abstraction reactions of a perfluoro-n-alkyl radical were measured in polar aqueous media. Most commercial fluoropolymers are now made by dispersion, emulsion, or suspension radical polymerization in aqueous media. Therefore it is also very important for the polymer industry to obtain the kinetic data of fluorinated radical reactions in aqueous solution.

Addition Reactions of Perfluoro-n-alkyl Radical in Aqueous Solution

Absolute rate constants of $\cdot CF_2CF_2OCF_2CF_2SO_3Na$ radical (abbreviated as $\cdot R_fSO_3Na$) addition to water-soluble alkenes containing ionic substituents (shown in Scheme 4-1) in aqueous solution are measured by LFP experiments.

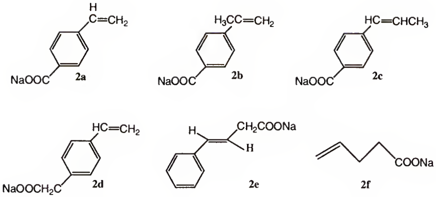

Scheme 4-1 Water-Soluble Alkenes

Equation 4-1 provides the addition reaction. Absolute rate constants k_{add} are determined to be from 1.88 x $10^{7}M^{-1}s^{-1}$ to 5.53 x $10^{8}M^{-1}s^{-1}$ for different alkenes. Thermodynamic, polar, and steric effects all play roles in such a reaction.

$$\mathbf{IR_fSO_3Na} \xrightarrow[H_2O]{hv,\ 308\ nm} \mathbf{\cdot R_fSO_3Na + R_1R_2C{=}CR_3R_4} \xrightarrow{k_{add}} \mathbf{R_1R_2\dot{C}\text{-}CR_3R_4R_fSO_3Na}\quad \textbf{(Eq. 4-1)}$$

The rate constants are compared with those of some analogous reactions, which have been determined in a non-polar organic solvent, F113. Aqueous reactions are all faster than the analogous reactions carried out in F113, and 3~9 folds rate increase are observed. Although the solvent effect is not large, it is unambiguous that the addition reactions of electrophilic perfluoro-n-alkyl radicals are faster in polar solvent water than in a non-polar organic solvent.

Hydrogen Atom Abstraction Reactions of Perfluoro-n-alkyl Radical in Aqueous Solution

The kinetics of H-abstraction reactions from a variety of organic compounds by perfluoro-n-alkyl radical ($\cdot R_fSO_3Na$) have been measured by competition kinetic methodology (shown in Scheme 4-2) in aqueous solution. Several competition reactions were conducted by using different pairs of hydrogen transfer agents and alkenes. Finally it was found that the competition experiment between H-abstraction reaction from $HSCH_2CH_2SO_3Na$ and addition reaction to $CH{=}CHCH_2CH_2COONa$ gave reliable results. Thus the absolute H-abstraction rate constant from $HSCH_2CH_2SO_3Na$ by the $\cdot R_fSO_3Na$ was obtained. Another competition of H-transfer from $HSCH_2CH_2SO_3Na$ with D-transfer from THF-d_8 gives the absolute D-transfer rate to $\cdot R_fSO_3Na$ radical in water.

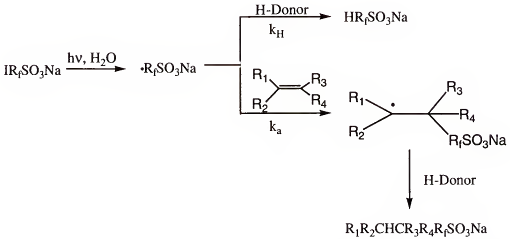

Scheme 4-2 Competition Reactions of Addition and H-Abstraction by $\cdot R_fSO_3Na$ Radical

The kinetics of hydrogen abstraction by $\cdot R_fSO_3Na$ radical from several types of functionalized organic compounds were then determined, with the competition between H-transfer agents and THF-d_8. The hydrogen atoms come from C-H bonds of alcohols, alkoxides, ethers, carbonyl compounds; S-H bond of a thiol; Si-H bond of silanes; and P-H bond of H_3PO_3.

A wide range of substrate reactivities (63,400-fold) was observed. The results imply that thermodynamic effects, transition state polar effects, and field effects all play a role in such H-abstraction reactions. Among the neutral hydrocarbon compounds, alcohols are more reactive than ketone and carboxylic acids. It is noticed that the α-CH bonds of alkoxides are so activated that the alkoxides are much more reactive than their corresponding alcohols towards the $\cdot R_fSO_3Na$ radical. The gas phase BDE's of the alcohols and alkoxides are calculated by Dolbier and his coworker. The α-CH bond is weakened greatly by the anionic oxygen.

Significant solvent effects are observed for the H-abstraction reactions by fluorinated radicals. It is found that H-abstraction reactions are faster in water than in the non-polar organic solvent, 1,3-BTB.

Kinetic isotope effects for H-abstraction reactions by $\cdot R_fSO_3Na$ radical in aqueous solution are also studied. Larger KIE's are observed for compounds having less reactive C-H bonds. A temperature dependence study of the KIE and DFT calculation indicate that there is tunneling effect involved in such a reaction.

CHAPTER 5
EXPERIMENTAL

General Procedures

Experimental text that mentions “commercially available reagents” indicates that such materials were purchased from Aldrich, Fisher, Lancaster, and CIL. All reagents were used without further purification unless otherwise indicated in the text. Anhydrous solvents were dried by distilling from the appropriate drying agent and used immediately.

NMR spectra were obtained on Varian VXR-300, Mercury-300, or Gem-300 spectrometers. Chemical shifts are reported in ppm downfield from internal TMS for ^1H and ^{13}C NMR spectra, $CFCl_3$ for ^{19}F NMR spectra. Kinetic ^{19}F NMR measurements were performed at 282 MHz using a Varian VXR-300 spectrometer.

Melting points were determined on a Thomas Hoover Capillary melting point apparatus and are uncorrected. MS were obtained in a Finnigan MAT95Q. UV spectra were obtained on a Cary 100 UV-Visible spectrophotometer.

Experiments for Chapter 2

Preparation of Sodium 5-Iodo-3-Oxaoctafluoropentanesulfonate (1)

NaOH (2.9657g, 74.14mmol) was dissolved in 20 ml H_2O in a 100ml round bottom flask equipped with a condenser and stirring bar. To the flask was added tetrafluoro-2-(tetrafluoro-2-iodoethoxy)ethanesulfonyl fluoride ($ICF_2CF_2OCF_2CF_2SO_2F$) (15.7931g, 37.07mmol). The reaction mixture was stirred overnight at 95°C. ^{19}F NMR showed the complete consumption of the starting material. The pH value of this solution was 7. Vacuum was applied to remove H_2O, giving a solid residue. 20ml ethanol was added to the solid to dissolve compound **1**, leaving NaF undissolved. NaF was filtered from the solution. The filtrate was concentrated by rotary evaporation to give a white solid residue. After recrystallization from water, the title compound was obtained in 87% yield. CHN analysis shows the compound is $ICF_2CF_2OCF_2CF_2SO_3Na \cdot H_2O$.

m.p. 151°C, decomposed. ^{19}F NMR ($D_2O/CFCl_3$ in C_6D_6) δ -69.16 (s, 2F), -83.02 (t, 2H, J = 12.1Hz), -86.35 (s, 2H), -118.42 (s, 2H). MS (FAB) 469 (M+Na). CHN analysis calcd for $C_4H_2F_8INaSO_5$: C, 10.35, H, 0.43; found C, 10.36, H, 0.26

Preparation of Sodium p-Vinylbenzoate (2a)[113]

p-Vinylbenzoic acid (0.2348g, 1.58mmol) was dissolved in 5ml methanol in a 25ml round bottom flask equipped with a magnetic stir bar. Two drops of phenolphthalein solution (0.1% in ethanol) was added to the flask. NaOH solution (0.96M in methanol) was added to the reaction mixture dropwisely until the color of the mixture turned to light pink. Methanol was removed by rotary evaporator, giving a solid residue. The solid was washed with diethyl ether for 3 times, dried under reduced pressure. The title compound was obtained in 85% yield.

1H NMR (D_2O) δ 7.84 (d, 2H, J = 8.1Hz), 7.55 (d, 2H, J = 8.1Hz), 6.84 (dd, 1H, J1 = 11.1Hz, J2 = 17.4 Hz)

Preparation of 4-Bromo-α-methylstyrene

Into a 250 ml three-necked round bottom flask equipped with a magnetic stir bar, condenser with nitrogen inlet, pressure-equalizing additional funnel, and a rubber septum was placed methyltriphenylphosphonium bromide (14.73g, 41mmol) suspended in 50ml anhydrous THF. The suspension was cooled to 0°C with ice bath. The reaction mixture was charged slowly with n-BuLi (2.5M in hexanes, 16.5ml, 41mmol) to give an orange solution. After one hour, 4'-bromoacetophenone (6.8g, 34mmol) with 20ml THF was added slowly to the flask from the additional funnel. Then the ice bath was removed and the flask was warmed to room temperature gradually. After the reaction mixture was stirred overnight, TLC analysis of a small aliquot of the reaction mixture showed complete consumption of the starting material. 50ml Brine was added to the mixture and the clear solution was extracted with three 100ml portions of benzene. The combined organic fractions were dried over $MgSO_4$, and benzene was removed by rotary evaporator. The liquid residue was purified with column chromatography (eluting solvent: hexanes) to give the title compound as a colorless liquid in 83% yield.

Preparation of 4-(α-Methyl)vinylbenzoic acid[114]

A two-neck 50ml round bottom flask equipped with magnetic stir bar, nitrogen inlet and rubber septum was flushed with nitrogen. 4-Bromo-α-methylstyrene (1.03g, 5.23mmol) was added to the flask with 20ml anhydrous diethyl ether and cooled to –30°C. The flask was charged slowly with n-BuLi (2.5M in Hexanes, 2.3 ml, 5.75 mmol). After the dry ice bath was removed, the temperature increased to room temperature. The mixture was allowed to stir for an additional 1 hour at room temperature before it was cooled to -70°C, and poured on dry ice powder, acidified with 5% HCl to pH = 3. The layers were separated, and the aqueous layer was washed with 20ml diethyl ether. The organic solution was washed once with 30ml 5% NaOH and once with 20ml H_2O. The aqueous layers were combined and acidified (pH = 2) with 10% HCl to give a white precipitate. This suspension was extracted with three 50ml portions of diethyl ether. The combined ether solution was dried over $MgSO_4$, and ether was removed by rotary evaporator to give the acid as a white solid in 84% yield. The product was recrystallized from water.

^1H NMR ($CDCl_3$): δ 8.07 (d, 2H, J = 8.3Hz), 7.56 (d, 2H, J = 8.3Hz), 5.50 (bs, 1H), 5.23 (bs, 1H), 2.19(s, 3H)

Preparation of Sodium 4-(α-methyl)Vinylbenzoate (2b)

4-(α-Methyl)benzoic acid (1.0216g, 6.30mmol) was dissolved in 10ml ethanol in a 25ml round bottom flask. NaOH solution (0.4835M, 6.31ml, 3.05mmol) was added to the flask, some white solid precipitated out. The solid was filtered and washed with ethanol, then dried under reduced pressure to give the title compound in 45% yield.

^1H NMR (D2O): δ 7.83 (d, 2H, J = 8.3Hz), 7.60 (d, 2H, J = 8.3Hz), 5.52 (s, 1H), 5.21 (s, 1H), 2.15 (s, 3H)

Preparation of 4-Bromo-β-methylstyrene

Into a 250 ml three-necked round bottom flask equipped with a magnetic stir bar, condenser with nitrogen inlet, pressure-equalizing additional funnel, and a rubber septum was placed ethyltriphenylphosphonium bromide (13.36g, 36mmol) suspended in 50ml anhydrous THF. The suspension was cooled to -5°C with salt ice bath. n-BuLi (2.5M in hexanes, 14.4ml, 36mmol) was added to the reaction mixture slowly to give a red solution. After one hour, 4-bromobenzaldehyde solution (5.55g, 30mmol in 50ml THF) was slowly added to the flask from the additional funnel. Then the ice bath was removed and the flask was warmed to room temperature gradually. After the reaction mixture was stirred for 10 hours, TLC analysis of a small aliquot of the reaction mixture showed complete consumption of the starting material. 50ml Brine was added to the reaction mixture and the clear solution was extracted with three 60ml portions of benzene. The combined organic fractions were dried over $MgSO_4$. Benzene was removed by rotary evaporator leaving the residue as a mixture of solid and oil. The oil was dissolved in 100ml diethyl ether and the undissolved solid was filtered. Ether was removed from the filtrate to give an oily residue, which was purified with column chromatography (eluting solvent as hexanes). The title compound was obtained as a colorless liquid in 90% yield.

^1H NMR ($CDCl_3$): δ 7.38-7.46 (m, 2H), 7.14-7.20 (m, 2H), [6.24-6.37 (m)+5.82 (dq)] (2H), 1.86 (m, 2H)

Preparation of 4-(β-Methyl)vinylbenzoic Acid

4-Bromo-β-methylstyrene (2.87g, 14.6mmol) was dissolved in 170ml anhydrous THF in a 3-neck round bottom flask equipped with a magnetic stir bar, a condenser with nitrogen inlet, and a rubber septum. The flask was cooled in a dry ice/isopropanol bath to -75°C. t-BuLi (1.7M in pentane, 17.2ml, 29.3mmol) was added to the flask via syringe slowly. The color of the solution turned to dark green. The solution was stirred at -75°C for an additional 1.5hours. CO_2 gas (generated from HCl and Na_2CO_3 and dried by passing through conc. H_2SO_4) was bubbled into the solution for 30 minutes. TLC analysis of a small aliquot of the reaction mixture showed complete consumption of the starting material. After the dry ice bath was removed and temperature increased to room temperature, 30ml water was added to the flask and the reaction mixture was acidified (pH = 1) with 10% HCl. The mixture was extracted with 30ml CH_2Cl_2 three times. The combined organic layers wete dried over $MgSO_4$. Rotary evaporating solvent gave the crude product in 97% yield. The solid product was recrystallized from ethyl acetate.

^{1}H NMR (Acetone-d6): δ 8.10-8.18 (m, 2H), 7.58-7.66 (m, 2H), 6.57-6.70 (m) + 6.07 (dq) (2H), 2.05 (m, 3H)

Preparation of Sodium 4-(β-Methyl)vinylbenzoate (2c)

Compound **2c** was prepared from 4-(β-methy)vinylbenzoic acid in a manner identical to the preparation of compound **1a**, with 69% yield.

Preparation of 4-Vinylphenylacetic Acid[115]

4-Vinylbenzyl chloride (4.69g, 30.7mmol) in 3ml CH_3CN was added to a mixture of 18-crown-6 (0.49g, 1.3mmol) and powdered KCN (2.99g, 46mmol) in 23ml anhydrous CH_3CN in a 3-neck round bottom flask equipped with a thermometer, nitrogen inlet, pressure-equalizing additional funnel, and a magnetic stir bar. The temperature of the reaction mixture rose quickly to 40°C and was kept at this temperature during the addition of 4-vinylbenzyl chloride. After the reaction mixture was stirred for an additional 15 hour, TLC (hexanes:ether = 5:1) analysis showed complete consumption of the starting material. CH_3CN was removed by rotary evaporator and the residue was partitioned between 25ml water and 30ml ether. The ethereal layer was washed once with water, twice with brine, dried over $MgSO_4$, and concentrated to afford a light yellow green liquid. The liquid was purified with column chromatography to give 4-vinylphenylacetonitrile in 64% yield.

In a 100ml 3-neck round bottom flask equipped with a magnetic stir bar, a condenser, and a nitrogen inlet, 4-vinylphenylacetonitrile (1.5g, 10.5 mmol) and hydroquinone (0.025g) were dissolved in 25ml 95% ethanol. KOH (87.7%, 4.75g, 74.4mmol) was added to the flask and the reaction mixture was heated at reflux for 5 hours with a slow stream of nitrogen passing through the flask to remove NH_3. TLC (hexanes: ethyl acetate = 1:1) analysis showed the complete consumption of the starting material. 30ml water was added to the flask, and the mixture was washed with two 30ml portions of diethyl ether. The aqueous solution was acidified (pH = 1) with concentrated HCl to and extracted with $CHCl_3$ (30ml x 3). The combined $CHCl_3$ layers were dried over $MgSO_4$, and evaporated to afford the title compound in 90% yield.

^{1}H NMR: δ 11.35 (bs, 1H), 7.38 (d, 2H, J = 7.8Hz), 7.24 (d, 2H, J = 8.7Hz), 6.70 (dd, 1H, J_1 = 10.8Hz, J_2 = 17.4Hz), 5.73 (d, 1H, J = 17.4Hz), 5.24 (d, 1H, J = 10.8Hz), 3.64 (s, 2H)

Preparation of Sodium 4-Vinylphenylacetate (2d)

Compound **2d** was prepared from 4-vinylphenylacetic acid in a manner identical to the preparation of compound **1a**, with 98% yield.

Preparation of Sodium trans-Styrylacetate (2e)

Compound **2d** was prepared from commercially available trans-styrylacetic acid in a manner identical to the preparation of compound **1a**, with 91% yield.

Preparation of Sodium Pentenoate (2f)

Pentenoic acid (3.04g, 30.4mmol) was dissolved in 5ml diethyl ether in a 3-neck round bottom flask equipped with a magnetic stir bar, a nitrogen inlet, and a rubber septum. NaOH solution (1.167g in 7ml water, 29.2mmol) was added to the flask via syringe. The reaction mixture was stirred at room temperature for 3 hours and then was washed with ether. A 500ml portion of acetone was added to the aqueous solution to precipitate the product. The precipitate was filtered and dried under reduced pressure to give the title compound in 87% yield.

^{1}H NMR (D2O): δ 5.86 (m, 1H), 4.94-5.07 (m, 2H), 2.24 (m, 4H)

General Procedure for Kinetic Study

601 mg IR_fSO_3Na was dissolved in 50ml H_2O to make a 0.027M solution. This solution is very stable and can be used as a stock solution. All the styrene solutions (ca. 0.03M) were made freshly and used within one and a half hour after being made.

The series of quartz cuvettes were charged with1.5ml stock solution of IR_fSO_3Na with pipette and sealed with rubber septa. They were all degassed by bubbling N_2 through the solution for 10-15 minutes. The styrene solution was prepared during this time, and immediately degassed by bubbling N_2 through the solution for 20-30 minutes. Then the quartz cuvettes were charged with different portions of styrene solution with micro-liter syringes. The mixture was shaken well and immediately irradiated by the laser shot at 308nm for 7-9 times to get an average 1st order growth curve for the generation of benzylic radical, which is monitored at 320nm by UV-vis. The 1st order rate constants were obtained from the fitting curve with the best R value and were plotted with the concentrations of styrene to give a 2nd order rate constant.

Tables of Kinetic Data

Table 5-1 Pseudo 1st Order Rate Constants of $\cdot R_fSO_3Na$ Radical Addition to **2a**

Entry	V_{2a} (μl)	C_{2a} (x 10^{-3} mol/l)	1st Order Rate (x 10^5 s^{-1})	R
1	25	0.520	1.82	0.981
2	45	0.923	2.78	0.990
3	70	1.41	4.02	0.986
4	100	1.98	4.89	0.996
5	130	2.53	5.38	0.992
6	160	3.06	6.84	0.993
7	200	3.73	9.10	0.995
8	250	4.53	11.6	0.983

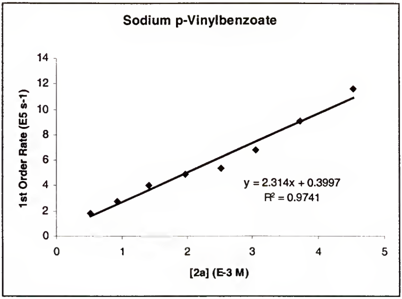

Figure 5-1 Plot of the Pseudo1st Order Rates vs. Concentration of **2a**

k_{2a} = 2.31 (± 0.15) x 10^8 M^{-1} s^{-1}

Table 5-2 Pseudo1st Order Rate Constants of $\cdot R_fSO_3Na$ Radical Addition to **2b**

Entry	V_{2b} (μl)	C_{2b} (x 10^{-3} mol/l)	1st Order Rate (x 10^5 s^{-1})	R
1	25	0.516	2.86	0.997
2	45	0.917	5.22	0.996
3	70	1.40	8.12	0.992
4	110	2.15	10.8	0.997
5	150	2.86	15.5	0.996
6	200	3.70	21.0	0.993

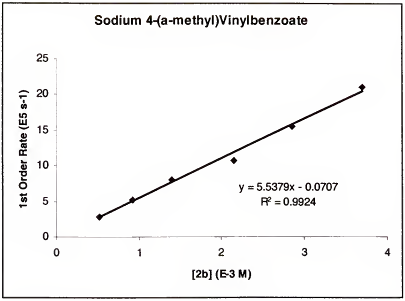

Figure 5-2 Plot of the Pseudo1st Order Rates vs. Concentration of **2b**

$k_{2b} = 5.54\ (\pm 0.24) \times 10^8\ M^{-1}\ s^{-1}$

Table 5-3 Pseudo1st Order Rate Constants of $\cdot R_fSO_3Na$ Radical Addition to **2c**

Entry	V_{2c} (μl)	C_{2c} (x 10^{-3} mol/l)	1st Order Rate (x 10^5 s^{-1})	R
1	75	1.55	0.819	0.976
2	100	2.04	0.884	0.986
3	150	2.96	1.06	0.963
4	200	3.84	1.48	0.978
5	250	4.66	1.85	0.962
6	300	5.43	2.00	0.946

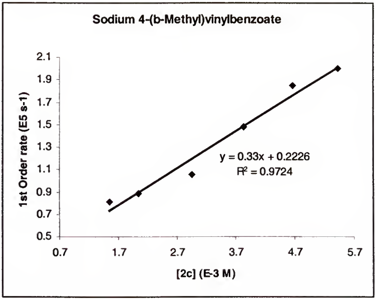

Figure 5-3 Plot of the Pseudo 1st Order Rates vs. Concentration of **2c**

$k_{2c} = 3.30\ (\pm 0.28) \times 10^7\ M^{-1}\ s^{-1}$

Table 5-4 Pseudo 1st Order Rate Constants of ·R_fSO_3Na Radical Addition to **2d**

Entry	V_{2d} (μl)	C_{2d} (x 10^{-3} mol/l)	1st Order Rate (x 10^5 s^{-1})	R
1	25	0.534	2.69	0.943
2	50	1.05	3.81	0.980
3	75	1.55	4.27	0.984
4	100	2.04	5.02	0.978
5	150	2.96	7.93	0.991
6	200	3.84	9.71	0.971
7	250	4.66	10.5	0.972

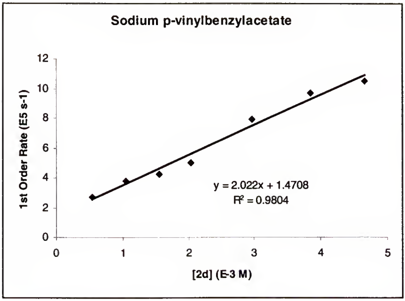

Figure 5-4 Plot of the Pseudo 1st Order Rates vs. Concentration of **2d**

$k_{2d} = 2.02\ (\pm 0.13) \times 10^8\ M^{-1}\ s^{-1}$

Table 5-5 Pseudo 1st Order Rate Constants of $\cdot R_fSO_3Na$ Radical Addition to **2e**

Entry	V_{2e} (μl)	C_{2e} (x 10^{-3} mol/l)	1st Order Rate (x 10^5 s^{-1})	R
1	250	4.66	0.726	0.904
2	300	5.43	0.906	0.930
3	350	6.17	0.982	0.916
4	400	6.86	1.18	0.973
5	450	7.52	1.30	0.916
6	500	8.15	1.37	0.974

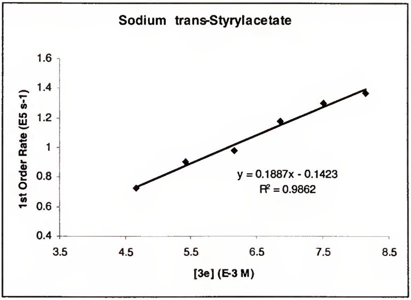

Figure 5-5 Plot of the Pseudo 1st Order Rates vs. Concentration of **2e**

$k_{2e} = 1.89\ (\pm 0.11) \times 10^7\ M^{-1}\ s^{-1}$

Table 5-6 Pseudo 1st Order Rate Constants of $\cdot R_fSO_3Na$ Radical Addition to **2f**

Entry	C_{2f}/ 10^{-3} mol/l	k_{exptl} / 10^5 s^{-1}	C_{2c} /10^{-3} mol/l	$k_{exptl} - k_{2c}$[**2c**] / 10^4 s^{-1}
1	1.09	1.25	1.98	5.97
2	1.61	1.38	1.95	7.36
3	2.12	1.64	1.92	10.1
4	3.08	1.75	1.86	11.4
5	4.00	1.80	1.81	12.0
6	4.86	2.03	1.76	14.5

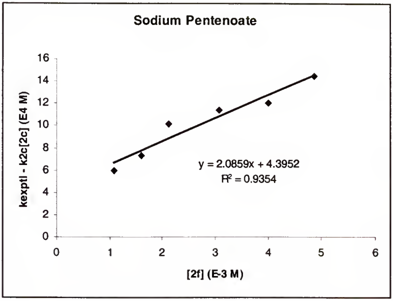

Figure 5-6 Plot of ($k_{exptl} - k_{2c}C_{2c}$) vs. Concentration of **2f**

k_{2f} = 2.08 (±0.27) x 10^7 M^{-1} s^{-1}

Experiments for Chapter 3

Preparation of Sodium 5-H-3-oxaoctafluoropentanesulfonate (3a)

$ICF_2CF_2OCF_2CF_2SO_3Na{\cdot}H_2O$ (0.28g, 0.60mmol) was dissolved in 45ml THF. The solution was degassed by passing nitrogen through for 30 minutes. After the solution was irradiated with UV light for 24 hours, ^{19}F NMR analysis showed complete consumption of the starting material. THF was removed by rotary evaporator. The solid residue was washed with hexanes, then with diethyl ether, and dried under reduced pressure to give the title compound in 88.3% yield.

m.p. :132°C, decomposed. ^1H NMR (Acetone-d6/TMS): δ 6.48 (tt, 1H, $J_1 = 3.42Hz$, $J_2 = 52Hz$), ^{19}F NMR (Acetone-d6/$CFCl_3$): δ -81.56 (m, 2F), -88.72 (bs, 2F), -117.62 (bs, 2F), -138.23 (dt, 2F, $J_1 = 4.3Hz$, $J_2 = 51.2Hz$). HRMS (FAB), (M+Na): calcd 342.9263; found 342.9256. CHN analysis calcd for $C_4F_8HNaO_4S{\cdot}H_2O$: C 14.21, H 0.89; found C 14.20, H 0.61

Preparation of Sodium 6,6,7,7-Tetrafluoro-7-(1,1,2,2-tetrafluoro-2-sodium sulfonate-ethoxy)-heptanate (4)

Tetrafluoro-2-(tetrafluoro-2-iodo-ethoxy)ethanesulfonyl fluoride ($ICF_2CF_2OCF_2CF_2SO_2F$, 6.56g, 15.4mmol), 4-pentenoic acid (0.91g, 9.09mmol), and AIBN (0.128g, 0.78mmol) were mixed in a Pyrex Rotaflo tube. The mixture was degassed by three cycles of freeze-pump-thaw, and then heated at 80°C for 2 days. ^1H NMR analysis showed complete consumption of 4-pentenoic acid.

The reaction mixture, 50ml ethanol, and activated zinc powder (2.8g, 43mmol) were mixed in a 3-neck round bottom flask equipped with a magnetic stir bar and a condenser. The flask was heated at 70°C for 2 hours, ^{19}F NMR showed complete consumption of the iodide compound. Ethanol was removed by rotary evaporator. Vacuum was applied to the residue to take away $HCF_2CF_2OCF_2CF_2SO_2F$.

The residue then was dissolved in 25ml ethanol in a 100ml round bottom flask with a magnetic stir bar. NaOH solution (1.102g in 10ml ethanol/5ml water, 27.55mol) was added to the flask. After being stirred at room temperature for 30 minutes, the mixture turned cloudy. The pH value of the mixture was 7. ^{19}F NMR analysis showed complete disappearance of $-SO_2F$ group. The reaction mixture was filtered, and the solvent in the filtrate was removed by rotary evaporator to give a solid residue. The solid was dissolved in 10ml water, then acidified with concentrated HCl to form white precipitate. The precipitate was filtered, dried under reduce pressure to give $NaSO_3(CF_2)_2O(CF_2)_2(CH_2)_4COOH$ in 26% overall yield.

^1H NMR (CD_3OD/CH_3OH): 2.34(t, 2H), 2.14 (m, 2H), 1.64 (m, 2H). ^{19}F NMR ($CD_3OD/CFCl_3$): -80.82 (m, 2F), -86.51 (m, 2F), -116.28 (m, 2F)

$NaSO_3(CF_2)_2O(CF_2)_2(CH_2)_4COOH$ (0.1435g, 0.342mmol) was dissolved in 5ml MeOH in a 25ml round bottom flask. One drop of phenolphthalein solution (0.1% in ethanol) was added to the flask. NaOH solution (ca. 0.402M in methanol) was added until the color of the solution turned to light pink. Methanol was removed, and the residue was washed with diethyl ether, dried under reduced pressure to afford the title compound in 94% yield.

^1H NMR (CD_3OD/CH_3OH): δ 2.23 (m, 2H), 2.13 (m, 2H), 1.63 (m, 4H). ^{19}F NMR ($CD_3OD/CFCl_3$): δ -82.46 (m, 2F), -88.20 (m, 2F), -117.95 (s, 2F), -118.12 (t, 2F, J = 17.09Hz). 13C NMR (CD_3OD/CH_3OH): δ 181.26, 37.88, 31.47, 26.89, 21.54. HRMS (FAB) calcd for $C_9F_8H_8Na_2O_6S$ 442.9787, found 442.9778

Preparation of Bromomethyldimethylsilane (9)[132]

(Bromomethyl)chlorodimethylsilane (2.33g, 12.4mmol) was dissolved in 25ml diethyl ether in a 3-neck round bottom flask equipped with a magnetic stir bar, a condenser with nitrogen inlet, and two rubber septa. The flask was charged with $LiAlH_4$ solution (1M in ether, 3.2ml, 3.2mmol) a syringe and the reaction mixture turned to cloudy. The reaction mixture was stirred at room temperature for two hours, and then cooled in ice bath. A portion of 10ml water was slowly added to the flask, the two-layer mixture was separated. Organic layer was washed with 10ml water once, and dried over $MgSO_4$. The ether was removed by distillation through a 12cm column. The residue was a mixture of the title compound and diethyl ether. ^1H NMR showed the yield of the reaction was 88%.

^1H NMR ($CDCl_3/CHCl_3$): δ 4.09 (hep-t, 1H, $J_1 = 2.44Hz$, $J_2 = 3.66Hz$), 2.52 (d, 2H, $J = 2.44Hz$), 0.21 (d, 2H, $J = 3.66Hz$). ^{13}C NMR ($CDCl_3/CHCl_3$): δ 15.27, -5.00.

Preparation of (Dimethylsilyl)acetic Acid (11)

Magnesium turning (1.97g, 82.1mmol), 5ml anhydrous diethyl ether and a crystal of iodine were mixed in a 3-neck flask equipped with a magnetic stir bar, a condenser with nitrogen inlet, and pressure-equalizing additional funnel. (Bromomethyl)dimethylsilane (9.41 g of 69% in ether, 43.3mmol) was dissolved in 30ml ether in the additional funnel, small portion of this solution was added to the flask to initiate the reaction. Then all of the silane solution was added to the flask in a rate to keep the mixture gently reflux. The reaction mixture was heated at reflux for another 30 minutes, and then was cooled to -8°C. CO_2 (generated from $CaCO_3$ + HCl and dried by passing through concentrated H_2SO_4) was bubbled into the solution for 30 minutes. 10% HCl was used to acidify the reaction mixture after it was warmed to room temperature.

The two layers were separated, organic layer was washed with brine (50ml x 2), dried over $MgSO_4$. After ether was removed by rotary evaporator, the title compound was obtained as a colorless liquid in 74% yield.

^1H NMR ($CDCl_3/CHCl_3$): δ 10.22 (bs, 1H), 4.11 (m, 1H), 2.02 (d, 2H, J = 3.07 Hz), 0.24 (d, 6H, J = 3.66Hz). ^{13}C NMR ($CDCl_3/CHCl_3$): δ 179.27, 23.99, -4.69

Preparation of (Dimethylsilyl)methyltrimethyl Ammonium Bromide (12)

(Bromomethyl)dimethylsilane (1.38g, 9.01mmol) was dissolved in 25ml CH_3CN in a 3-neck round bottom flask equipped with a magnetic stir bar and a gas inlet. Trimethylamine was bubbled into the solution, white precipitate was formed. The solid was filtered, washed with diethyl ether, dried under reduced pressure. ^1H NMR showed there was a peak at 3.20ppm, its integral was much more than that of other peaks. The compound was used in H-abstraction kinetic study without further purification.

^1H NMR (D_2O/H_2O): δ 4.21 (bs, 1H), 3.20 (s), 0.28 (d, 6H, J = 3.6Hz). ^{13}C NMR (D_2O): δ 56.75, 55.58, -5.06.

Preparation of 1-(Benzyloxy)-3-bromopropane (14)[133]

Into a chilled (5-10°C) mixture of 26.76g (0.161mol) 1-(Benzyloxy)-3-propanol and 42.23g (0.161mol) triphenylphosphine in a 250 ml 3-neck round bottom flask equipped with a mechanical stirring was added 28.66g (0.161mol) NBS in small portions to keep the low temperature (after half of the NBS was added, the mixture turned very sticky and the stirring rod couldn't move. 50ml cyclohexane was added to the reaction mixture to make the stirring rod move). The ice bath was removed, and the reaction proceeded for another 16 hours. A portion of 200 ml benzene was added to the flask. The mixture was stirred, and then filtered. The filtrate was washed with 400ml of 5% NaS_2O_3

solution, 0.5N NaOH (420ml x 3), brine (350ml x 2) and dried over $MgSO_4$. Benzene was rotary evaporated and the residue was triturated with 150ml diethyl ether. After the solid was filtered, ether was removed from the filtrate by rotary evaporator, and column chromatography (hexanes: diethyl ether = 5:1) afforded 19g (52%) of the bromide as colorless liquid.

Synthesis of Tris(3-benzyloxypropyl) Silane (15)[134]

Into a 100ml 3-neck round bottom flask equipped with a magnetic stir bar, a condenser with a nitrogen inlet, and an additional funnel, 0.44g (18mmol) magnesium powder and 0.8g (3.49mmol) 3-benzoxylpropylbromide were mixed. 5ml anhydrous diethyl ether was charged into the flask to initiate the reaction. A solution of 1-(benzyloxy)-3-bromopropane (3.8g, 16.59mmol), trichlorosilane (0.6g, 4.4mmol) in 35ml diethyl ether was added drop wisely to the flask through the additional funnel to keep a gentle reflux. The mixture was heated at reflux for another 3 hours, and cooled in ice bath. 20ml H_2O was slowly added, 5 ml 10% HCl was used to neutralize the reaction mixture. The 2 layers were separated, and the aqueous layer was extracted with ether twice. The combined ether layer was washed with brine and dried over $MgSO_4$. Ether was rotary evaporated and the residue was purified by column chromatography (hexanes: ether = 5:1) to give the silane as a colorless liquid in 70% yield.

^1H NMR ($CDCl_3$/TMS): δ 7.35 (m, 15 H), 4.52 (s, 6H), 3.77 (hept, 1 H, J = 3.2 Hz), 3.45 (t, 6H, J = 6.8 Hz), 1.68 (m, 6 H), 0.66 (td, 6 H, J = 3.2 Hz, J = 8.3 Hz). ^{13}C NMR ($CDCl_3$/$CHCl_3$) 138.57, 128.32, 127.62, 127.46, 72.88, 72.81, 24.76, 7.31.

HRMS(FAB): calcd for $C_{30}H_{40}O_3Si$ 476.2747, found 476.2772.

Synthesis of Tris(3-hydroxypropyl)silane (16)

Tris(3-benzyloxypropyl)silane (0.64g, 1.35mmol) was dissolved in 40 ml ethanol in a 3-neck round bottom flask equipped with a magnetic stir bar, a gas inlet connected with hydrogen cylinder and a rubber septum. The system was flushed with N_2, charged with 10% Pd/C (0.26g, 0.08mmol), then filled with H_2. The absorption of H_2 was very obvious as soon as the stirring started. After 3 hours of stirring at room temperature, the resulting suspension was filtered through celite. The filtrate was evaporated and the residue was solidified with diethyl ether to afford the silane (**16**) as a white solid in 97% yield.

m.p.: 89-91°C. ^1H NMR (D_2O/H_2O): δ 3.54 (t, 6H, J = 6.6Hz), 1.57 (m, 6H), 0.60 (m, 6H). ^{13}C NMR (CD_3OD/CH_3OH) 66.02, 27.64, 12.45. HRMS (FAB): calcd for $C_9H_{21}SiO_3$ (M-1) 205.1260, found 205.1252

Preparation of Sodium Trifluoroethoxide

NaH (0.5338g, 22.24mmol) was suspended in 30 ml anhydrous diethyl ether in a 3-neck round bottom flask equipped with a magnetic stir bar, pressure-equalizing additional funnel, and a condenser with nitrogen inlet. Trifluoroethanol (2.94g, 29.39mmol) was mixed with 15ml ether in the additional funnel and added to the flask dropwisely. Gas evolved during the addition. The reaction mixture became a clear solution after the addition of trifluoroethanol. Ether was removed and the residue was dried under reduced pressure to afford the title compound as a white solid in almost quantitative yield.

^1H NMR (D_2O/H_2O): δ 3.90 (m, 2H). ^{19}F NMR (D_2O): δ 77.13 (m, 3F)

Preparation of Sodium 1,1,1-3,3,3-Hexafluoro-2-propoxide

NaH (0.5123g, 21.34mmol) was suspended in 20 ml anhydrous diethyl ether in a 3-neck round bottom flask equipped with a magnetic stir bar, pressure-equalizing additional funnel, and a condenser with nitrogen inlet. 1,1,1,3,3,3-Hexafluoro2-propanol (4.95g, 29.46mmol) was mixed with 15ml ether in the additional funnel and added to the flask dropwisely. Gas evolved during the addition. The reaction mixture became a clear solution after the addition of 1,1,1,3,3,3-hexafluoro2-propanol. Nitrogen was used to blow out ether and the residue was dried under reduced pressure to give the title compound in almost quantitative yield.

^{1}H NMR (CD_3CN/CH_3CN): δ 4.44 (m, 1H). ^{19}F NMR (CD_3CN): δ -76.55 (d, 6F, J = 6.94Hz).

General Procedure for Kinetic Study

The kinetic studies were run in pyrex NMR tubes containing a sealed capillary tube ($CFCl_3$ in C_6D_6) as the internal standard. For each kinetic study, a group of samples were prepared at the same time. The NMR tubes were capped with rubber septa, wrapped with Teflon tape before chemicals being added. The IR_fSO_3Na was used as a stock solution (17.8% by weight) and added to the NMR tubes with a micro-syringe. All liquid chemicals were added with syringes and weighed on the balance. The samples were degassed by 3 cycles of freeze-pump-thaw. After ^{19}F NMR spetra were taken, they were irradiated in a RPR-204 Rayonet photochemical reactor. ^{19}F NMR was taken again after 24 hours unless otherwise mentioned in the text. The acquisition time of NMR was at least 15 minutes to assure accurate integration. The product ratios were obtained from the ratios of integration of CF_2H and CF_2D signals. The conversion and yield were obtained from the integration of CF_2I peak in the starting material and (CF_2H+CF_2D) peaks in the products based on the internal standard.

Tables of Kinetic Data

Table 5-7 Rate Data for $HSCH_2CH_2SO_3Na$ (**17**)/$CH_2{=}CHCH_2CH_2COONa$ (**2f**) Competition towards $\cdot R_fSO_3^-Na^+$ Radical

Entry	[**17**] / mol·l^{-1}	[**17**] / [**2f**]	[**3a**] / [**4**]	Yield (%)
1	0.106	0.993	0.0190	98
2	0.142	1.32	0.0493	93
3	0.178	1.66	0.112	98
4	0.213	1.99	0.153	98
5	0.249	2.32	0.190	99
6	0.320	2.98	0.260	99

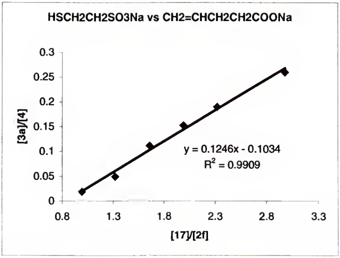

Figure 5-7 Plot of Products Ratio (**3a/4**) versus Substrates Ratio (**17/2f**)

k_H/k_a = Slope = 0.125 (± 0.006)

Intercept = -0.103 (± 0.012)

$R^2 = 0.991$

Table 5-8 Rate Data for Methanol/THF-d8 Competition towards $\cdot R_fSO_3^-Na^+$ Radical

$[IR_fSO_3Na]$ (mol· l^{-1})	[THF-d8] (mol· l^{-1})	$[CH_3OH]$/[THF-d8]	$[HR_fSO_3Na]$/ $[DR_fSO_3Na]$	Yield (%)
0.012	1.19	2.40	1.23	98
0.012	1.19	4.55	2.13	100
0.012	1.18	5.60	2.58	100
0.012	1.20	6.56	3.05	100

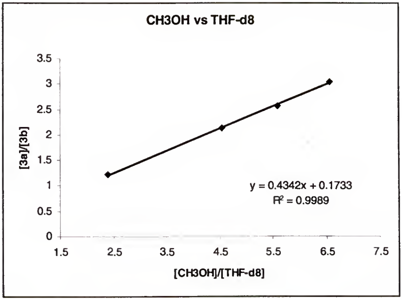

Figure 5-8 Plot of [**3a**]/[**3b**] vs. $[CH_3OH]$/[THF-d8]

$k_H/k_{D\ THF\text{-}d8}$ = Slope = 0.434 (± 0.010)

Intercept = 0.173 (±0.051)

$R^2 = 0.999$

Table 5-9 Rate Data for Ethanol/THF-d8 Competition towards $\cdot R_fSO_3^-Na^+$ Radical

$[IR_fSO_3Na]$ (mol· l^{-1})	[THF-d8] (mol· l^{-1})	$[CH_3CH_2OH]$/ [THF-d8]	$[HR_fSO_3Na]$/ $[DR_fSO_3Na]$	Yield (%)
0.011	1.10	0.884	2.93	97
0.011	1.09	1.11	3.67	94
0.011	1.10	1.40	4.51	91
0.011	1.10	1.82	5.73	91
0.011	1.09	2.23	6.67	96
0.011	1.10	2.80	7.62	100

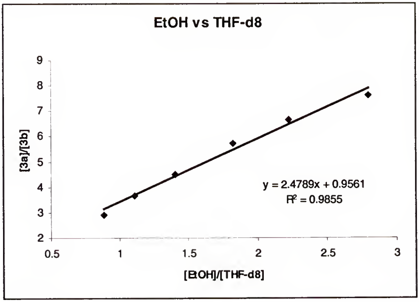

Figure 5-9 Plot of [3a]/[3b] vs. [EtOH]/[THF-d8]

$k_H/k_{D\ THF\text{-}d8}$ = Slope = 2.48 (± 0.15)

Intercept = 0.956 (±0.275)

$R^2 = 0.986$

Table 5-10 Rate Data for Isopropanol/THF-d8 Competition towards $\cdot R_fSO_3^-Na^+$ Radical

$[IR_fSO_3Na]$ (mol· l^{-1})	[THF-d8] (mol· l^{-1})	[i-PrOH]/ [THF-d8]	$[HR_fSO_3Na]$/ $[DR_fSO_3Na]$	Yield (%)
0.011	1.09	0.213	2.73	100
0.011	1.08	0.313	4.20	100
0.011	1.10	0.421	5.88	100
0.011	1.09	0.525	6.35	100
0.011	1.09	0.636	8.71	100
0.011	1.09	0.745	9.63	100

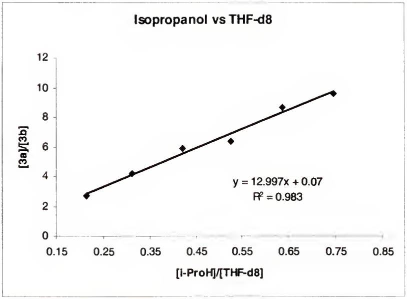

Figure 5-10 Plot of **[3a]**/**[3b]** vs. [Isopropanol]/[THF-d8]

$k_H/k_{D\ THF\text{-}d8}$ = Slope = 13.0 (± 0.8)

Intercept = 0.070 (±0.435)

$R^2 = 0.983$

Table 5-11 Rate Data for Ethylene Glycol/THF-d8 Competition towards $\cdot R_fSO_3^-Na^+$ Radical

$[IR_fSO_3Na]$ (mol· l^{-1})	[THF-d8] (mol· l^{-1})	[Ethylene Glycol]/ [THF-d8]	$[HR_fSO_3Na]$/ $[DR_fSO_3Na]$	Yield (%)
0.012	1.20	0.313	0.557	97
0.012	1.22	0.607	0.963	99
0.012	1.20	0.913	1.38	100
0.012	1.19	1.33	1.97	100
0.012	1.19	1.76	2.47	100
0.012	1.19	2.35	3.16	100

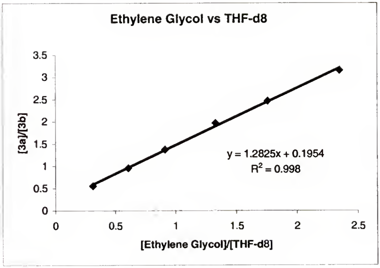

Figure 5-11 Plot of [3a]/[3b] vs. [Ethylene Glycol]/[THF-d8]

$k_H/k_{D\ THF\text{-}d8}$ = Slope = 1.28 (± 0.03)

Intercept = 0.195 (±0.040)

$R^2 = 0.998$

Table 5-12 Rate Data for 2,3-Butanediol/THF-d8 Competition towards $\cdot R_fSO_3^-Na^+$ Radical

$[IR_fSO_3Na]$ (mol· l^{-1})	[THF-d8] (mol· l^{-1})	[2,3-butanediol]/ [THF-d8]	$[HR_fSO_3Na]$/ $[DR_fSO_3Na]$	Yield (%)
0.013	1.33	0.162	1.23	64
0.013	1.33	0.348	2.36	62
0.013	1.33	0.524	3.42	64
0.013	1.33	0.696	4.58	62
0.013	1.33	0.870	5.21	66
0.013	1.32	1.05	6.14	70

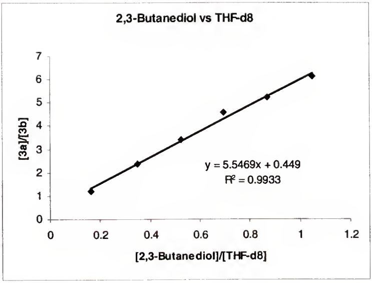

Figure 5-12 Plot of [3a]/[3b] vs. [2,3-Butanediol]/[THF-d8]

$k_H/k_{D\ THF\text{-}d8}$ = Slope = 5.55 (± 0.23)

Intercept = 0.449 (±0.155)

$R^2 = 0.993$

Table 5-13 Rate Data for Methyl Glycolate/THF-d8 Competition towards $\cdot R_fSO_3Na$ Radical

$[IR_fSO_3Na]$ (mol· l^{-1})	[THF-d8] (mol· l^{-1})	[Methyl Glycolate]/ [THF-d8]	$[HR_fSO_3Na]$/ $[DR_fSO_3Na]$	Yield (%)
0.011	1.19	0.405	0.450	93
0.011	1.20	0.816	0.804	90
0.011	1.21	1.24	1.15	100
0.011	1.19	2.09	1.66	90
0.011	1.17	3.04	2.14	98
0.011	1.17	4.33	2.83	94

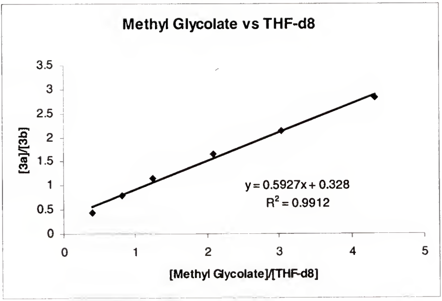

Figure 5-13 Plot of [**3a**]/[**3b**] vs. [Methyl Glycolate]/[THF-d8]

$k_H/k_{D\ THF\text{-}d8}$ = Slope = 0.593 (± 0.028)

Intercept = 0.328 (±0.067)

$R^2 = 0.991$

Table 5-14 Rate Data for Trifluoroethanol/THF-d8 Competition towards $\cdot R_fSO_3Na$ Radical

$[IR_fSO_3Na]$ (mol· l^{-1})	[THF-d8] (mol· l^{-1})	[Trifluoroethanol]/ [THF-d8]	$[HR_fSO_3Na]$/ $[DR_fSO_3Na]$	Yield (%)
0.011	0.232	4.27	0.158	100
0.011	0.223	6.69	0.203	100
0.011	0.223	8.82	0.260	100
0.011	0.221	11.1	0.286	100
0.011	0.218	14.6	0.348	100
0.011	0.218	17.9	0.421	100

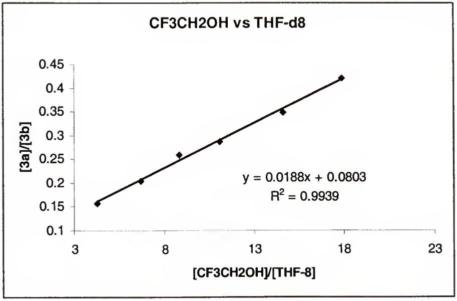

Figure 5-14 Plot of [3a]/[3b] vs. $[CF_3CH_2OH]/[THF\text{-}d8]$

$k_H/k_{D\ THF\text{-}d8}$ = Slope = 0.0188 (± 0.0007)

Intercept = 0.0803 (±0.0085)

$R^2 = 0.994$

Table 5-15 Rate Data for Hexafluoroisopropanol/CD_3OD Competition towards $\cdot R_fSO_3Na$ Radical

$[IR_fSO_3Na]$ (mol· l^{-1})	$[CD_3OD]$ (mol· l^{-1})	$[(CF_3)_2CHOH]/[CD_3OD]$	$[HR_fSO_3Na]/[DR_fSO_3Na]$	Yield (%)
0.011	2.20	0.314	0.121	94
0.011	2.16	0.473	0.472	93
0.011	2.20	0.617	0.872	94
0.011	2.18	0.779	1.30	93
0.011	2.19	0.971	1.87	95
0.011	2.19	1.16	2.11	93

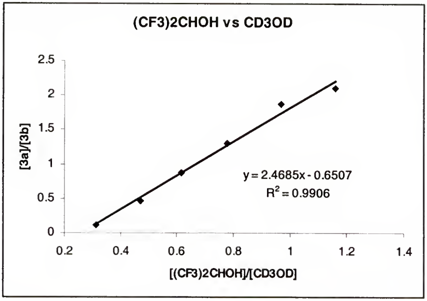

Figure 5-15 Plot of [**3a**]/[**3b**] vs. $[(CF_3)_2CHOH]/[CD_3OD]$

$k_H/k_{D\ CD3OD}$ = Slope = 2.47 (± 0.12)

Intercept = -0.651 (±0.093)

$R^2 = 0.991$

Table 5-16 Rate Data for CH_3OH/CD_3OD Competition towards $\cdot R_fSO_3Na$ Radical

$[IR_fSO_3Na]$ (mol· l^{-1})	$[CD_3OD]$ (mol· l^{-1})	$[CH_3OH]/[CD_3OD]$	$[HR_fSO_3Na]/[DR_fSO_3Na]$	Yield (%)
0.011	4.41	0.103	1.45	100
0.011	4.39	0.209	2.65	98
0.011	4.44	0.306	4.01	100
0.011	4.44	0.456	5.90	100
0.011	4.42	0.606	7.57	99
0.011	4.41	0.801	9.26	100

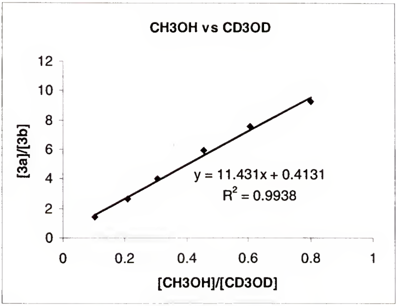

Figure 5-16 Plot of **[3a]**/**[3b]** vs. $[CH_3OH]/[CD_3OD]$

$k_H/k_{D\ CD3OD}$ = Slope = 11.4 (± 0.4)

Intercept = 0.413 (±0.215)

$R^2 = 0.994$

Table 5-17 Rate Data for Sodium Trifluoroethoxide/THF-d8 Competition towards $\cdot R_fSO_3Na$ Radical

$[IR_fSO_3Na]$ (mol· l^{-1})	[THF-d8] (mol· l^{-1})	$[CF_3CH_2ONa]$ [THF-d8]	$[HR_fSO_3Na]$/ $[DR_fSO_3Na]$	Yield (%)
0.011	1.09	0.103	1.91	100
0.011	1.09	0.128	2.52	100
0.011	1.09	0.154	3.23	100
0.011	1.08	0.181	3.79	100
0.011	1.08	0.207	4.46	100
0.011	1.09	0.231	5.44	100

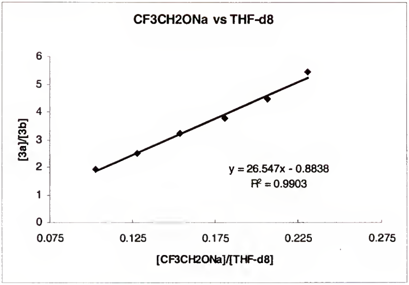

Figure 5-17 Plot of [3a]/[3b] vs. $[CF_3CH_2ONa]$/[THF-d8]

$k_H/k_{D\ THF\text{-}d8}$ = Slope = 26.5 (± 1.3)

Intercept = -0.884 (±0.228)

$R^2 = 0.990$

Table 5-18 Rate Data for Sodium Hexafluoroisopropoxide/THF-d8 Competition towards $\cdot R_fSO_3Na$ Radical

$[IR_fSO_3Na]$ (mol· l^{-1})	[THF-d8] (mol· l^{-1})	$[(CF_3)_2CHONa]$/ [THF-d8]	$[HR_fSO_3Na]$/ $[DR_fSO_3Na]$	Yield (%)
0.011	1.06	0.102	2.36	100
0.011	1.08	0.125	2.88	100
0.011	1.08	0.151	3.65	100
0.011	1.09	0.176	4.28	100
0.011	1.09	0.200	4.92	100
0.011	1.10	0.223	5.83	100

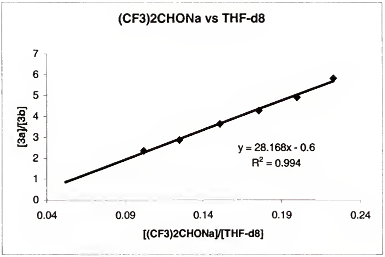

Figure 5-18 Plot of **[3a]**/**[3b]** vs. $[(CF_3)_2CHONa]$/[THF-d8]

k_H/k_D THF-d8 = Slope = 28.2 (± 1.1)

Intercept = -0.600 (±0.184)

$R^2 = 0.994$

Table 5-19 Rate Data for Sodium Hexafluoroisopropoxide/CD_3OD Competition towards $\cdot R_fSO_3Na$ Radical

$[IR_fSO_3Na]$ (mol· l^{-1})	$[CD_3OD]$ (mol· l^{-1})	$[(CF_3)_2CHONa]/[CD_3OD]$	$[HR_fSO_3Na]/[DR_fSO_3Na]$	Yield (%)
0.011	6.64	0.0165	8.52	100
0.011	6.62	0.0193	10.1	100
0.011	6.55	0.0223	12.1	100
0.011	6.60	0.0249	14.9	100
0.011	6.57	0.0278	16.0	100
0.011	6.57	0.0306	18.1	100

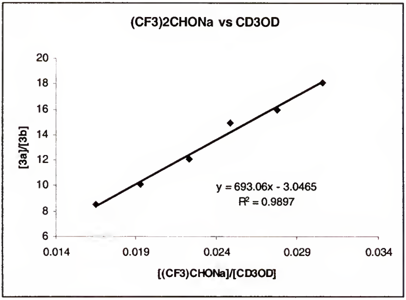

Figure 5-19 Plot of [3a]/[3b] vs. $[CF_3CH_2ONa]/[CD_3OD]$

$k_H/k_{D\,CD3OD}$ = Slope = 693 (±35)

Intercept = -3.05 (±0.85)

$R^2 = 0.990$

Table 5-20 Rate Data for Ethylene Glycol Dimethyl Ether/THF-d8 Competition towards $\cdot R_fSO_3Na$ Radical

$[IR_fSO_3Na]$ (mol· l^{-1})	[THF-d8] (mol· l^{-1})	$[(CH_3OCH_2)_2]$/ [THF-d8]	$[HR_fSO_3Na]$/ $[DR_fSO_3Na]$	Yield (%)
0.011	1.07	0.414	0.792	100
0.011	1.06	0.807	1.35	100
0.011	1.07	1.18	1.88	100
0.011	1.07	1.58	2.35	100
0.011	1.07	1.95	2.82	100
0.011	1.06	2.34	3.35	100

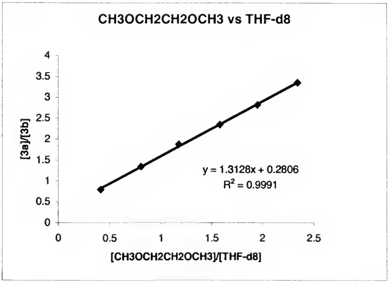

Figure 5-20 Plot of **[3a]**/**[3b]** vs. $[CH_3OCH_2CH_2OCH_3]$/[THF-d8]

$k_H/k_{D\ THF\text{-}d8}$ = Slope = 1.31 (±0.02)

Intercept = 0.280 (±0.030)

$R^2 = 0.999$

Table 5-21 Rate Data for THF/THF-d8 Competition towards $\cdot R_fSO_3Na$ Radical

$[IR_fSO_3Na]$ ($mol\cdot l^{-1}$)	[THF-d8] ($mol\cdot l^{-1}$)	[THF]/ [THF-d8]	$[HR_fSO_3Na]/$ $[DR_fSO_3Na]$	Yield (%)
0.013	1.29	0.204	1.67	100
0.013	1.28	0.415	3.47	100
0.013	1.28	0.605	5.03	100
0.013	1.28	0.809	6.68	100
0.013	1.30	0.990	7.40	100
0.013	1.28	1.22	9.99	100

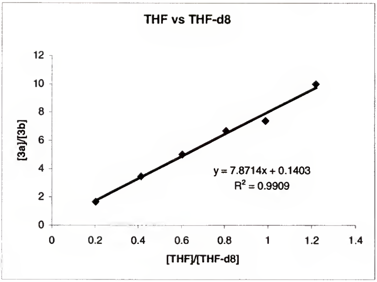

Figure 5-21 Plot of **[3a]**/**[3b]** vs. [THF]/[THF-d8]

$k_H/k_{D\ THF\text{-}d8}$ = Slope = 7.87 (± 0.38)

Intercept = 0.140 (±0.296)

$R^2 = 0.991$

Table 5-22 Rate Data for Acetone/THF-d8 Competition towards $\cdot R_fSO_3^-Na^+$ Radical

$[IR_fSO_3Na]$ (mol· l^{-1})	[THF-d8] (mol· l^{-1})	[Acetone]/ [THF-d8]	$[HR_fSO_3Na]$/ $[DR_fSO_3Na]$	Yield (%)
0.012	1.19	2.39	0.0953	96
0.012	1.19	3.57	0.117	100
0.012	1.19	4.46	0.126	100
0.012	1.19	5.65	0.144	100

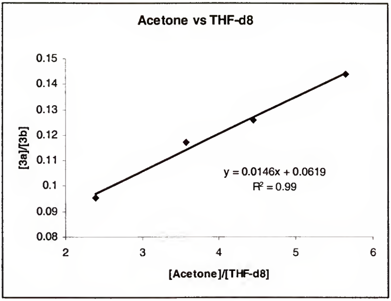

Figure 5-22 Plot of [3a]/[3b] vs. [Acetone]/[THF-d8]

$k_H/k_{D\ THF\text{-}d8}$ = Slope = 0.0146 (± 0.0010)

Intercept = 0.0619 (±0.0043)

$R^2 = 0.990$

Table 5-23 Rate Data for Acetic Acid/THF-d8 Competition towards $\cdot R_fSO_3^-Na^+$ Radical

$[IR_fSO_3Na]$ (mol· l^{-1})	[THF-d8] (mol· l^{-1})	[Acetic Acid]/ [THF-d8]	$[HR_fSO_3Na]$/ $[DR_fSO_3Na]$	Yield (%)
0.012	1.18	3.10	0.0542	100
0.012	1.19	4.45	0.0589	100
0.012	1.20	5.76	0.0676	100
0.012	1.19	7.23	0.0685	100
0.012	1.19	8.60	0.0756	100
0.012	1.18	10.0	0.0881	100

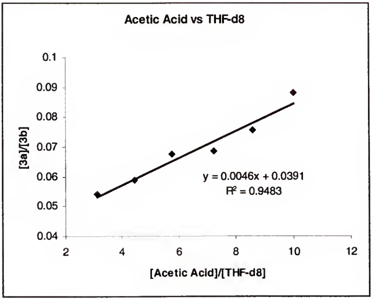

Figure 5-23 Plot of [3a]/[3b] vs. [Acetic Acid]/[THF-d8]

$k_H/k_{D\ THF\text{-}d8}$ = Slope = 0.00455 (± 0.00053)

Intercept = 0.0391 (±0.0037)

$R^2 = 0.948$

Table 5-24 Rate Data for Sodium Acetate/THF-d8 Competition towards $\cdot R_fSO_3Na$ Radical

$[IR_fSO_3Na]$ (mol$\cdot$ l^{-1})	[THF-d8] (mol$\cdot$ l^{-1})	$[CH_3COONa]$/ [THF-d8]	$[HR_fSO_3Na]$/ $[DR_fSO_3Na]$	Yield (%)
0.011	0.214	3.53	0.182	100
0.011	0.217	4.62	0.225	100
0.011	0.217	5.78	0.277	100
0.011	0.217	6.94	0.308	100
0.011	0.214	9.70	0.381	100
0.011	0.212	12.2	0.431	100

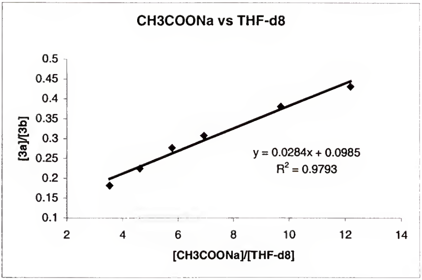

Figure 5-24 Plot of **[3a]**/**[3b]** vs. $[CH_3COONa]$/[THF-d8]

$k_H/k_{D\ THF\text{-}d8}$ = Slope = 0.0284 (± 0.0020)

Intercept = 0.0985 (±0.0159)

$R^2 = 0.979$

Table 5-25 Rate Data for Propionic Acid/THF-d8 Competition towards · $R_fSO_3^-Na^+$ Radical

$[IR_fSO_3Na]$ (mol· l^{-1})	[THF-d8] (mol· l^{-1})	$[CH_3CH_2COOH]$/ [THF-d8]	$[HR_fSO_3Na]$/ $[DR_fSO_3Na]$	Yield (%)
0.012	1.20	1.48	0.382	93
0.012	1.20	2.55	0.534	100
0.012	1.20	3.61	0.749	100
0.012	1.20	4.66	0.923	100
0.012	1.19	5.82	1.16	100

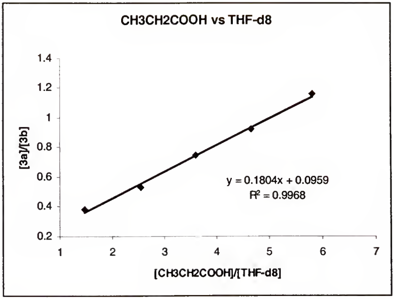

Figure 5-25 Plot of [**3a**]/[**3b**] vs. $[CH_3CH_2COOH]$/[THF-d8]

k_H/k_D THF-d8 = Slope = 0.180 (± 0.006)

Intercept = 0.0959 (±0.0234)

$R^2 = 0.997$

Table 5-26 Rate Data for Sodium Propionate/THF-d8 Competition towards · $R_fSO_3^-Na^+$ Radical

$[IR_fSO_3Na]$ (mol· l^{-1})	[THF-d8] (mol· l^{-1})	$[CH_3CH_2COONa]$/ [THF-d8]	$[HR_fSO_3Na]$/ $[DR_fSO_3Na]$	Yield (%)
0.013	1.28	0.288	0.181	98
0.013	1.29	0.484	0.265	96
0.013	1.29	0.778	0.373	95
0.013	1.29	1.13	0.464	94
0.013	1.28	1.42	0.610	95

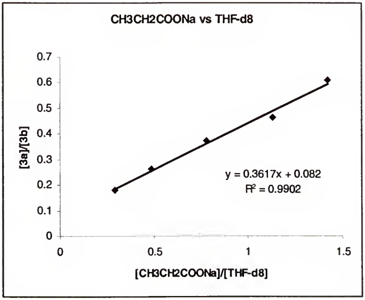

Figure 5-26 Plot of **[3a]**/**[3b]** vs. $[CH_3CH_2COONa]$/[THF-d8]

$k_H/k_{D\ THF\text{-}d8}$ = Slope = 0.362 (± 0.021)

Intercept = 0.0820 (±0.0190)

$R^2 = 0.990$

Table 5-27 Rate Data for 2-Mercaptoethanesulfonic Acid, Sodium Salt/THF-d8 Competition towards · $R_fSO_3^-Na^+$ Radical

$[IR_fSO_3Na]$ (mol· l^{-1})	[THF-d8] (mol· l^{-1})	$[HSCH_2CH_2SO_3Na]$/ [THF-d8]	$[HR_fSO_3Na]$/ $[DR_fSO_3Na]$	Yield (%)
0.011	0.677	0.174	20.1	97
0.011	0.677	0.232	27.3	97
0.011	0.675	0.291	29.1	97
0.011	0.673	0.349	38.9	96
0.011	0.675	0.408	41.0	96
0.011	0.682	0.460	48.7	97

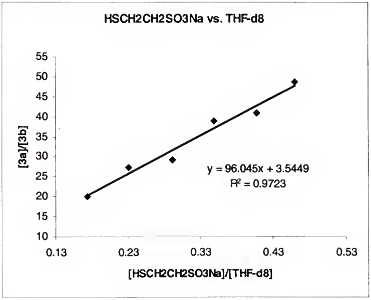

Figure 5-27 Plot of **[3a]**/**[3b]** vs. $[HSCH_2CH_2SO_3Na]$/[THF-d8]

$k_H/k_{D\ THF\text{-}d8}$ = Slope = 96.0 (± 8.1)

Intercept = 3.54 (±2.70)

$R^2 = 0.972$

Table 5-28 Rate Data for $(HOCH_2CH_2CH_2)_3SiH$ **(16)**/THF-d8 Competition towards $\cdot R_fSO_3Na$ Radical

$[IR_fSO_3Na]$ ($mol \cdot l^{-1}$)	[THF-d8] ($mol \cdot l^{-1}$)	[Silane **16**]/ [THF-d8]	$[HR_fSO_3Na]$/ $[DR_fSO_3Na]$	Yield (%)
0.0079	0.487	0.131	3.46	100
0.0079	0.479	0.160	4.04	100
0.0079	0.483	0.185	5.12	100
0.0079	0.485	0.211	5.74	100
0.0079	0.489	0.261	7.02	100

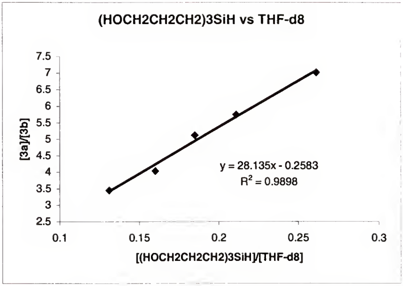

Figure 5-28 Plot of [**3a**]/[**3b**] vs. $[(HOCH_2CH_2CH_2)_3SiH]$/[THF-d8]

$k_H/k_{D\ THF\text{-}d8}$ = Slope = 28.1 (± 1.6)

Intercept = -0.258 (±0.321)

$R^2 = 0.990$

Table 5-29 Rate Data for $Me_3N^+CH_2SiMe_2H$ Br^- (**12**)/THF-d8 Competition towards $\cdot R_fSO_3Na$ Radical

$[IR_fSO_3Na]$ ($mol \cdot l^{-1}$)	[THF-d8] ($mol \cdot l^{-1}$)	[Silane **12**]/ [THF-d8]	$[HR_fSO_3Na]$/ $[DR_fSO_3Na]$	Yield (%)
0.011	0.655	0.0673	1.01	100
0.011	0.671	0.164	3.05	100
0.011	0.662	0.333	6.85	100
0.011	0.672	0.492	9.63	100

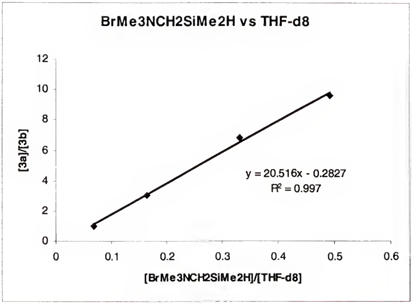

Figure 5-29 Plot of [3a]/[3b] vs. $[BrMe_3NCH_2SiMe_2H]$/[THF-d8]

$k_H/k_{D\ THF\text{-}d8}$ = Slope = 20.5 (± 0.8)

Intercept = -0.283 (±0.245)

$R^2 = 0.997$

Table 5-30 Rate Data for Phosphorus Acid/THF-d8 Competition towards ·R_fSO_3Na Radical

[IR_fSO_3Na] (mol· l^{-1})	[THF-d8] (mol· l^{-1})	[H_3PO_3]/ [THF-d8]	[HR_fSO_3Na]/ [DR_fSO_3Na]	Yield (%)
0.011	1.08	0.271	1.73	100
0.011	1.09	0.536	2.79	100
0.011	1.09	0.804	3.68	100
0.011	1.09	1.07	4.79	100
0.011	1.09	1.34	5.46	100
0.011	1.09	1.61	6.43	100

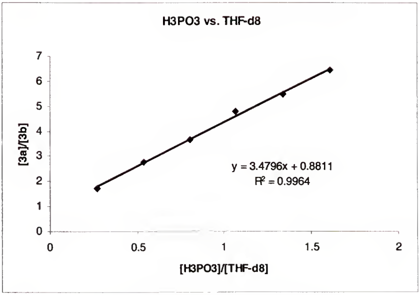

Figure 5-30 Plot of [**3a**]/[**3b**] vs. [H_3PO_3]/[THF-d8]

$k_H/k_{D\ THF\text{-}d8}$ = Slope = 3.48 (± 0.10)

Intercept = 0.881 (±0.109)

$R^2 = 0.996$

Table 5-31 Rate Data for $(CH_3)_2CHOH/(CD_3)_2CDOD$ Competition towards $\cdot R_fSO_3Na$ Radical

$[IR_fSO_3Na]$ (mol· l^{-1})	$[(CD_3)_2CDOD]$ (mol· l^{-1})	$[(CH_3)_2CHOH]/[(CD_3)_2CDOD]$	$[HR_fSO_3Na]/[DR_fSO_3Na]$	Yield (%)
0.011	0.688	0.150	1.04	100
0.011	0.704	0.334	1.99	100
0.011	0.694	0.492	2.98	100
0.011	0.704	0.656	4.05	100
0.011	0.694	0.832	4.95	100
0.011	0.694	1.00	5.96	100

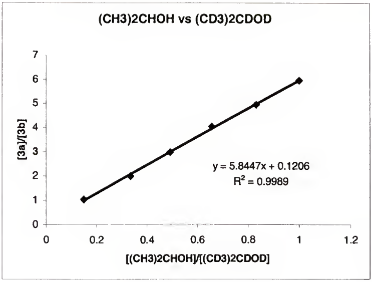

Figure 5-31 Plot of **[3a]**/**[3b]** vs. $[(CH_3)_2CHOH]/[(CD_3)_2CDOD]$

k_H/k_D = Slope = 5.84 (± 0.10)

Intercept = 0.121 (±0.063)

$R^2 = 0.999$

Table 5-32 Rate Data for CH_3CH_2OH/CD_3CD_2OD Competition towards $\cdot R_fSO_3Na$ Radical

$[IR_fSO_3Na]$ (mol· l^{-1})	$[CD_3CD_2OD]$ (mol· l^{-1})	$[CH_3CH_2OH]/[CD_3CD_2OD]$	$[HR_fSO_3Na]/[DR_fSO_3Na]$	Yield (%)
0.011	1.24	0.123	1.17	91
0.011	1.25	0.266	2.30	99
0.011	1.23	0.400	3.42	100
0.011	1.24	0.521	4.34	100
0.011	1.24	0.753	6.52	99
0.011	1.22	1.03	9.12	100

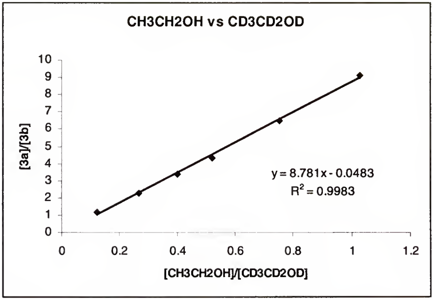

Figure 5-32 Plot of [**3a**]/[**3b**] vs. $[CH_3CH_2OH]/[CD_3CD_2OD]$

k_H/k_D = Slope = 8.78 (± 0.18)

Intercept = -0.048 (±0.109)

$R^2 = 0.998$

Table 5-33 Rate Data for $(CH_3)_2CO/(CD_3)_2CO$ Competition towards $\cdot R_fSO_3Na$ Radical

$[IR_fSO_3Na]$ (mol· l^{-1})	$[(CD_3)_2CO]$ (mol· l^{-1})	$[(CH_3)_2CO]/[(CD_3)_2CO]$	$[HR_fSO_3Na]/[DR_fSO_3Na]$	Yield (%)
0.011	2.40	0.110	1.88	86
0.011	2.40	0.167	2.84	89
0.011	2.38	0.208	3.44	89
0.011	2.41	0.282	4.77	90
0.011	2.42	0.305	5.35	88
0.011	2.43	0.407	6.86	92

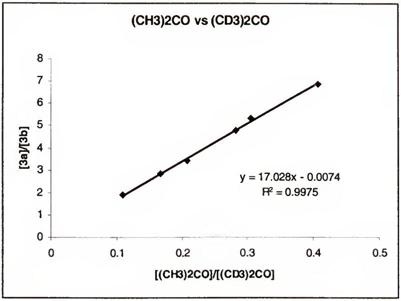

Figure 5-33 Plot of [3a]/[3b] vs. $[(CH_3)_2CO]/[(CD_3)_2CO]$

k_H/k_D = Slope = 17.0 (± 0.4)

Intercept = -0.007 (±0.112)

$R^2 = 0.998$

Table 5-34 Rate Data for CH_3COOH/CD_3COOD Competition towards $\cdot R_fSO_3Na$ Radical

$[IR_fSO_3Na]$ (mol· l^{-1})	$[CD_3COOD]$ (mol· l^{-1})	$[CH_3COOH]/[CD_3COOD]$	$[HR_fSO_3Na]/[DR_fSO_3Na]$	Yield (%)
0.011	3.15	0.100	2.38	84
0.011	3.12	0.151	3.60	89
0.011	3.12	0.206	5.10	88
0.011	3.10	0.256	6.03	93
0.011	3.12	0.303	6.90	96
0.011	3.12	0.352	8.03	94

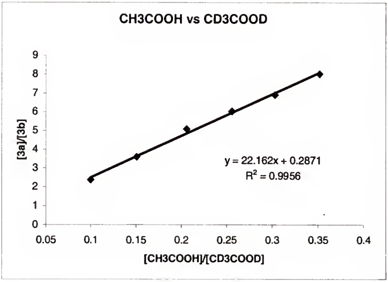

Figure 5-34 Plot of [3a]/[3b] vs. $[CH_3COOH]/[CD_3COOD]$

k_H/k_D = Slope = 22.2 (± 0.7)

Intercept = 0.287 (±0.179)

$R^2 = 0.996$

Table 5-35 Rate Data for CH_3CH_2OH/t-$BuSiMe_2D$ Competition towards $\cdot C_4F_9$ Radical in 1,3-BTB at 308K, Initiated with $(tBuON)_2$

$[C_4F_9I]$ (mol· l^{-1})	[t-$BuSiMe_2D$] (mol· l^{-1})	$[CH_3CH_2OH]$/ [t-$BuSiMe_2D$]	$[C_4F_9H]$/ $[C_4F_9D]$	Yield (%)
0.059	0.544	2.99	0.230	32
0.053	0.548	4.07	0.255	51
0.052	0.542	5.26	0.261	61
0.053	0.548	6.95	0.303	62
0.053	0.542	9.32	0.338	74
0.053	0.544	11.6	0.412	80

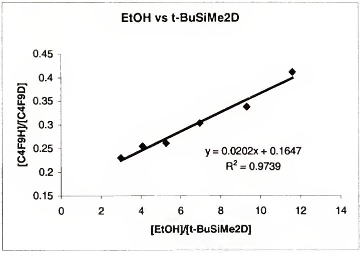

Figure 5-35 Plot of $[C_4F_9H]/[C_4F_9D]$ vs. $[CH_3CH_2OH]$/[t-$BuSiMe_2D$]

$k_H/k_{D\ t\text{-}BuSiMe2D}$ = Slope = 0.0202 (± 0.0016)

Intercept = 0.165 (±0.012)

$R^2 = 0.974$

$k_H = 3.01\ (\pm 0.65) \times 10^3\ M^{-1}s^{-1}$

APPENDIX
SELECTED ^{19}F NMR SPECTRA

The following spectra have been included in this dissertation as they have been critical in the determination of absolute rate constants using competition kinetic method. The spectra have been presented in the same order as discussed in chapter 3.

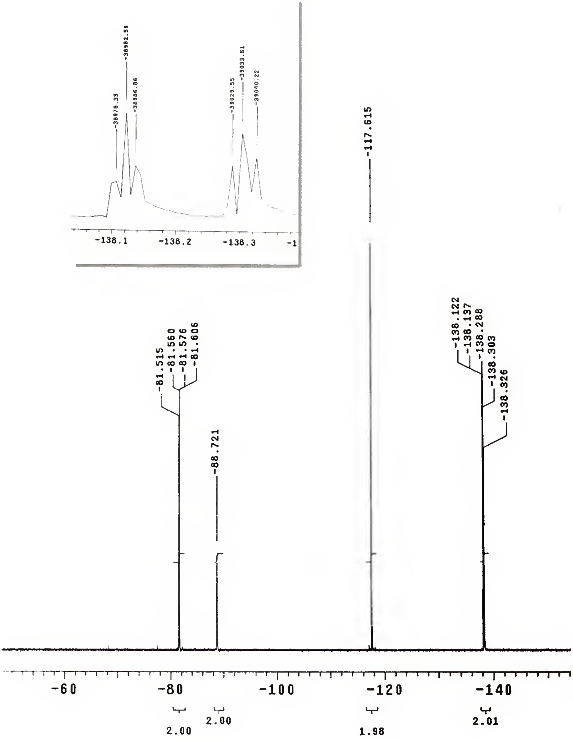

Figure A-1 ^{19}F NMR Spectrum of Compound $HCF_2CF_2OCF_2CF_2SO_3Na$ (**3a**)

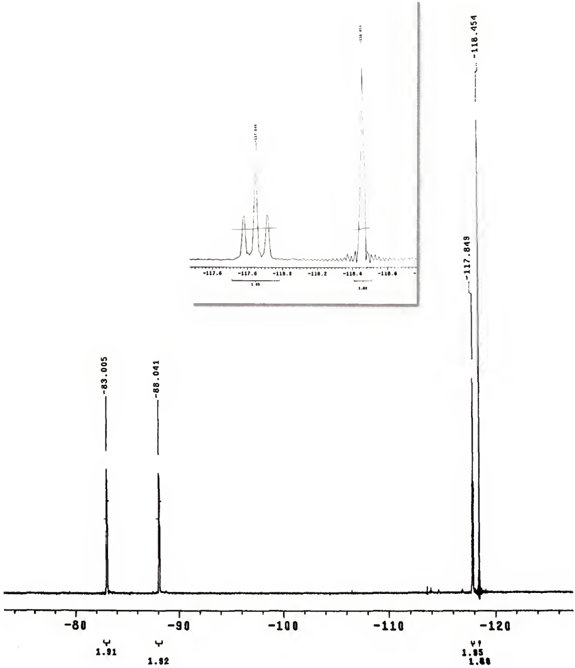

Figure A-2 ^{19}F NMR of Compound $NaSO_3(CF_2)_2O(CF_2)_2(CH_2)_4CO_2Na$ (**4**) ($D_2O/CFCl_3$ in C_6D_6 in a capillary tube)

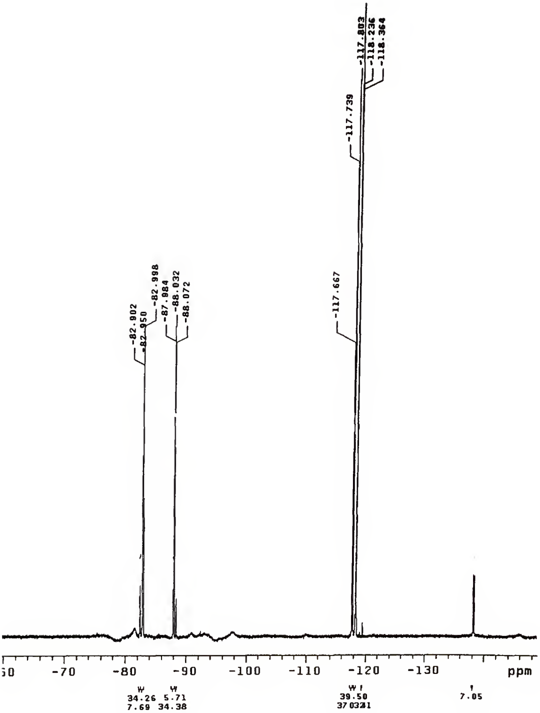

Figure A-3 A Typical ^{19}F NMR Spectrum of the Competition Reaction Between $HSCH_2CH_2SO_3Na$ and $CH_2=CHCH_2CH_2CO_2Na$ towards $\cdot R_fSO_3Na$ Radical ($D_2O/CFCl_3$ in C_6D_6 in a capillary tube)

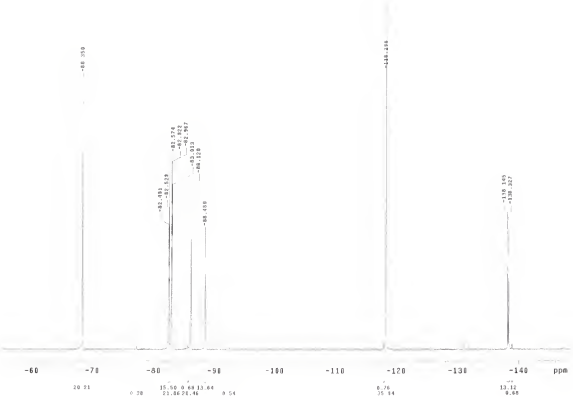

Figure A-4 A Typical ^{19}F NMR Spectrum of the Competition Between $HSCH_2CH_2SO_3Na$ and THF-d8 towards $\cdot R_fSO_3Na$ Radical ($D_2O/CFCl_3$ in C_6D_6 in a capillary tube)

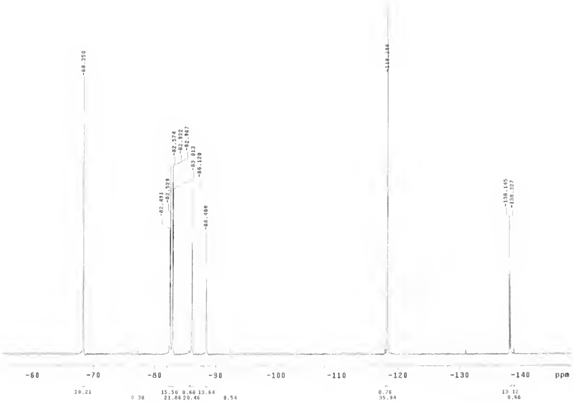

Figure A-4 A Typical ^{19}F NMR Spectrum of the Competition Between $HSCH_2CH_2SO_3Na$ and THF-d8 towards $\cdot R_fSO_3Na$ Radical

REFERENCES

(1) Giese, B. *Radicals in Organic Synthesis: Formation of Carbon-Carbon Bonds*; Pergamon Press: Oxford:, 1986.

(2) Jasperse, C. P.; Curran, D. P.; Fevig, T. L. *Chem. Rev.* **1991**, *91*, 1237-1286.

(3) Dowd, P.; Zhang, W. *Chem. Rev.* **1993**, *93*, 2091-2115.

(4) Curran, D. P.; Sisko, J.; Yeske, P. E.; Liu, H. *Pure Appl. Chem.* **1993**, *65*, 1153-1159.

(5) Koert, U. *Angew. Chem., Int. Ed. Engl.* **1996**, *35*, 405-407.

(6) Easton, C. J. *Chem. Rev.* **1997**, *97*, 53-82.

(7) Yet, L. *Tetrahedron* **1999**, *55*, 9349-9403.

(8) Capek, I.; Chern, C. S. *Adv. Polym. Sci.* **2001**, *155*, 101-165.

(9) Coessens, V.; Pintauer, T.; Matyjaszewski, K. *Progress in Polymer Science* **2001**, *26*, 337-377.

(10) Patten, T. E.; Matyjaszewski, K. *ADV. MATER.* **1998**, *10*, 901.

(11) Leffler, J. E. *An Introduction to Free Radicals*; John Wiley & Sons, Inc.:, 1993.

(12) Wentrup, C. *Reactive Molecules*; John Wiley & Sons:, 1984.

(13) Tedder, J. M.; Walton, J. C. *Acct. Chem. Res.* **1976**, *9*, 183-191.

(14) Fischer, H.; Paul, H. *Acc. Chem. Res.* **1987**, *20*, 200-206.

(15) Newcomb, M. *Tetrahedron* **1993**, *49*, 1151-1176.

(16) Tedder, J. M.; Walton, J. C. *Tetrahedron* **1980**, *36*, 701-707.

(17) Tedder, J. M. *Tetrahedron* **1982**, *38*, 313-329.

(18) Ingold, K. U. *Pure Appl. Chem.* **1984**, *56*, 1767-1779.

(19) Giese, B.; Meister, J. *Angew. Chem., Int. Ed. Engl.* **1977**, *16*, 178-179.

(20) Giese, B.; Meixner, J. *Chem. Ber.* **1981**, *114*, 2138-2145.

(21) Sakurai, H.; Hayashi, S.; Hosomi, A. *Bull. Chem. Soc. Japan* **1971**, *44*, 1945.

(22) Jones, M. J.; Moad, G.; Rizzardo, E.; Solomon, D. H. *J. Org. Chem.* **1989**, *54*, 1607-1611.

(23) Wong, M. W.; Radom, L. *J. Phys. Chem.* **1995**, *99*, 8582-8588.

(24) Lias, S. G.; Bartmess, J. E.; Liebman, J. F.; Holmes, J. L.; Levin, R. D.; Mallard, W. G. *J. Phys. Chem. Ref. Data* **1988**, *17*, 1-861.

(25) Hammond, G. S. *J. Am. chem. Soc.* **1955**, *77*, 334-338.

(26) Abell, P. I. *Comprehensive Chemical Kinetics*; Elsevier Amsterdam:, 1976; 18.

(27) Hoyland, J. R. *Theor. Chim. Acta.* **1971**, *22*, 229.

(28) Houk, K. N.; Paddon-Row, M. N.; Spellmeyer, D. C.; Rondan, N. G.; Nagase, S. J. *J. Org. Chem.* **1986**, *51*, 2874-2879.

(29) Zipse, H.; He, J.; Houk, K. N.; Giese, B. *J. Am. Chem. Soc.* **1991**, *113*, 4324-4325.

(30) Wong, M. W.; Pross, A.; Radom, L. *J. Am. Chem. Soc.* **1994**, *116*, 6284-6292.

(31) Pryor, W. A.; F.Y.Tang; Tang, R. H.; Church, D. F. *J. Am. Chem. Soc.* **1982**, *104*, 2885-2891.

(32) Henderson, R. W.; R.D. Ward, J. *J. Am. Chem. Soc.* **1974**, *96*, 7556-7557.

(33) Pryor, W. A.; Tonellato, U.; Fuller, D. L.; Jumonville, S. *J. Org. Chem.* **1969**, *34*, 2018.

(34) Sakurai, H.; Hosomi, A. *J. Am. Chem. Soc.* **1967**, *89*, 458.

(35) Howard, J. A.; Chenier, J. H. B. *J. Am. Chem. Soc.* **1973**, *95*, 3054-3055.

(36) Michejda, C. J.; Hoss, W. P. *J. Am. Chem. Soc.* **1970**, *92*, 6298.

(37) Huyser, E. S. *J. Am. Chem. Soc.* **1960**, *82*, 394-396.

(38) Avila, D. V.; Ingold, K. U.; Lusztyk, J.; Jr., W. R. D.; Pan, H.-Q.; Muir, M. *J. Am. Chem. Soc.* **1994**, *116*, 99-104.

(39) Tedder, J. M. *Angew. Chem., Int. Ed. Engl.* **1982**, *21*, 401-410.

(40) Giese, B. *Angew. Chem., Int. Ed. Engl.* **1989**, *28*, 969-980.

(41) Giese, B. *Angew. Chem., Int. Ed. Engl.* **1983**, *22*, 753-764.

(42) Beckwith, A. L. J. *Tetrahedron* **1981**, *37*, 3073-3100.

(43) Low, H. C.; Tedder, J. M.; Walton, J. C. *J. Chem. Soc. Faraday I* **1976**, *72*, 1707-1714.

(44) Sloan, J. P.; Tedder, J. M.; Walton, J. C. *J. Chem. Soc. Perkin II* **1975**, 1841-1845.

(45) Cape, J. N.; Greig, A. C.; Tedder, J. M.; Walton, J. C. *J. Chem. Soc. Faraday I* **1975**, *71*, 592-601.

(46) Stefani, A. P.; Herk, L.; Szwarc, M. *J. Am. Chem. Soc.* **1961**, *83*, 4732-4736.

(47) Moad, G.; Solomon, D. H. *The Chemistry of Free Radical Polymerization*; First edition ed.; Pergamon:, 1995.

(48) Flemming, I. *Frontier Orbitals and Organic Chemical Reactions*; Wiley: Chichester:, 1976.

(49) Salem, L. *J. Am. Chem. Soc.* **1968**, *90*, 543-552.

(50) Fukui, K. *Fortschr. Chem. Forsch.* **1970**, *15*, 1.

(51) Fukui, K. *Theory of Orientation and Stereoselection*; Springer-Verlag: Berlin:, 1975.

(52) Houk, K. N. *Acc. Chem. Res.* **1975**, *8*, 361-369.

(53) Sustmann, R.; Trill, H. *Angew. Chem., Int. Ed. Engl.* **1972**, *11*, 838-840.

(54) Bamford, C. H. *Comprehensive Polymer Science (Eds. G.C. Eastmond, A. Ledwith, S. Russo, P. Sigwalt)*; Pergamon: London:, 1988; 3, P.216.

(55) Rüchardt, C. *Top. Curr. Chem.* **1980**, *88*, 1.

(56) Evans, M. G.; Polanyi, M. *Trans. Faraday Soc.* **1938**, *34*, 11.

(57) Trotman-Dickenson, A. F. *Chem. Ind.* **1965**, 379.

(58) Pross, A.; Yamataka, H.; Nagase, S. *J. Phys. Org. Chem.* **1991**, *4*, 135-140.

(59) Gilliom, R. D. *J. Mol. Struct.* **1986**, *138*, 157-161.

(60) Gray, P. A.; Herod, A. A.; Jones, A. *Chem. Rev.* **1971**, *71*, 247.

(61) Rüchardt, C. *Angew. Chem., Internat. Ed.* **1970**, *9*, 830.

(62) Carisson, D. J.; Ingold, K. U. *J. Am. Chem. Soc.* **1967**, *89*, 4885-4891.

(63) Carisson, D. J.; Ingold, K. U. *J. Am. Chem. Soc.* **1968**, *90*, 7047-7055.

(64) Malatesta, V.; Ingold, K. U. *J. Am. Chem. Soc.* **1981**, *103*, 3094-3098.

(65) Norman, R. O. C. *Pure Appl. Chem* **1979**, *51*, 1009-1019.

(66) Chatgilialoglu, C.; Ingold, K. U.; Scaiano, J. C. *J. Am. Chem. Soc.* **1981**, *103*, 7739-7742.

(67) Avila, D. V.; Brown, C. E.; Ingold, K. U.; Lusztyk, J. *J. Am. Chem. Soc.* **1993**, *115*, 466-470.

(68) Paul, H.; Small, R. D.; Scaiano, J. C. *J. Am. Chem. Soc.* **1978**, *100*, 4520-4527.

(69) Scaiano, J. C. *J. Am. Chem. Soc.* **1980**, *102*, 5399-5440.

(70) Avila, D. V.; Ingold, K. U.; Lusztyk, J.; Jr., W. R. D.; Pan, H.-Q. *J. Am. Chem. Soc.* **1993**, *115*, 1577-1579.

(71) Kazanis, S.; Azarani, A.; Johnston, L. J. *J. Phys. Chem.* **1991**, *95*, 4430-4435.

(72) Rios, L. A.; W.R. Dolbier, J.; Paredes, R.; Lusztyk, J.; Ingold, K. U.; Jonsson, M. *J. Am. Chem. Soc.* **1996**, *118*, 11313-11314.

(73) Banks, R. E.; Smart, B. E.; Tatlow, J. C. *Organofluorine Chemistry - Principles and Commercial Application*; Plenum Press: New York and London, 1994.

(74) Dolbier, W. R., Jr. *Top. Curr. Chem.* **1997**, *192*, 97-163.

(75) Brace, N. O. *J. Fluorine Chem.* **1999**, *93*, 1-25.

(76) Brace, N. O. *J. Fluorine Chem.* **1999**, *96*, 101-127.

(77) Brace, N. O. *J. Fluorine Chem.* **2001**, *108*, 147-175.

(78) Huang, W. Y. *J. Fluorine Chem.* **1992**, *58*, 1-8.

(79) Takeyama, Y.; Ichinose, Y.; Oshima, K.; Utimoto, K. *Tetra. Lett.* **1989**, *30*, 3159-3162.

(80) Ren, Y.; Lodge, T. P.; Hillmyer, M. A. *Macromolecules* **2001**, *34*, 4780-4787.

(81) Ameduri, B.; Boutevin, B.; F. Guida-Pietrasanta, e. a. *J. Fluorine Chem.* **2001**, *107*, 397-409.

(82) Balague, J.; Ameduri, B.; Boutevin, B.; Caporiccio, G. *J. Fluorine Chem.* **2000**, *102*, 253-268.

(83) Delest, B.; Shtarev, A. B.; Jr., W. R. D. *Tetrahedron* **1998**, *54*, 9273-9280.

(84) Dolbier, W. R., Jr.; Rong, X.-X.; Bartberger, M.; Koroniak, H.; Smart, B. E.; Yang, Z.-Y. *J. Chem. Soc. Trans. 2* **1998**, 219-231.

(85) Dolbier, W. R., Jr.; Li, A.-R.; Smart, B. E.; Yang, Z.-Y. *J. Org. Chem.* **1998**, *63*, 5687-5688.

(86) Rong, X. X.; Pan, H. Q.; W.R. Dolbier, J. *J. Am. Chem. Soc.* **1994**, *116*, 4521-4522.

(87) Shtarev, A. B.; Tian, F.; W.R. Dolbier, J. *J. Am. Chem. Soc.* **1999**, *121*, 7335-7341.

(88) Dolbier, W. R., Jr.; Li, A.-R. *J. Chem. Soc. Perk T 2* **1998**, 79-82.

(89) Dolbier, W. R., Jr. *Chem. Rev.* **1996**, *96*, 1557-1584.

(90) Avila, D. A.; Ingold, K. U.; Lusztyk, J.; W.R. Dolbier, J.; Pan, H. Q. *J. Org. Chem.* **1996**, *61*, 2027-2030.

(91) McMillen, D. F.; Golden, D. M. *Annu. Rev. Phys. Chem.* **1982**, *33*, 493-532.

(92) Stein, S. E.; Rukkers, J. M.; Brown, R. L. "NIST Standard Reference Database 25: NIST Structures and Properties Database and Estimation Program," National Institute of Standards and Technology, 1991.

(93) Dolbier, W. R., Jr.; Rong, X. X. *Tetra. Lett.* **1994**, *35*, 6225-6228.

(94) Paleta, O.; Církva, V.; Kvícala, J. *J. Fluorine Chem.* **1996**, *80*, 125-134.

(95) Církva, V.; Polák, R.; Paleta, O. *J. Fluorine Chem.* **1996**, *80*, 135-144.

(96) Shtarev, A. B.; W.R. Dolbier, J.; Smart, B. E. *J. Am. Chem. Soc.* **1999**, *121*, 2110-2114.

(97) Liguori, L.; Bjørsvik, H.-R.; Fontana, F.; Minisci, F. *Chem. Commun.* **1997**, 1501-1502.

(98) Tanko, J. M.; Suleman, N. K. *Energetics of Organic Free Radicals: Solvent Effects in the Reactions of Neutral Free radicals*; Blackie Academic & Professional:, 1996, P.224.

(99) Walling, C.; Wagner, P. J. *J. Am. Chem. Soc.* **1964**, *86*, 3368.

(100) Li, C.-J. *Chem. Rev.* **1993**, *93*, 2023-2035.

(101) Lubineau, A.; Auge, J.; Queneau, Y. *Synthesis* **1994**, 741-760.

(102) Kumar, A. *Chem. Rev.* **2001**, *101*, 1-20.

(103) Light, J.; Breslow, R. *Tetra. Lett.* **1990**, *31*, 2957-2958.

(104) Rai, R.; Collum, D. B. *Tetra. Lett.* **1994**, *35*, 6221-6224.

(105) Jang, D. O. *Tetra. Lett.* **1996**, *37*, 5367-5368.

(106) Yamazaki, A.; Togo, H.; Nogami, G.; Yokoyama, M. *Bull. Chem. Soc. Japan* **1997**, *70*, 2519-2523.

(107) Yorimitsu, H.; Wakabayashi, K.; Shinokubo, H.; Oshima, K. *Tetra. Lett.* **1999**, *40*.

(108) Yorimitsu, H.; Nakamura, T.; Shinokubo, H.; Oshima, K.; Omoto, K.; Fujimoto, H. *J. Am. Chem. Soc.* **2000**, *122*, 11041-11047.

(109) Hamilton, C. J.; Tighe, B. J. *Comprehensive Polymer Science (Eds. G.C. Eastmond, A. Ledwith, S. Russo, P. Sigwalt)*, 1988; 3, p.261.

(110) Van Doremaele, G. H. J.; Schoonbrood, H. A. S.; German, A. L. *Comprehensive Polymer Science (Eds. S.L. Aggarwal, S. Russo)*, 1992; Fist Supplement, P.41.

(111) Putnam, R. E. *Comprehensive Polymer Science (Eds. G.C. Eastmond, A. Ledwith, S. Russo, P. Sigwalt*, 1988; 3. P.321.

(112) Feiring, A. E.; Krespan, C. G.; Resnick, P. R.; Smart, B. E. *United States Patent 5,182,342* **1993**.

(113) Inoki, M.; Akutsu, F.; Kitayama, Y.; Kasashima, Y.; Naruchi, K. *Macromol. Chem. Phys.* **1998**, *199*, 619-622.

(114) Letsinger, R. L.; Hamiton, S. B. *J.Am.Chem.Soc.* **1959**, *81*, 3009.

(115) Wright, S. W.; McClure, L. D. *Org. Prep. Proced. Int.* **1994**, *26*, 602-605.

(116) Hansch, C.; Leo, A.; Taft, R. W. *Chem. Rev.* **1991**, *91*, 165-195.

(117) Brace, N. O. *J. Org. Chem.* **1971**, *36*, 1904.

(118) Bullock, G.; Cooper, R. *Trans. Faraday Soc.* **1970**, *66*, 2055-2064.

(119) Hudlicky, M. *Chemistry of organic Fluorine Compounds: A laboratory Manual with Comprehensive Literature Coverage*; 2nd Ed. ed.; John Wiley & Sons Inc.: New York, 1976; P.550.

(120) Baker, J. M.; W.R. Dolbier, J. Unpublished results. Structure were optimized and vibrational grequency calculations were performed using B3LYP and the 6-31G9d) basis set. Thermal energies were obtained using frequencies scales by 0.9804 at 298.15K ans 1atm. Single-point energies were calculated using B3LYP and the 6-311+G(2df,2p) basis set.

(121) Evans, D. A.; Golob, A. M. *J. Am. Chem. Soc.* **1975**, *97*, 4765-4766.

(122) Evans, D. A.; Baillargeon, D. J.; Nelson, J. V. *J. Am. Chem. Soc.* **1978**, *100*, 2242-2244.

(123) Carey, F. A.; Sundberg, R. J. *Advanced Organic Chemistry, part B*; Plenum Press, New York:, 1990; P.321.

(124) Russell, G. A. *Free Radicals Vol. I*; John Wiley &Sons:, 1973; p.311.

(125) Newcomb, M.; G.Glenn, A.; Manek, M. B. *J. Org. Chem.* **1989**, *54*, 4603.

(126) Tronche, C.; Martinez, F.; Horner, J.; Newcomb, M. *Tetra. Lett.* **1996**, *37*, 5845.

(127) Ha, C.; Horner, J.; Newcomb, M.; Varick, T. *J. Org. Chem.* **1993**, *58*, 1194.

(128) Graham, S. R.; Murphy, J. A.; Coates, D. *Tetra. Lett.* **1999**, *40*, 2415-2416.

(129) Cradlebaugh, J.; Zhang, L.; W.R. Dolbier, J., Unpublished results.

(130) Hess, B. A., Jr. *J. Org. Chem.* **2001**, *66*, 5897-5900.

(131) Baker, J. M.; Dolbier, W. R., Jr. Unpublished Results. Calculation used (V)B3LYP/6-311+g(2df, 2p)//(U)B3LYP/6-31g(d) basis set.

(132) R.Carleer; Anteunis, M. J. O. *Organic Magnetic Resonance* **1980**, *13*, 253-258.

(133) Heathcock, C. H.; Keinman, E. F.; Binkley, E. S. *J. Am. Chem. Soc.* **1982**, *104*, 1054-1068.

(134) Zhun, V. I.; Tsvetkov, A. L.; Sheludyakov, V. D.; etc. *J. General. Chem. of USSR* **1988**, 1425-1431.

BIOGRAPHICAL SKETCH

Li Zhang was born on April 28, 1972 in Huhuhot, People's Republic of China to Gui-lin Tian and An-zhe Zhang. She has one older sister. Li lived in Huhuhot until she was seventeen years old, when she completed high school. She then attended Ji-Lin University and received a Bachelor of Science degree in chemistry.

In 1993, Li went to Shanghai Institute of Organic Chemistry for the graduate study in organic chemistry, where she received a Master of Science degree after three years. She worked on the synthesis and properties of novel fluoro-containing polyesters under the supervisory of Dr. Wei-yuan Huang.

Li came to the United States and started her Ph.D. program in the Department of Chemistry at the University of Florida in spring, 1997. She joined Professor Dolbier's group by then. She has been performing research in different areas. Some of these areas include reactivities of fluorinated radicals and kinetic study of α-halomethylammonium salts.

At the time of this writing, Li has accepted a position as a postdoctoral fellow in Research Triangle Institute.

I certify that I have read this study and that in my opinion it conforms to acceptable standards of scholarly presentation and is fully adequate, in scope and quality, as a dissertation for the degree of Doctor of Philosophy.

William R Dolbier

William R. Dolbier, Jr. Chair
Professor of Chemistry

I certify that I have read this study and that in my opinion it conforms to acceptable standards of scholarly presentation and is fully adequate, in scope and quality, as a dissertation for the degree of Doctor of Philosophy.

Merle A. Battiste

Merle A. Battiste
Professor of Chemistry

I certify that I have read this study and that in my opinion it conforms to acceptable standards of scholarly presentation and is fully adequate, in scope and quality, as a dissertation for the degree of Doctor of Philosophy.

Kirk S. Sch

Kirk S. Schanze
Professor of Chemistry

I certify that I have read this study and that in my opinion it conforms to acceptable standards of scholarly presentation and is fully adequate, in scope and quality, as a dissertation for the degree of Doctor of Philosophy.

Robert K. Kennedy
Professor of Chemistry

I certify that I have read this study and that in my opinion it conforms to acceptable standards of scholarly presentation and is fully adequate, in scope and quality, as a dissertation for the degree of Doctor of Philosophy.

Wolfgang M. Sigmund
Assistant Professor of Materials Science
and Engineering

This dissertation was submitted to the Graduate Faculty of the Department of Chemistry in the College of Liberal Arts and Sciences and to the Graduate School and was accepted as partial fulfillment of the requirements for the degree of Doctor of Philosophy.

December, 2001

Dean, Graduate School